

JULIUS-MAXIMILIANS UNIVERSITÄT WÜRZBURG

DOCTORAL THESIS

**Quantitative genetics - from genome
assemblies to neural network aided
omics based prediction of quantitative
traits**

Author:

Jan Alexander
FREUDENTHAL

Supervisor:

Prof. Arthur KORTE

A thesis submitted in fulfillment of the requirements

for the degree of Ph.D.

in the

Research group for evolutionary genomics

GSLs

October 29, 2019

Declaration of Authorship

I, Jan Alexander FREUDENTHAL, declare that this thesis titled, “Quantitative genetics - from genome assemblies to neural network aided omics based prediction of quantitative traits” and the work presented in it are my own. I confirm that:

- This work was done wholly or mainly while in candidature for a research degree at this University.
- Where any part of this thesis has previously been submitted for a degree or any other qualification at this University or any other institution, this has been clearly stated.
- Where I have consulted the published work of others, this is always clearly attributed.
- Where I have quoted from the work of others, the source is always given. With the exception of such quotations, this thesis is entirely my own work.
- I have acknowledged all main sources of help.
- Where the thesis is based on work done by myself jointly with others, I have made clear exactly what was done by others and what I have contributed myself.

Signed:

Date:

“Wit beyond measure is man’s greatest treasure”

Rowena Rawenclaw

JULIUS-MAXIMILIANS UNIVERSITÄT WÜRZBURG

Abstract

Faculty Name

GSLs

Ph.D.

**Quantitative genetics - from genome assemblies to neural network aided omics
based prediction of quantitative traits**

by Jan Alexander FREUDENTHAL

The Thesis Abstract is written here (and usually kept to just this page). The page is kept centered vertically so can expand into the blank space above the title too...

Acknowledgements

The acknowledgments and the people to thank go here, don't forget to include your project advisor. . .

Contents

Declaration of Authorship	i
Abstract	iii
Acknowledgements	iv
1 Benchmarking of Chloroplast Genome Assembly tools	1
1.1 Introduction	1
1.1.1 Motivation	1
1.1.2 Extraction of chloroplast reads from whole genome data and general assembly workflow	4
Purpose and scope of benchmarking the landscape of chloro- plast assembly tools	5
1.2 Material and Methods	6
1.2.1 Methods	6
Data and code availability	6
Tools	6
Standardization and reproducibility	7
1.2.2 Data	8
Simulated	8
Real data set	8
Novel data sets	9
1.2.3 Evaluation	9
Quantitative	9

Consistency	10
1.3 Results	11
1.3.1 Quantitative	11
Simulated data	11
Real data sets	13
Consistency	15
Novel	16
1.4 Discussion	17
1.5 Conclusion & outlook	22
2 Understanding the haplotype structure of Arabidopsis thaliana	23
2.1 Introduction	23
2.2 Haplotyping of A. thaliana	23
2.3 Results	23
2.4 Disucssion	23
3 GWAS-Flow a gpu-accelerated software for large-scale genome-wide association studies	30
3.1 Introduction	30
3.2 Methods	32
GWAS Model	32
The GWAS-Flow Software	32
Calculation of permutation-based thresholds for GWAS	33
Benchmarking	34
3.3 Results	35
3.4 Disucssion	36
4 Genomic prediction of phenotypic values of quantitative traits using artificial neural networks	40
4.1 Introduction	40

4.1.1	A brief history of machine learning	40
	Basic perceptron model	40
	Activation functions	42
	Gradient descent algorithm	45
	Optimizers	47
	Backpropagation	49
	Regularization parameters	49
4.1.2	On the nature of quantitative traits	51
4.1.3	Artificial selection in plant and animal breeding in the ge- nomics era	55
	Introduction to genomic selection	55
	Genomic BLUP and Bayesian methods	57
4.1.4	Genomic selection using artificial neural networks	57
4.2	Proof of concept for ANN-based genomic selection	60
4.3	Material	62
4.3.1	DH populations derived from MAZE landraces	62
4.3.2	<i>A. thaliana</i>	62
4.4	Methods	62
4.4.1	ANN	62
4.4.2	GBLUP	62
4.5	Results	62
4.6	Discussion	62
5	GWAS	63
5.1	Reevaluation of 463 phenotypes from the AraPheno database	63
5.1.1	Introduction	63
5.1.2	Material and Methods	63
5.1.3	Results	63
5.1.4	Results	63

5.1.5	Disucssion	63
5.2	GWAS in DH landrace populatios of maze across and within environ- ments	63
5.2.1	Introduction	63
5.2.2	Material and Methods	63
5.2.3	Results	63
5.2.4	Results	63
5.2.5	Disucssion	63
A	Source code GWAS-Flow	64
A.1	gwas.py	64
A.2	main.py	67
A.3	herit.py	72
	Bibliography	74

List of Figures

1.1	Structure of a chloroplast genome	3
1.2	Chloroplast genome assembly workflow	5
1.3	Score of assemblies of simulated data sets	12
1.4	Scores of assemblies from real data sets	15
1.5	Comparison between two runs with the same assembler for consistency testing	16
1.6	Upset plot comparing the success rates for novel data sets	17
1.7	Upset plot comparing the success rates of all assemblers	19
1.8	AliTV plot of alignments of assemblies of <i>Oryza brachyantha</i> of all assemblers	21
2.1	Haplotype structure of chromosome 1 of <i>A. thaliana</i>	24
2.2	Haplotype structure of chromosome 2 of <i>A. thaliana</i>	25
2.3	Haplotype structure of chromosome 3 of <i>A. thaliana</i>	26
2.4	Haplotype structure of chromosome 4 of <i>A. thaliana</i>	27
2.5	Haplotype structure of chromosome 5 of <i>A. thaliana</i>	28
2.6	blabl	29
3.1	Computation time vs number of markers	36
3.2	Computations time vs accessions	37
3.3	Computational time of GWA Analyses on real <i>A. thaliana</i> data sets . .	39
4.1	Basic perceptron model	40
4.2	Schematic layout of a simple multi-layer perceptron	42

4.3	Popular activation functions for neural networks	43
4.4	Training vs. validation loss over time	50

List of Tables

1.1	Data selection criteria for real data sets from SRA	9
1.2	Scores of assemblies of simulated data	13
1.3	Mean scores of chloroplast genome assemblers	14
4.1	Simple simulated phenotypes and genotypes for genomic prediction with genotypes $G_1 \dots G_4$, M_1 and M_2 and phenotypes based on addi- tive effects or <i>and</i> , <i>or</i> , <i>xor</i> logic gates.	60
4.2	Results of genomic prediction from phenotypes and genotypes in ta- ble 4.1	61

List of Abbreviations

Adadelata	Adaptive delta
Adagrad	Adaptive Gradient Algorithm
Adam	Adaptive Moment estimation
ANN	Artificial Neural Network
AUC	Area Under the Curve
BLUE	Best Linear Unbiased Estimator
BLUP	Best Linear Unbiased Predictor
BP	Base Pair
CPU	Core Processing Unit
DH	Doubled Haploid
DNA	DeoxyriboNucleic Acid
DNA	RiboNucleic Acid
EMMA	Efficient Mixed Model Associations
FCL	Fully Connected Layer
GBLUP	Genomic Best Linear Unbiased Predictor
GD	Gradient Descent
GP	Genomic Prediction
GPU	Graphical Processing Unit
GS	Genomic Selection
GUI	Graphical User Interface
GWAIS	Genome Wide Interaction Association Studies
GWAS	Genome Wide Association Studies
HDF	Hierarchical Data Format

IR	I nverted R epeat
LCL	L ocally C onected L ayer
LD	L inkage D isequilibrium
LMM	L inear M ixed M odel
LSC	L arge S ingle C opy
MLP	M ulti L ayer P erceptron
ML	M achine L earning
MSE	M ean S quare E rror
Nadam	N esterov- a ccelerated A daptive M oment E stimation
NAG	N esterov A ccelerated M omentum
QTL	Q uantitative T rait L ocus
ReLU	R ectified L inear U nits
RKHS	R eproducing K ernel H ilbert S paces
RMSE	R oot M ean S quare E rror
RMSProp	R oot M ean S quare P ropagation
ROC	R eciever O perating C haracteristics
RSS	R esidual S um of S quares
SGD	S tochastic G radient D escent
SNP	S ingle N ucleotide P olymorphism
SSC	S mall S ingle C opy
TRN	T Rai N ing subset
TST	T e S Ting subset
WGS	W hole G enome S equencing
XOR	e Xclusive O R
MBP	M ega B ase P air
SRA	S equence R ead A rchive
NCBI	N ational C enter for B iotechnological I nformation
GPL	G eneral P ublic L icense

HPC	H igh P erformance C omputing
GEBC	G enomic E stimated B reeding V alues

For/Dedicated to/To my...

1 Benchmarking of Chloroplast Genome Assembly tools

This chapter orientates on *Freudenthal et al., 2019b* only the chapters from the publication which the author majorly contributed are included. If not cited otherwise the plots even though they were published along the aforementioned paper, were designed and generated by the author.

1.1 Introduction

1.1.1 Motivation

Certain organelles like mitochondria and chloroplasts contain their own genetic information from which they are able to synthesize certain proteins independent of the core genome. Evolutionary this developed during endosymbiosis. Its underlying theory seeks to explain how eukaryotic cells formed from prokaryotes *Mereschkowsky, 1905; Kutschera and Niklas, 2005*. The widely acknowledged theory explains how in the early evolution of eukaryotes, other cells were incorporated in those cells from which today's known organelles descent. In the case of a chloroplast this was most likely a photosynthetic bacteria or similar organism *Archibald, 2015*. Until today the structure of chloroplast genomes resembles more that of a prokaryotic genome than that of its eukaryotic host cells. A typical chloroplast genome consists of circular DNA with a size between 120 kBP to 160 kBP *Palmer, 1985*. The first chloroplast have been sequenced as early as 1986 and were isolated from *Marchantia polymorpha* and *Nico Ohyama et al., 1986; Shinozaki et al., 1986*. Complete reviews of

the genome structure of chloroplast genomes were written by Green, 2011; Wicke et al., 2011. Chloroplast genomics is widely applied in evolutionary studies Martin et al., 2002; Xiao-Ming et al., 2017. The genome has been reduced in size over the course of evolution through endosymbiotic gene transfer Martin et al., 2002; Deiner et al., 2017. This is still an ongoing process, which can be observed *in vitro* Bock, 2017; Fuentes et al., 2014; Stegemann and Bock, 2009. Up to 14 % of the the core genome of *Arabidopsis thaliana* is made up of genes previously located on the chloroplast (fancy citation), while 100-120 genes remain on the chloroplast Wicke et al., 2011 itself, which by far would not be enough to function independently. Chloroplast genomes are much smaller than core genomes e.g *A. thaliana* has a core genome size of ca. 125 MBP and are highly conserved with a large gene content, therefore polymorphisms are more likely to cause functional changes in the metabolism. Single chloroplast contain up to hundreds of copies of its genome Kumar, Oldenburg, and Bendich, 2014; Bendich, 1987. Photosynthetic activate cells contain multiple chloroplasts, therefore the copy number of the chloroplast genomes is much higher than the number of core genomes per cell which is most cases is 1.

Structurally chloroplast genomes are made up of 4 distinct regions: two inverted repeats (IR) - IR_A and IR_B - ranging from 10 kbp to 76 kbp. They divide the genome into two areas: the large single copy (LSC) and the small single copy (SSC) as shown in 1.1 Palmer, 1985. Taking into account that the majority of assembly tools has been designed to assemble linear core genomes, the structure of chloroplast genomes is a major obstacle when wanting to assemble those genomes with modern short read technologies, especially solving and aligning the IR Wang et al., 2018.

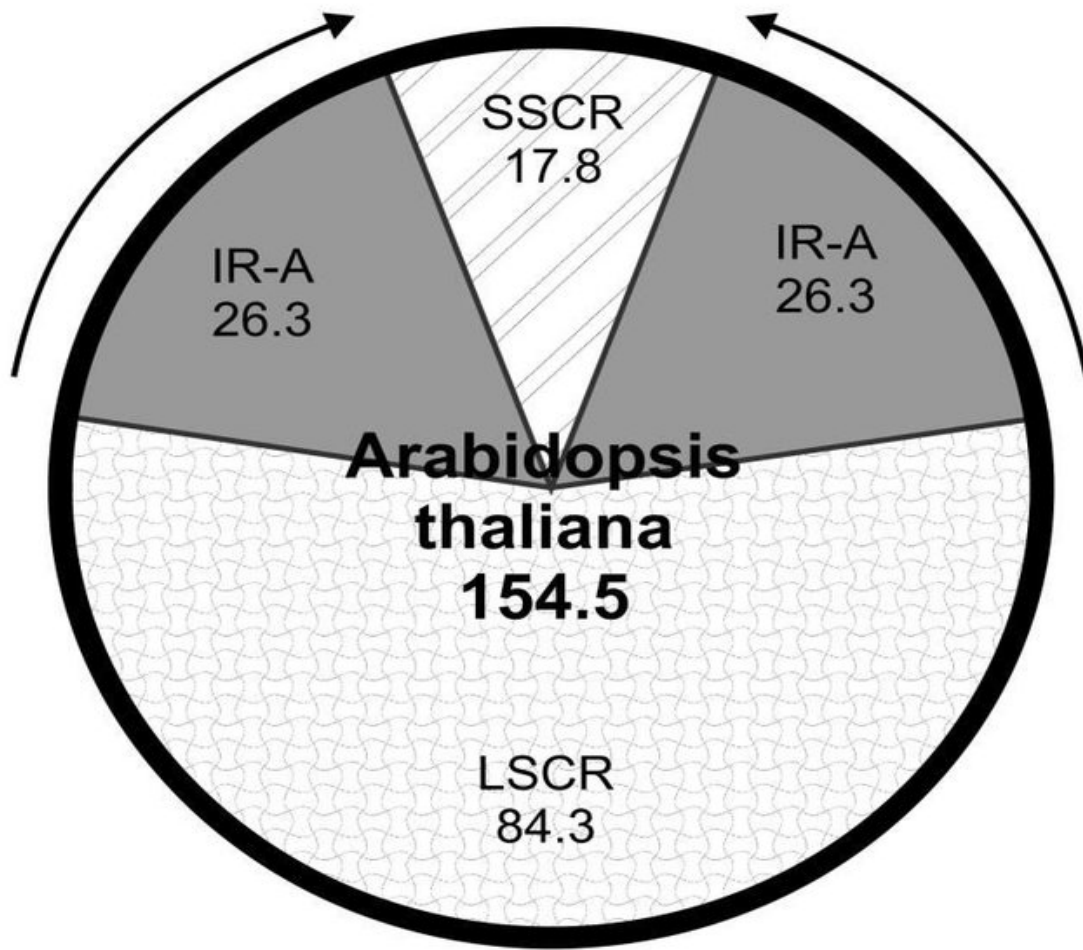


FIGURE 1.1: Structure of the chloroplast genome of *A. thaliana* with SSC-Region and LSC-Region. Length of the genome and its parts in kbp. Graphic from Olejniczak et al., 2016

Chloroplast genomes present biologist with many obstacles of which heteroplasmy stands out and immensely complicated genome assemblies and downstream analyses Corriveau and Coleman, 1988; Chat et al., 2002. Heteroplasmy describes the phenomenon of co-existence of multiple versions of the chloroplast genomes in a single organism and single cells of that respective organism. The underlying evolutionary mechanisms behind heteroplasmy are no fully elucidated and eventually existing fitness advantages fueling heteroplasmy cannot be explained satisfactory by evolutionary methods Scarcelli et al., 2016. There is a variety of databases containing short read data for species without an chloroplast genome available. For

example NCBI's the short read archive (SRA) *Leinonen et al., 2010*. Because most plant DNA extraction protocols use green leaf tissue as basis, they usually contain a large amount of plastid DNA. Having larger number of assembled and annotated chloroplast genomes publicly available would be beneficial for evolutionary studies and could be a useful addition to bar-coding and super-barcoding *Coissac et al., 2016* and other biotechnological applications *Daniell et al., 2016*. To achieve this there is a variety of tools available. The study presented in this chapter, assesses the availability, usability and overall performance of 7 of those tools and ultimately makes use of the newly gained insights to attempt *de novo* assemble more than 100 chloroplast

1.1.2 Extraction of chloroplast reads from whole genome data and general assembly workflow

There is a variety of strategies to assemble chloroplast genomes from raw sequencing data *Twyford and Ness, 2017*. In general the process involves three steps: (i) extraction of plastid reads from the WGS data, (ii) assembly of the plastid genome, (iii) solving the circular structure of the chromosome with the IRs. There are two distinct ways to tackle step (i): The first one is to map all the reads to a reference chloroplast *Vinga et al., 2012*, which works reasonably well if there is one available for the same, or at least a closely related species. The second is to make use of the much larger coverage of chloroplast DNA compared to core DNA, with a k-mer analysis *Chan and Ragan, 2013*, this is for example done by *chloroExtractor* *Ankenbrand et al., 2018*. The third way to accomplish this is to combine as done by *NOVOPlasty* *Dierckxsens, Mardulyn, and Smits, 2017*. Figure 1.2 shows the general workflow of chloroplast assembly too.

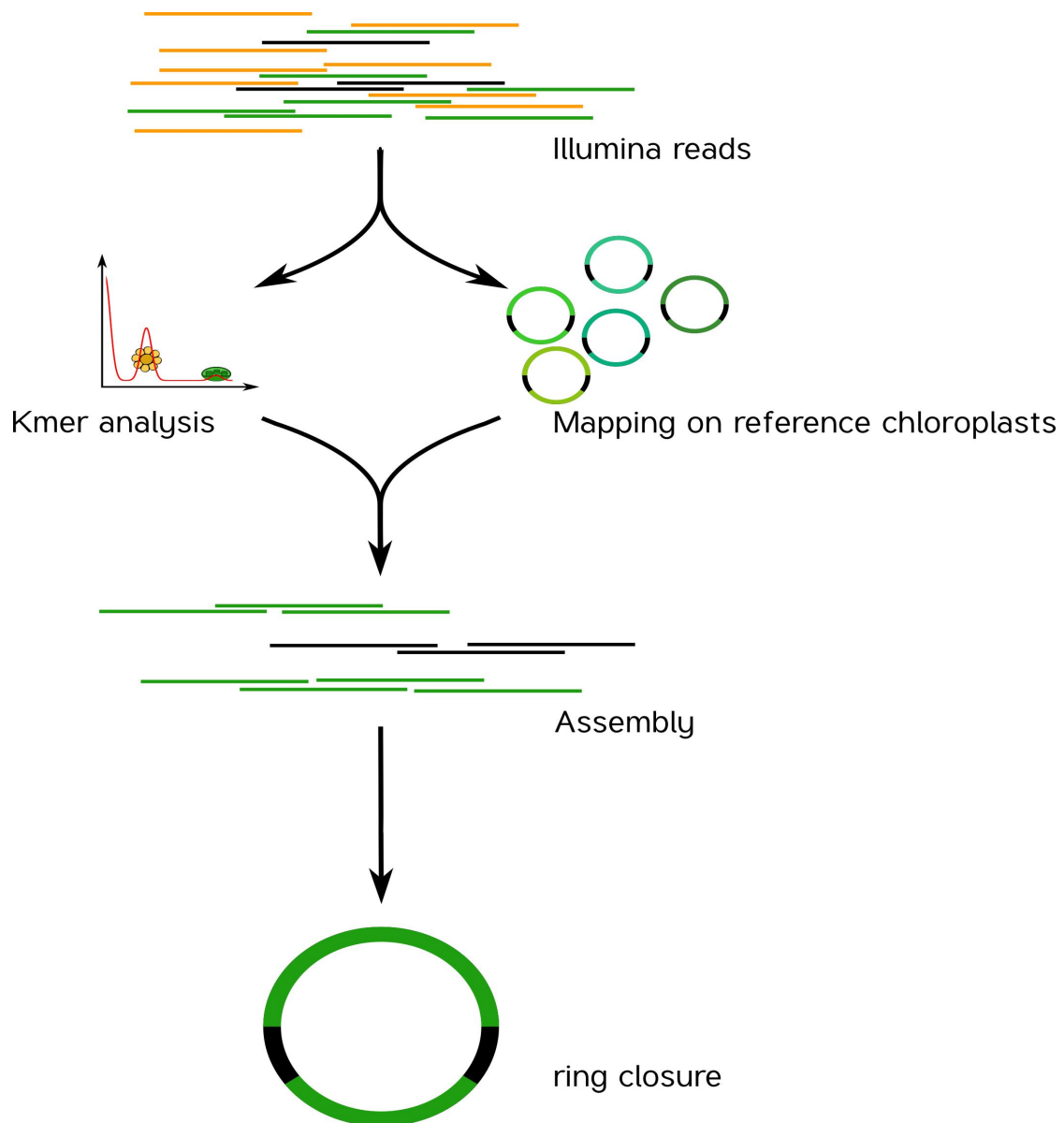


FIGURE 1.2: Standard workflow of chloroplast genome assembly.
Graphic from Ankenbrand et al., 2018

Purpose and scope of benchmarking the landscape of chloroplast assembly tools

The purpose of this study is to provide insights into the landscape of chloroplast assembly tools, to recommend best practices for organelle genome assemblies and to provide *de novo* assemblies for many species and family's without a reference chloroplast available so far. To be included into this study the software including

the source code must be publicly available and published under the terms of a liberal free open source software e.g. GPL or MIT-license. The study was also limited to paired-end Illumina data sets as their sole input source, because they are abundantly available for this benchmark. The seven tools that met the requirements and were therefore included in this study were: chloroExtractor, ORG.Asm, Fast-Plast, IOGA, NOVOPlasty, GetOrganelle and Chloroplast assembly protocol. As later thoroughly described in section 1.3, there are huge differences between those tools and some will not be recommended to be used in scientific applications, while others stand out for most but not all cases.

1.2 Material and Methods

1.2.1 Methods

Data and code availability

All the source code and data used in the scope of this study is publicly available under the terms of the MIT-License. The source code has been published on github [GitHub Repository for Benchmark Project](#) and archived on zenodo [Förster and Ankenbrand, 2019](#). The docker images are available on dockerhub [Docker Hub Group for Benchmark Project](#)

Tools

There were certain requirements to be met to be included into the study as aforementioned. The only technical requirements was, being able to assemble chloroplast genomes from paired-end Illumina reads. The other requirements were due to reproducibility. (i) The software must be open-source and available under the terms of a liberal software license. In the authors opinion obscuring reproducibility

under paywalls cannot be considered good scientific practice. (ii) It must be a command line tool, GUI-only tools are not suited for highly repetitive automated analyses. In total there were 7 tools that met those requirements: (i) *chloroExtractor* Ankenbrand et al., 2018; (ii) *Chloroplast assembly protocol* Sancho et al., 2018; (iii) *GetOrganelle* Jin et al., 2018; (iv) *ORG.Asm* Coissac et al., 2016; (v) *IOGA* Bakker et al., 2016; (vi) *Fast-Plast* McKain and Afinit, 2017; (vii) *NOVOPlasty* Dierckxsens, Mardulyn, and Smits, 2017. There are other tools available, that did not meet the requirements.

Standardization and reproducibility

The main goal of the study was to provide deep insights into the landscape of chloroplast assembly tools. To accomplish that we tried to use the highest standards in bioinformatics when it comes to standardization and reproducibility. Along the study we also wanted to publish easy and ready-to-use versions of all the involved programs, working with standardized input. To accomplish that we decided to make use of containerization in form of docker containers Merkel, 2014 to work with the containers in a closed HPC environment we decided a related software - singularity Kurtzer, Sochat, and Bauer, 2017. Therefore users do not have anything else to do than provide two files one for the forward reads (*forward.fq*) and one for the reverse reads (*reverse.fq*). Both files are required to be in FASTQ format. If docker or singularity are installed no further setup is required, because all dependencies and packages are installed and run from the containers on any given environment. Besides the individual output files, recording the process of the respective program, all programs write the assembly products in to files called *output.fa* in FASTA format. For the quantitative and consistency measurements the singularity containers were run on the Julia HPC-Cluster of the University of Würzburg using the SLURM workload manager Jette, Yoo, and Grondona, 2002. All runs for all assemblies were set with a time limit of 48h. This was necessary because some assemblers e.g. IOGA,

if not finishing after at least 12 hours appear to continue in some kind of loop and never finish.

1.2.2 Data

Three different data sets were used for this study. (i) Simulated data from *A. thaliana* chloroplasts. (ii) real data with known reference chloroplast to rate the success of the assemblies. (iii) Novel data sets from NCBI's SRA without a known reference chloroplast to apply the gained knowledge for the *de novo* assembly of more than 100 chloroplasts.

Simulated

For first steps in any benchmarking process it is always useful to start with simulated data, where the investigators have full control over all the parameters involved. In the case of the present study the data's input parameters thought to be influential on the outcome were: The read length, the ratio between chloroplast and core genome reads. The simulations were based on data from the TAIR10 genome *Berardini et al., 2015* and performed using *seqkit Shen et al., 2016*. Ratios simulated were: 0:1, 1:10, 1:1000 and 1:1000, with read length of 150 and 250 bp. The simulated data consisted either of 2 million read pairs or the full data available. The simulation process is documented and the code and the data is available on github and zenodo *Ankenbrand and Förster, 2019*

Real data set

Real data was selected from the SRA database table 1.1 lists the search terms that had to be met according to the aforementioned search terms.

TABLE 1.1: Data selection criteria for real data sets from SRA

choice	option	explanation
green plants	Organism	include only photosynthetic plants e.g. no algae
wgs	Strategy	only data from wgs projects included
Illumina	Platform	include only paired-en Illumina reads
biomol DNA	Properties	include only biomol. DNA samples (e.g. no RNA)
paired	Layout	exclude single-end reads
random	Selection	
public	Access	Only publicly available data included

In total this resulted in 369 data sets representing a broad variety of the plant kingdom with many different families and genera included.

Novel data sets

To assess the performance on assemblies without a published chloroplast on CpBase *CpBase* 105 data sets were selected from SRA, it was emphasized that such data sets were selected, with the next relatives with a reference chloroplast as distantly related as possible in taxonomic terms according to NCBI *NCBI Taxonomy*

1.2.3 Evaluation

Quantitative

Each assembly from each assembler was compared to their respective reference genome by alignment using minimap2 *Li, 2018* and based on those alignments scores were calculated following equation 1.1 from 0 to 100 with 100 being a perfect score. Four different metrics contributed equally to the final score. (i) The coverage of the assembled genome compared to the reference genome cov_{ref} as an estimate for the completeness. (ii) The vice versa case cov_{qry} as a measure for the correctness of the

assembly. (iii) The success of resolving the IR correct, estimated from the size difference from the reference and the newly assembled genome is: $\min \left\{ \frac{cov_{qry}}{cov_{ref}}, \frac{cov_{ref}}{cov_{qry}} \right\}$. (iv) The number of total contigs were weighted as $\frac{1}{n_{contigs}}$ giving a chloroplast with 1 contig the optimal score.

$$score = \frac{1}{4} \cdot \left(cov_{ref} + cov_{qry} + \min \left\{ \frac{cov_{qry}}{cov_{ref}}, \frac{cov_{ref}}{cov_{qry}} \right\} + \frac{1}{n_{contigs}} \right) \cdot 100 \quad (1.1)$$

While it is difficult to assess the success or failure of assemblies on a continuous scale, equation 1.1 allows for objective and unbiased measurements. SNPs or other small variants do not influence the outcome of the score, because it is much more likely that there are due to in-species variation of the plastid's genome and not caused by the assembly, and even if the latter is true it would be difficult to evaluate that.

Consistency

In any given bioinformatical application consistency is a desired trait. All software (exceptions excluded) should given repeatedly the same input provide the same output. The same obviously or even more so holds true for assembly tools. To evaluate the reproducibility of the 7 tools. All the 369 real data sets described in section 1.2.2 has been used twice for assembly with each assembler and scored twice with equation 1.1. The correlation between the first and the second scores and runs was used the measure for the robustness of a program.

1.3 Results

1.3.1 Quantitative

Simulated data

The simulated data was assembled and scored with all the tools as described above. Figure 1.3 shows as a tile plot the results for all data sets and assemblers. While at first sight there is no clear correlation with the input data sets. It is obvious that there are grave differences between the assemblers. Two programs namely Chloroplast assembly protocol and IOGA failed to correctly assemble a single chloroplast genome. IOGA even fails to provide output at all for the majority of the data sets. While those two stand out as a negative example Fast-Plast and GetOrganelle stand out as a positive example perfectly or nearly perfectly assembling all the data sets, with GetOrganelle surpassing the performance of Fast-Plast. In the middle of the field are chloroExtractor, ORG.As and NOVOPlasty performing reasonably well, but sometimes lacking to solve the IRs and the circular structure.

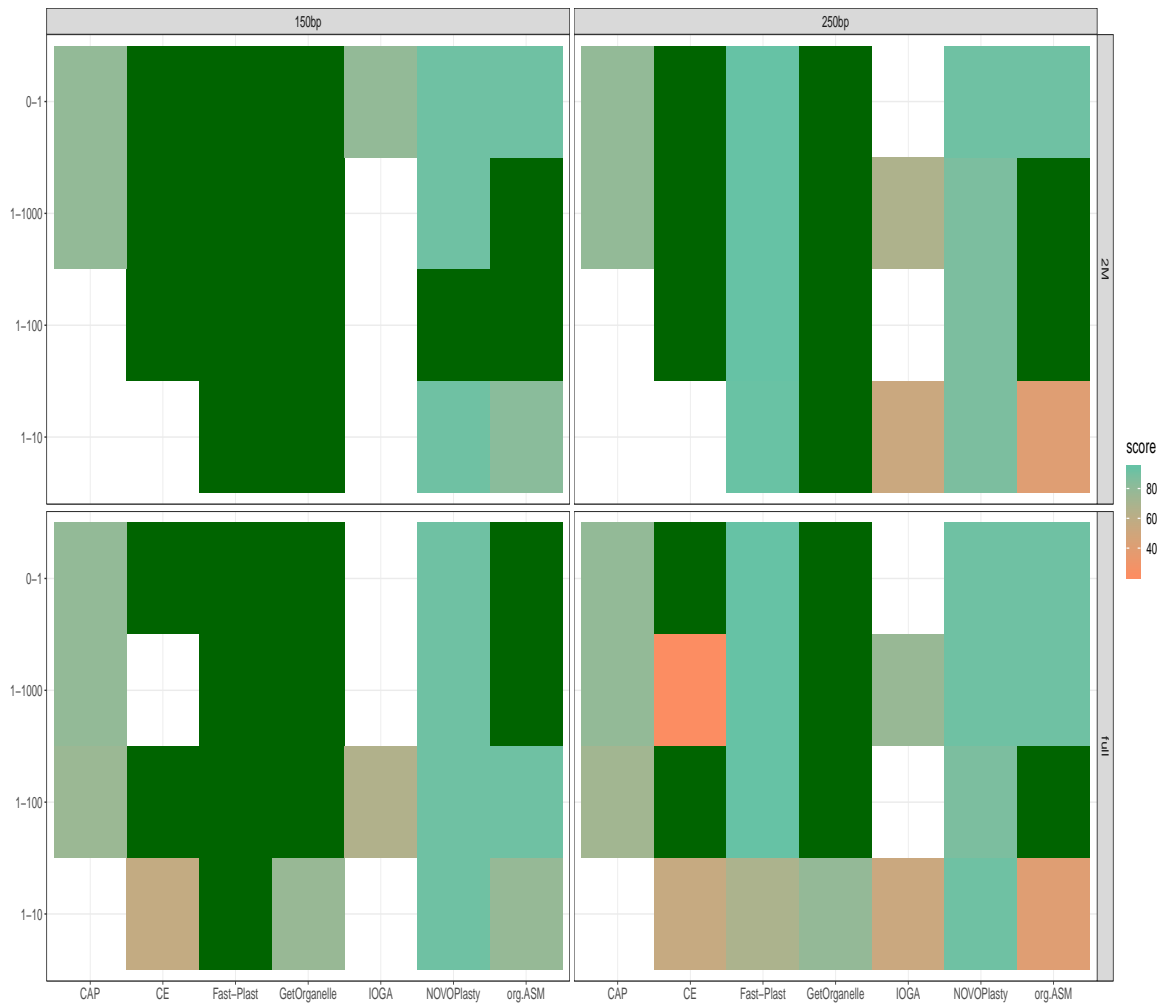


FIGURE 1.3: Results of assemblies executed with simulated data sets.

While there is a significant difference between the assemblers the same is not necessarily true in general for the other varying parameters. While Fast-Plast deals with the shorter reads of 150 bp much better than with the longer reads of 250 bp. The outcome of the other assemblies does not seem to be influenced by that. There is no difference between the full and the subsampled data sets. And while all assemblers appear to be more challenge by low chloroplast to core genome ratios of 1:10 larger ratios do not affect the quality of the result as expected. Table 1.2 shows all the individual results for all data sets and assemblers. For the fields with no entry the respective assembler failed to provide an output.

TABLE 1.2: Scores of assemblies of simulated data

	data set	CAP	CE	Fast-Plast	GetOrganelle	IOGA	NOVOPlasty	org.ASM
1	sim_150bp.0-1	79.10	100.00	99.48	100.00		91.52	100.00
2	sim_150bp.0-1.2M	79.10	100.00	99.72	100.00	79.10	91.52	91.50
3	sim_150bp.1-10		56.44	100.00	76.98		91.52	78.00
4	sim_150bp.1-10.2M			99.97	100.00		91.52	82.72
5	sim_150bp.1-100	75.72	100.00	99.48	100.00	66.09	91.52	91.50
6	sim_150bp.1-100.2M		100.00	99.47	100.00		100.00	100.00
7	sim_150bp.1-1000	79.10		99.72	100.00		91.52	100.00
8	sim_150bp.1-1000.2M	79.10	100.00	99.72	100.00		91.52	100.00
9	sim_250bp.0-1	79.10	100.00	93.82	100.00		91.52	91.50
10	sim_250bp.0-1.2M	79.10	100.00	93.83	100.00		91.52	91.50
11	sim_250bp.1-10		54.98	68.45	78.89	52.71	91.52	40.20
12	sim_250bp.1-10.2M			93.00	100.00	52.67	87.40	40.20
13	sim_250bp.1-100	72.81	100.00	93.82	100.00		87.40	100.00
14	sim_250bp.1-100.2M		100.00	93.83	100.00		87.40	100.00
15	sim_250bp.1-1000	79.10	21.30	93.83	100.00	76.96	91.52	91.50
16	sim_250bp.1-1000.2M	79.10	100.00	93.83	100.00	67.55	87.40	100.00

Real data sets

Table 1.3 gives the results from the assemblies of 369 data sets with 7 assemblers. Similar to the results of the previous section there is a significant difference between the tools. Likewise GetOrganelle is the most successful assembler by a large margin with 210 of 369 perfectly assembled chloroplast genomes, failing to provide output for only 9 data sets, resulting in a media score > 99. Contrary to GetOrganelle, Chloroplast assembly protocol and IOGA fail to completely assemble a single genome. The performance of Fast-Plast could be considered reasonably well, completing approximately half as many genomes as GetOrganelle and being the only other tool whose average score is larger than 90. Similar to the trials with the simulated data in chapter 1.3.1 in the middle of the field are chloroExtractor, NOVOPlasty and ORG.Asm.

TABLE 1.3: Mean scores of chloroplast genome assemblers

	assembler	Median	IQR	N_perfect	N_tot
1	CAP	45.25	50.19	0	369
2	CE	56.55	71.50	14	369
3	Fast-Plast	92.80	23.59	113	369
4	GetOrganelle	99.83	20.94	210	360
5	IOGA	71.10	11.21	0	338
6	NOVOPlasty	75.95	48.69	58	369
7	org.ASM	67.35	91.69	46	348

Figure 1.4 emphasizes the large differences between the assemblers shown in table 1.3. The swarm plots show some distinct bands for some assemblers e.g. NOVOPlasty and ORG.Asm, suggesting that multiple assemblies fail to be solved into a single contig genome at a certain point. As thoroughly discussed in section 1.4 just from this swarm plot it is debatable if all the tools could be recommended for the purpose they were designed for.

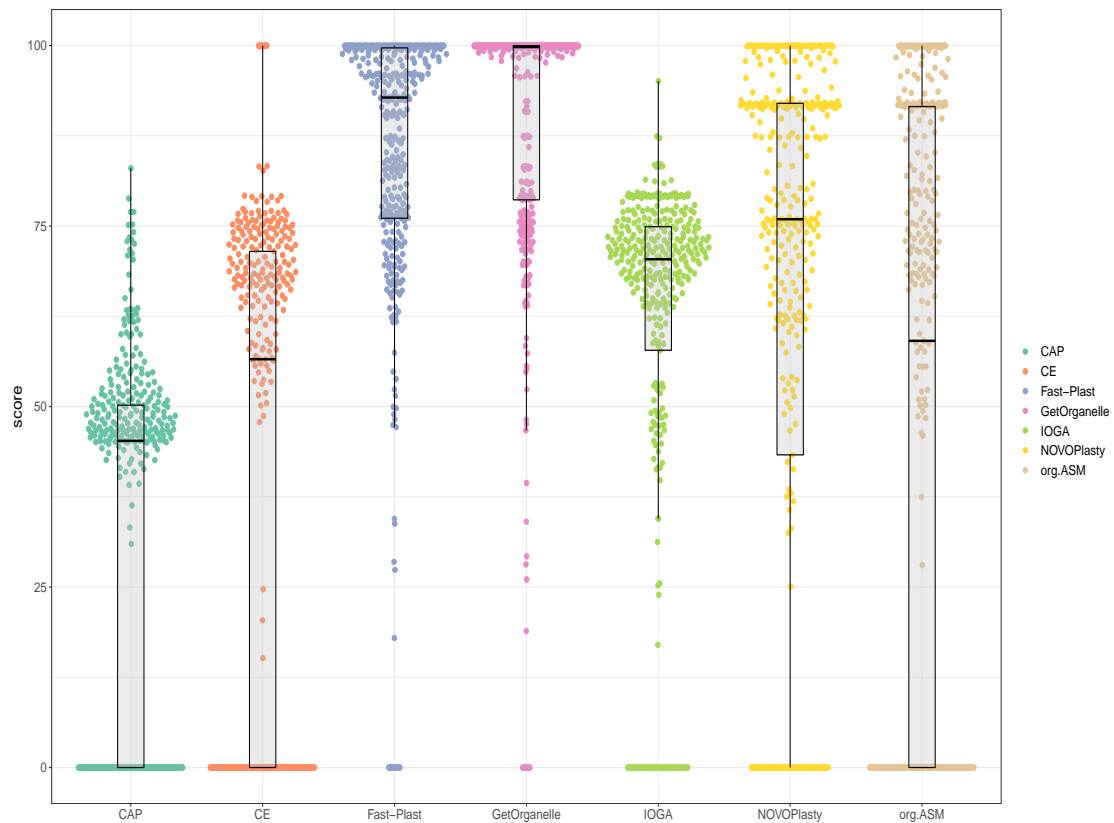


FIGURE 1.4: Box and swarm plots depict the results from the scoring shown in 1.1

Consistency

Consistency testing was done by re-running every assembly for the real data sets twice and comparing the scores. `chloroExtractor` was the only tool that was 100 % consistent over 2 runs. Followed by `Fast-Plast` and `NOVOPlasty`. The consistency plot figure 1.5 for both of them results in an arrowhead shaped plot. With the main differences between the first and second run in the best scores. All other assemblers appear to produce the same output in the two runs except if they fail to complete the assembly at all. This is less pronounced for `Chloroplast assembly protocol` and `GetOrganelle` and is a grave issue for `ORG.ASM` and `IOGA`.

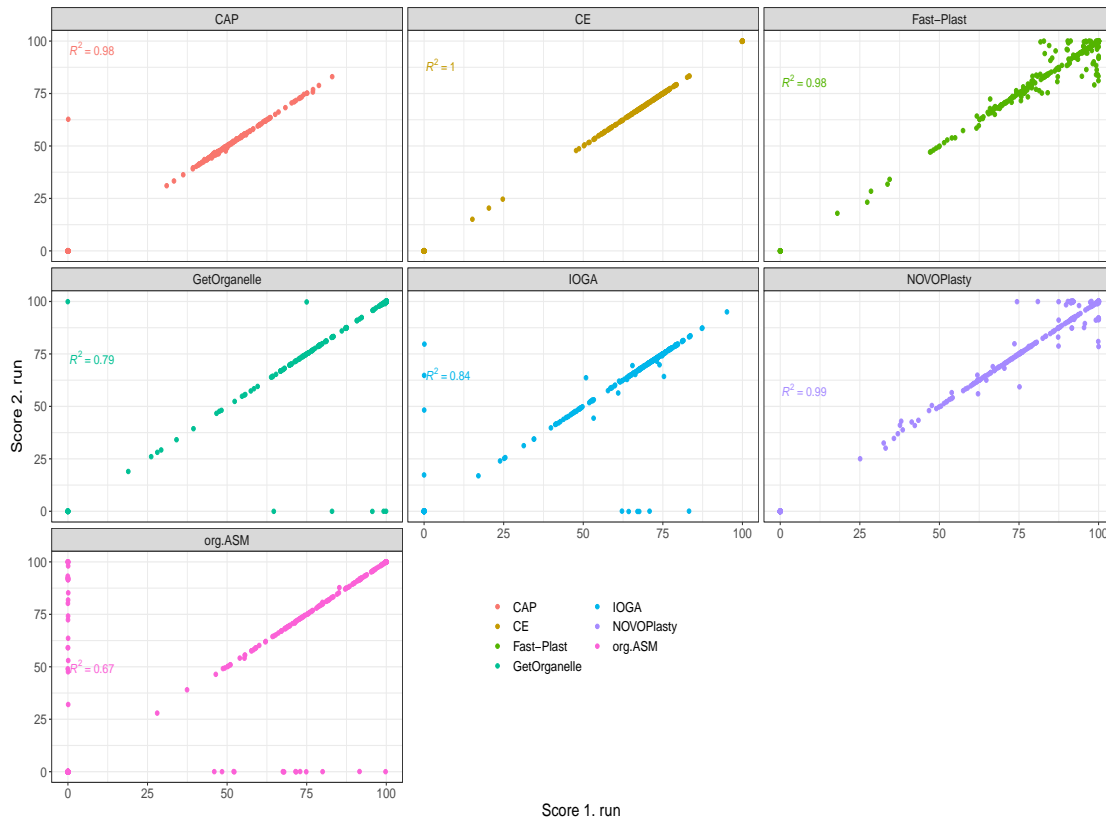


FIGURE 1.5: Swarm plots depict the results from the scoring shown in 1.1 for two independent runs for each assembler on each of the data sets

Novel

The final assessment in the scope of the study was to test the assemblers on novel data sets without a published chloroplast. This step is important for two reasons. (i) There could be the possibility that certain tools perform well on known chloroplasts because they somehow of knowledge over those and simply apply it during those assemblies and therefore the previous results will not be able to generalize on unknown data. (ii) To apply and test the gained insights in the hope of providing the scientific community with a larger variety of published chloroplast genomes. Again the most successful assembler was GetOrganelle, with 49 out of 105 data sets completely assembled. Lacking a reference genome the success had to be defined differently and equation 1.1 was not suitable to evaluate the novel assemblies.

Metrics influencing the score of the novel assemblies were the number of contigs, solving the IRs and the size of the SSC and LSC. This known to the authors might be very biased and not true for all chloroplast and assumes that all chloroplast genomes follow the general structure for their genomes described in chapter 1.1. Figure 1.6 compares the results for the assemblies with at least one successful assembly.

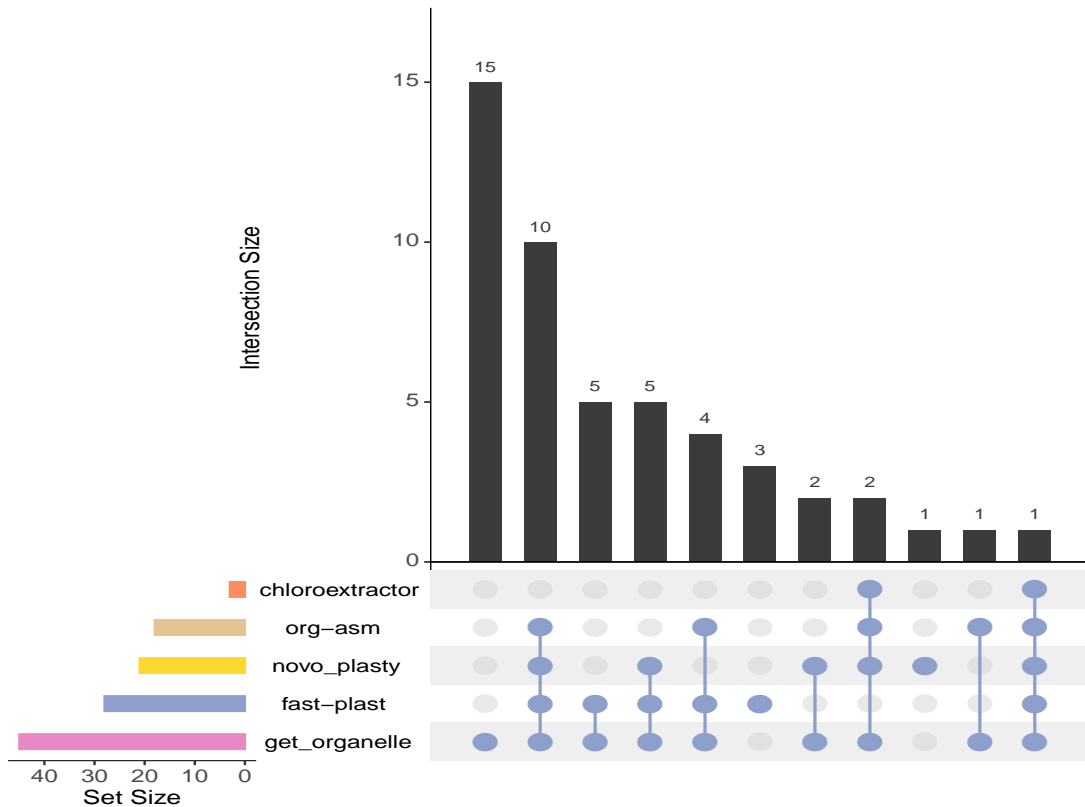


FIGURE 1.6: Upset plot comparing the success rates of the different assemblers

1.4 Discussion

The study compromised of two goals. (i) to assess the overall performance of a variety of tools designed specifically for the assembly of circular chloroplast genomes from paired-end Illumina data and (ii) to *de novo* assemble a variety of yet unpublished chloroplast genomes from existing data. To accomplish the first goal 16 simulated and 369 simulated data sets were used adding up to a total of 5166 assemblies

for the real data sets and 112 for the simulated data, along 735 assemblies for the novel data sets, thus underlying the statistical powers of this benchmarking study. The most successful tools were GetOrganelle and Fast-Plast which are recommended to be used complementary, because as shown in figure 1.7 they succeed for the most data sets compared to other assemblers and accomplish to satisfactory assemble chloroplast genomes where the other fails. If both of them fail it might be worthwhile to repeat the runs because other results could be expected as shown in the scatter plots of figure 1.5, especially Fast-Plast might be able to improve the previously achieved score. Only if both of them fail it might, even though improbable, that NOVOPlast might lead to a successful assembly. The other assemblers should be used with caution. While chloroExtractor might be good for a quick overview due to its relatively low demand in computational time *Freudenthal et al., 2019b*; Chloroplast assembly protocol, ORG.As and IOGA are not recommended to be used as the primary tools in organelle genome assembly projects, as used in this study.

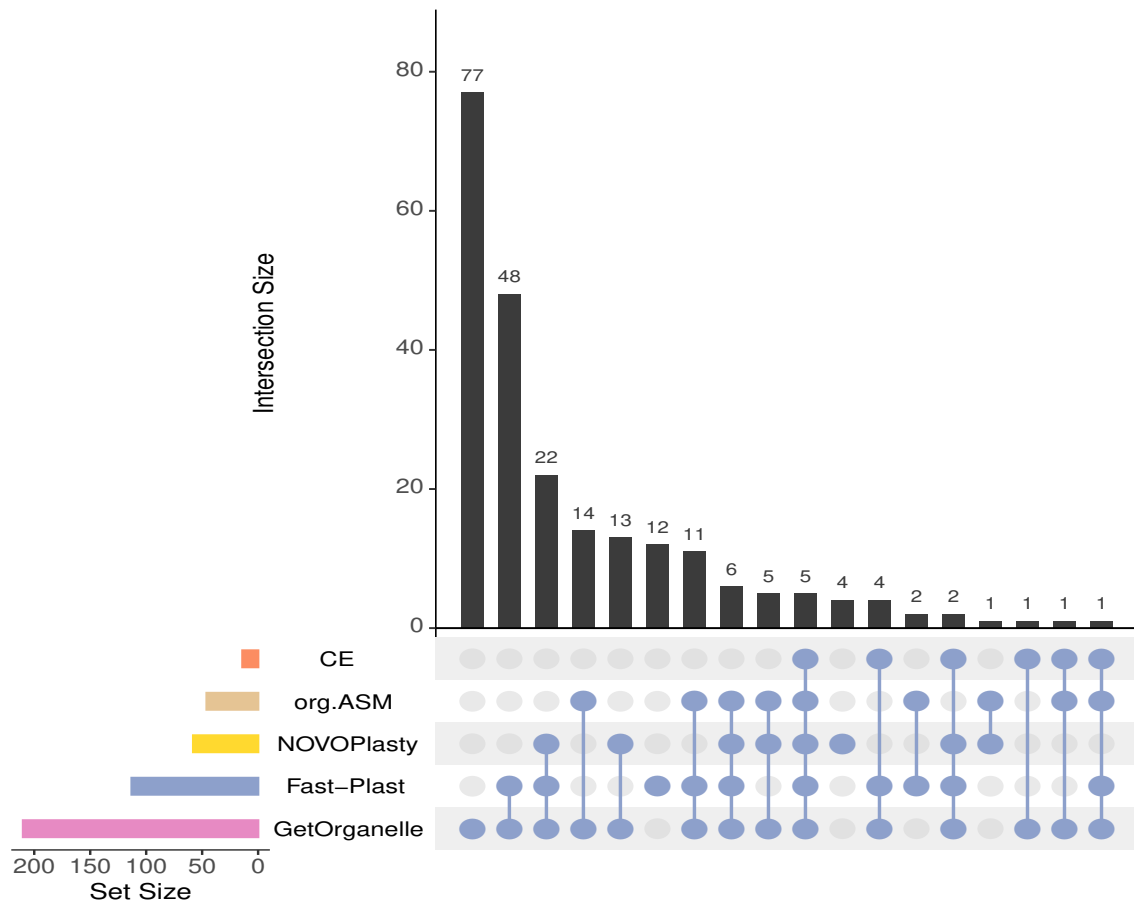


FIGURE 1.7: Upset plot showing the intersections of success rates between assemblers. A successful assembly was defined with a score > 99 according to equation 1.1. The colored, horizontal barplot indicates the total number of successful assemblies for an individual tool. The black, vertical barplot gives the magnitude of the intersection between the assemblers indicated with the dot. Therefore the first bar is to be interpreted as follows: 77 data sets were only successfully assembled by chloroExtractor, likewise 48 genomes were assembled completely by GetOrganelle and Fast-Plast and so on.

It might be possible that overall performance of a specific tool might change significantly by fine tuning the input parameters of the tool, which was purposely not done in the scope of the present study, because this study was designed to mimic

the behavior have end-users and not developers of such tools and the assumption is proposed that end-users with little experience in bioinformatics would be inclined to use the basic configurations of such a tool.

While there is a huge differences for all assemblers they are presented with the same challenges and the bottlenecks are similar for each of them, the success rate of passing those differs however. Figure 1.8 shows the alignment of the 7 chloroplast genomes of *Oryza brachyantha* a grass distantly related to cultivated rice *Oryza sativa* and the respective reference genome. For the need of a linear representation of the circular genome the convention is to present chloroplast genomes in the order LSC - IRa - SSC - IRb. *O. brachyantha* was chosen because multiple tools successfully or at least almost assembled the full genome. Only Chloroplast assembly protocol is singled out, which only managed to assemble a few fragments on the SCC and the IRs on many contigs. A common mistake is to return 3 contigs as IOGA did. They represent the LSC the SSC and one IR but failed to resolve those regions into a one circular contig. GetOrganelle and Fast-Plast were able to reproduce the structure of the reference, while chloroExtractor flipped the LSC and NOVOPlasty and ORG.Asm were not able to construct the single contig into the conventional structure. All of this are common mistakes appearing more or less rare in all the assemblers. This could be a good starting point for the developers to further improve their tools. In this example all but Chloroplast assembly protocol were able to construct all the parts of the chloroplast's genome, and the main mistake was to resolve the structure of the genome into a circular, one contig version.

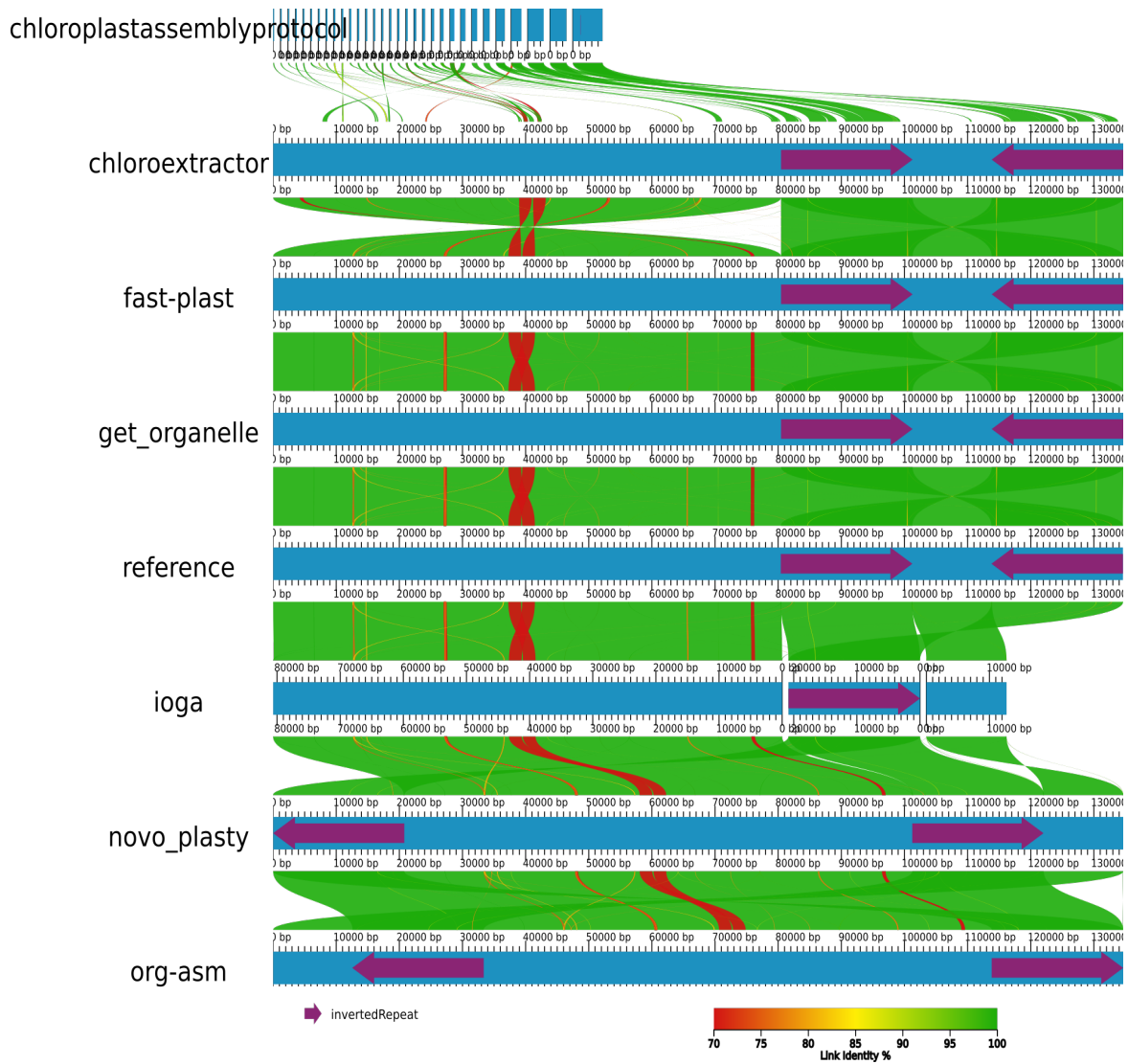


FIGURE 1.8: AliTV plot [Ankenbrand et al., 2017](#) from [Freudenthal et al., 2019b](#) showing the alignments of *Oryza brachyantha* chloroplast genomes from all 7 assemblers. Regions in adjacent assemblies are connected with colored ribbons for similar regions in alignment with the identity coded as described in the legend. The purple arrows indicate the IR regions

1.5 Conclusion & outlook

Organelle genomics is promising field in plant genetics. As described in section 1.1 chloroplast genomes are well-suited for applications in evolutionary sciences, taxonomy and barcoding applications. Alike its mother branch genomics for comparative chloroplast genomics its just as crucial to obtain high quality genomes. And the quality is mainly influenced by two major factors: the quality of the genome sequencing protocol and the quality of the assembly. As shown the latter varies massively between tools and not all tools are recommend equally from the conclusions drawn for the above experiments. All tools have room for improvement, this is meant to criticize the respectable work of the developers, but to encourage them to further develop tools and publish them under terms of liberal software licenses for the greater benefit of the entire scientific community.

2 Understanding the haplotype structure of *Arabidopsis thaliana*

2.1 Introduction

Recombination and LD in *A. thaliana* Kim et al., 2007 LD in *A. thaliana* Nordborg et al., 2002 Evolution of selfing Tang et al., 2007 Evolution and genetic differentiation among relatives of *Arabidopsis thaliana* Koch and Matschinger, 2007 FLC haplotypes Li et al., 2014

2.2 Haplotyping of *A. thaliana*

2.3 Results

2.4 Disucssion

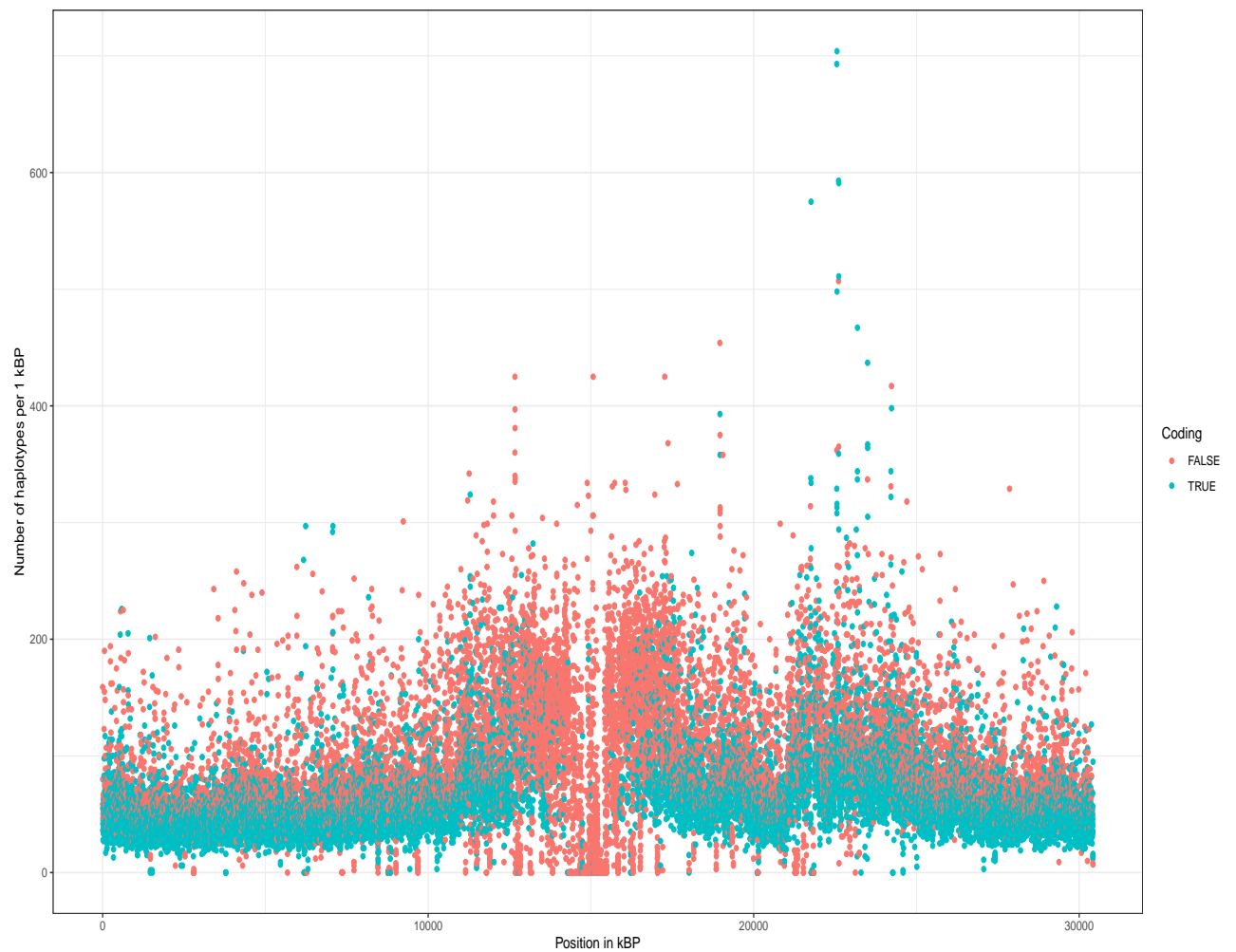


FIGURE 2.1: The number of segregating haplotypes with a polymorphism in at least one position over a stretch of 1 kBP.

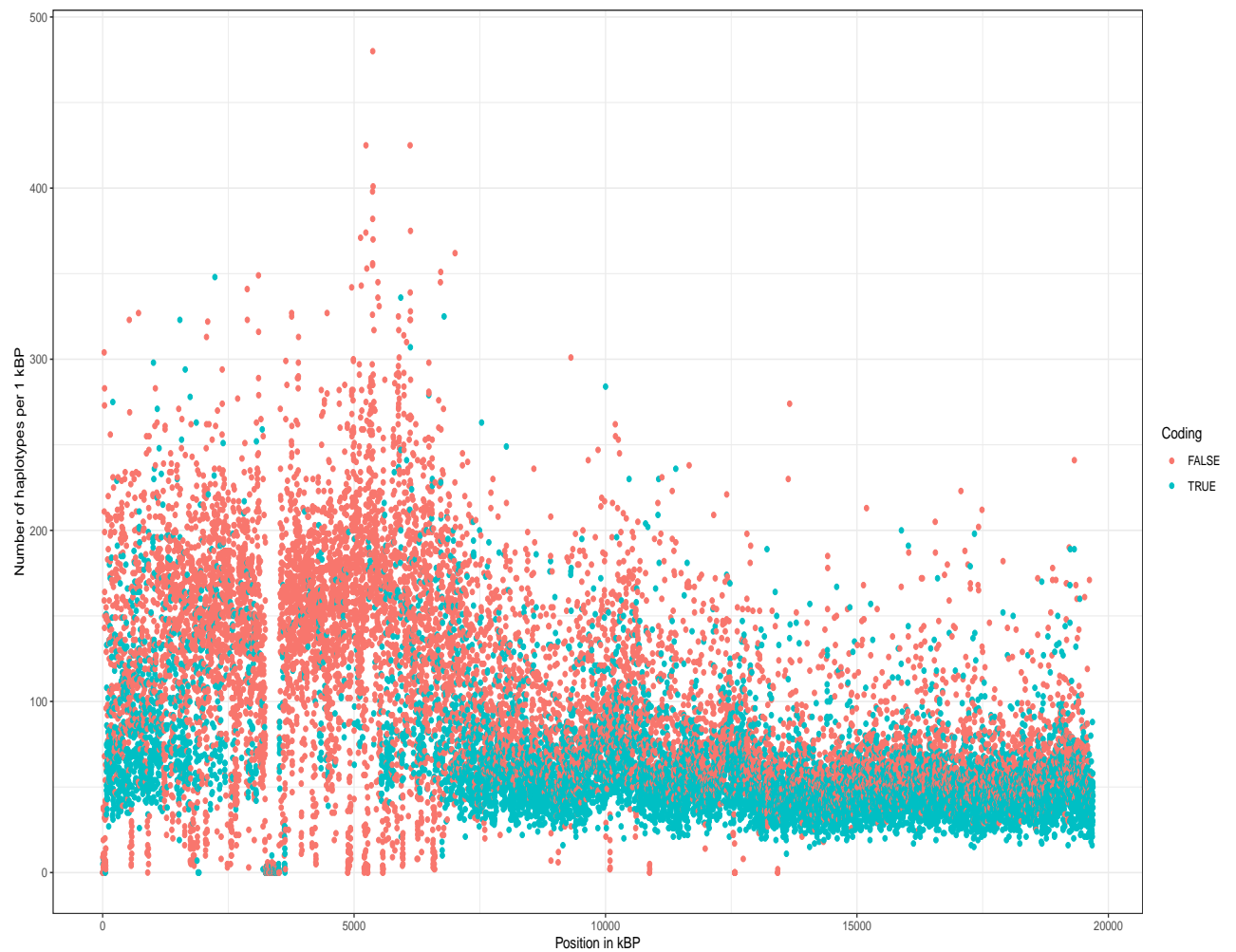


FIGURE 2.2: Number of segregating haplotypes with a polymorphism in at least one position over a stretch of 1 kBP.

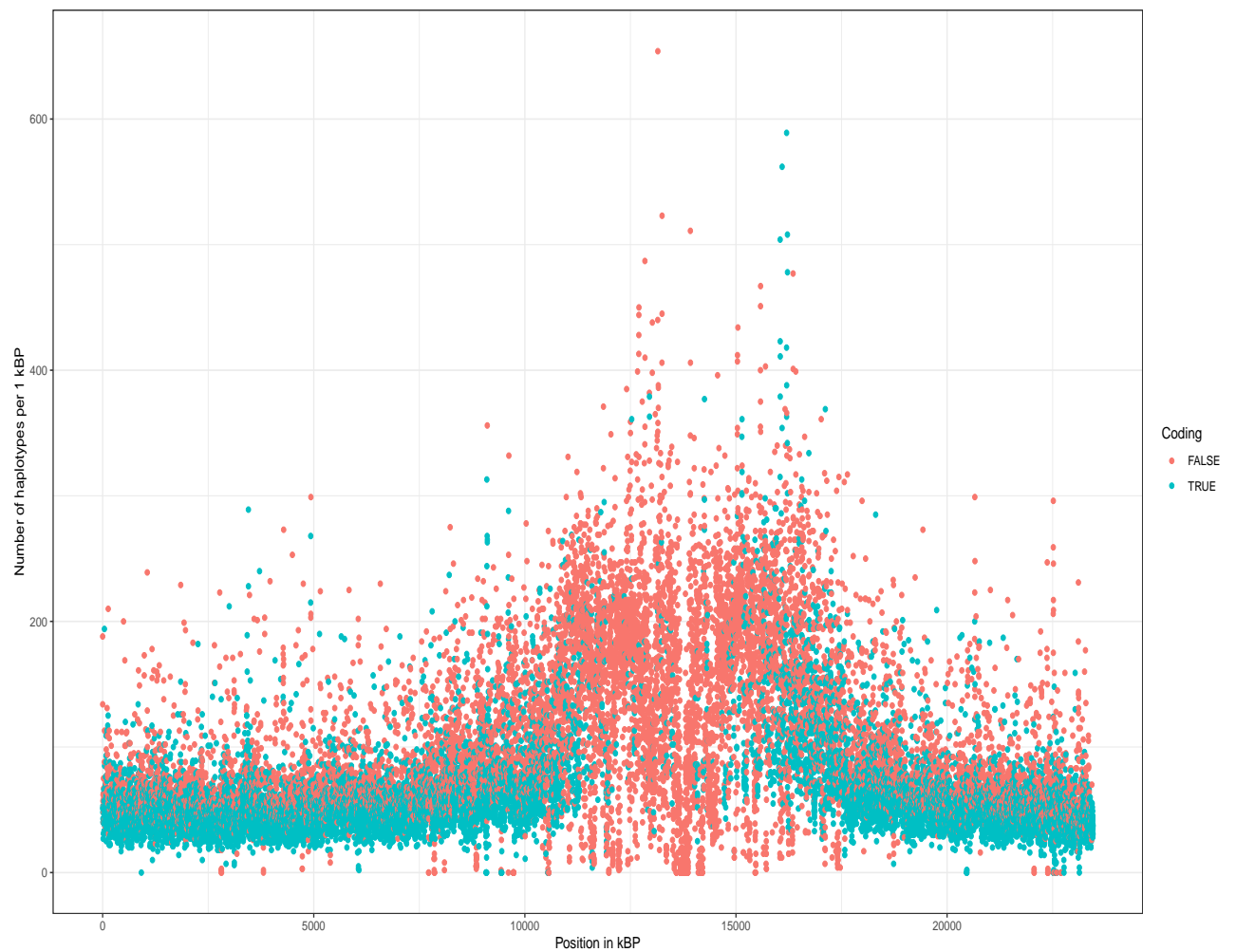


FIGURE 2.3: Number of segregating haplotypes with a polymorphism in at least one position over a stretch of 1 kBP.

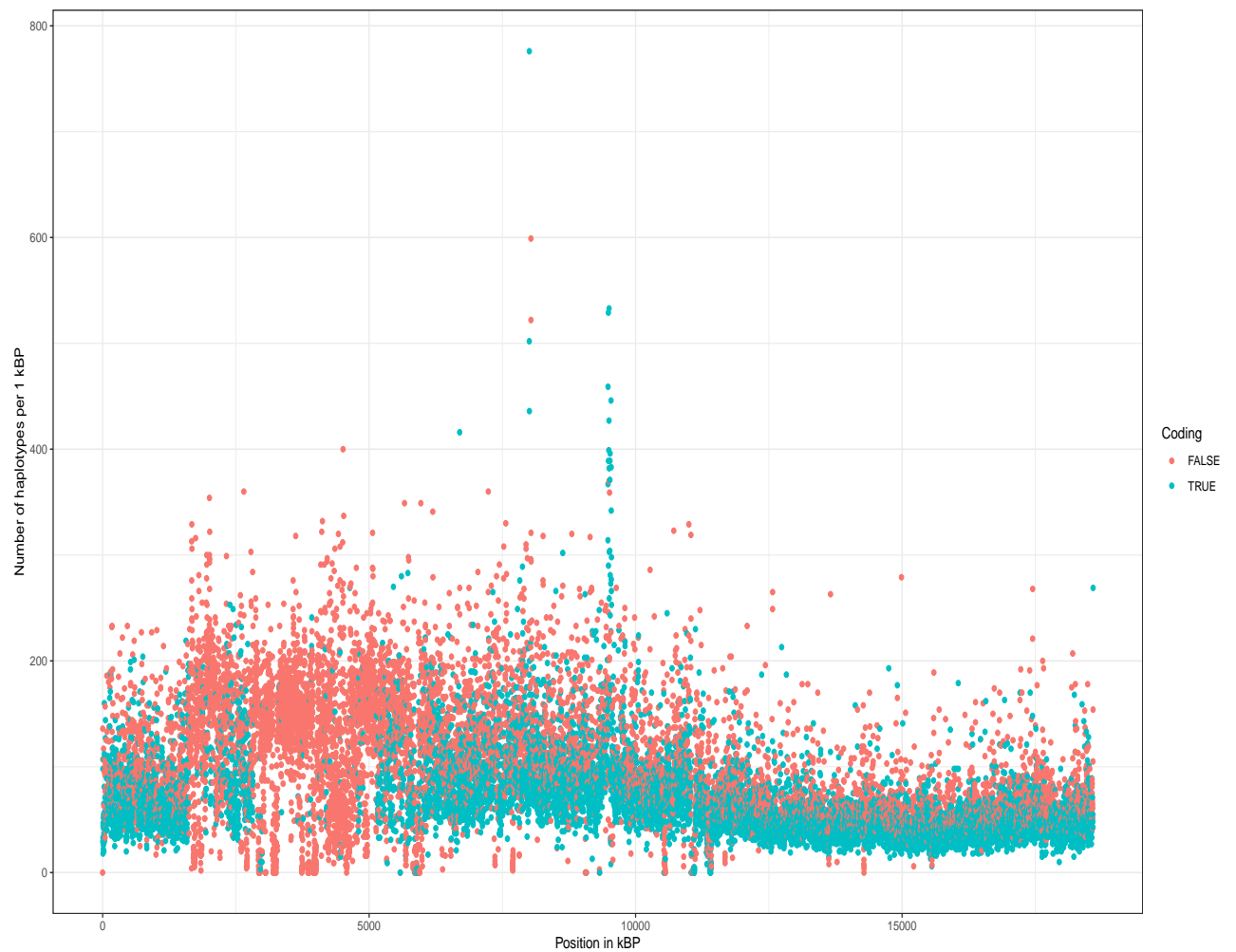


FIGURE 2.4: Number of segregating haplotypes with a polymorphism in at least one position over a stretch of 1 kBP.

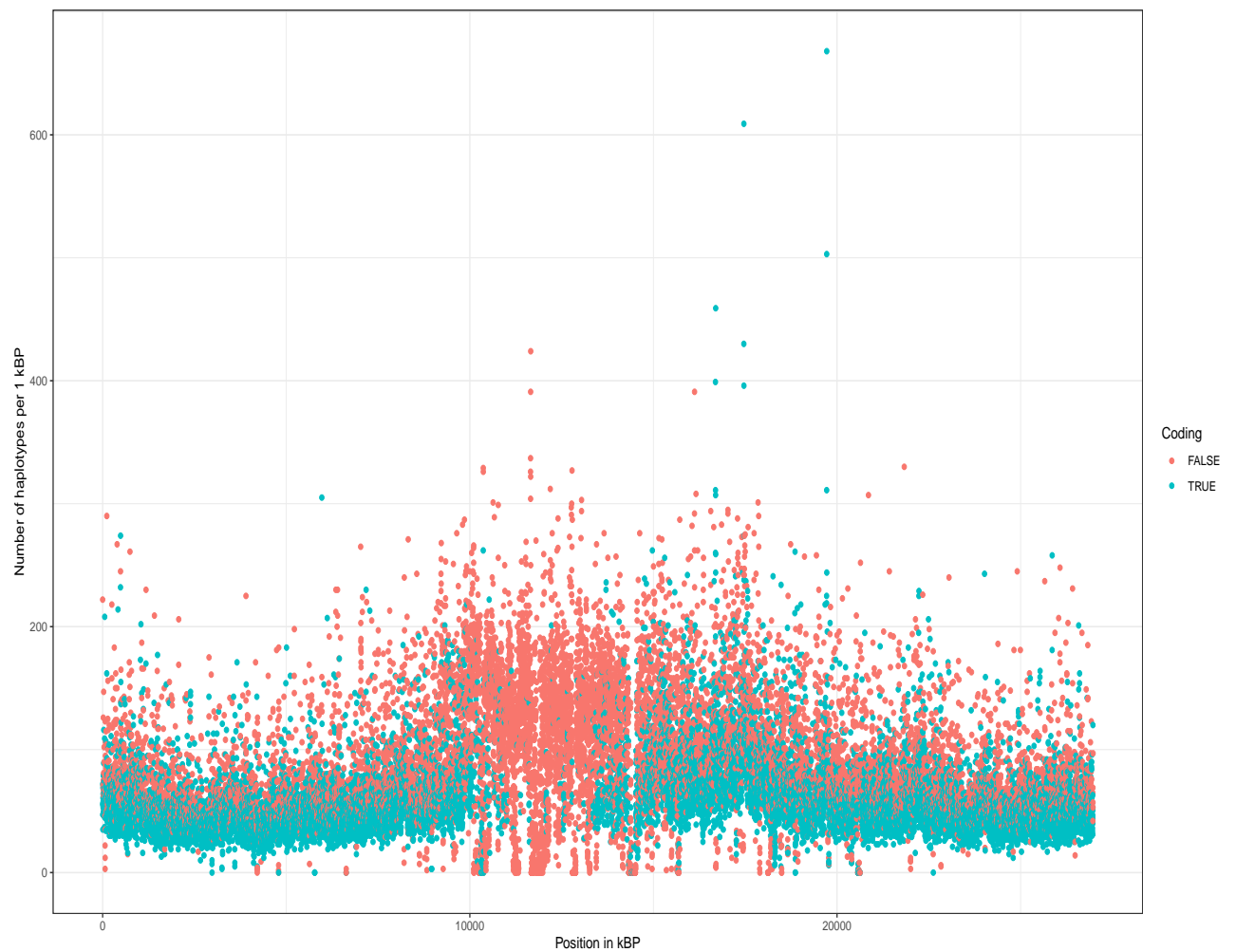


FIGURE 2.5: Number of segregating haplotypes with a polymorphism in at least one position over a stretch of 1 kBP.

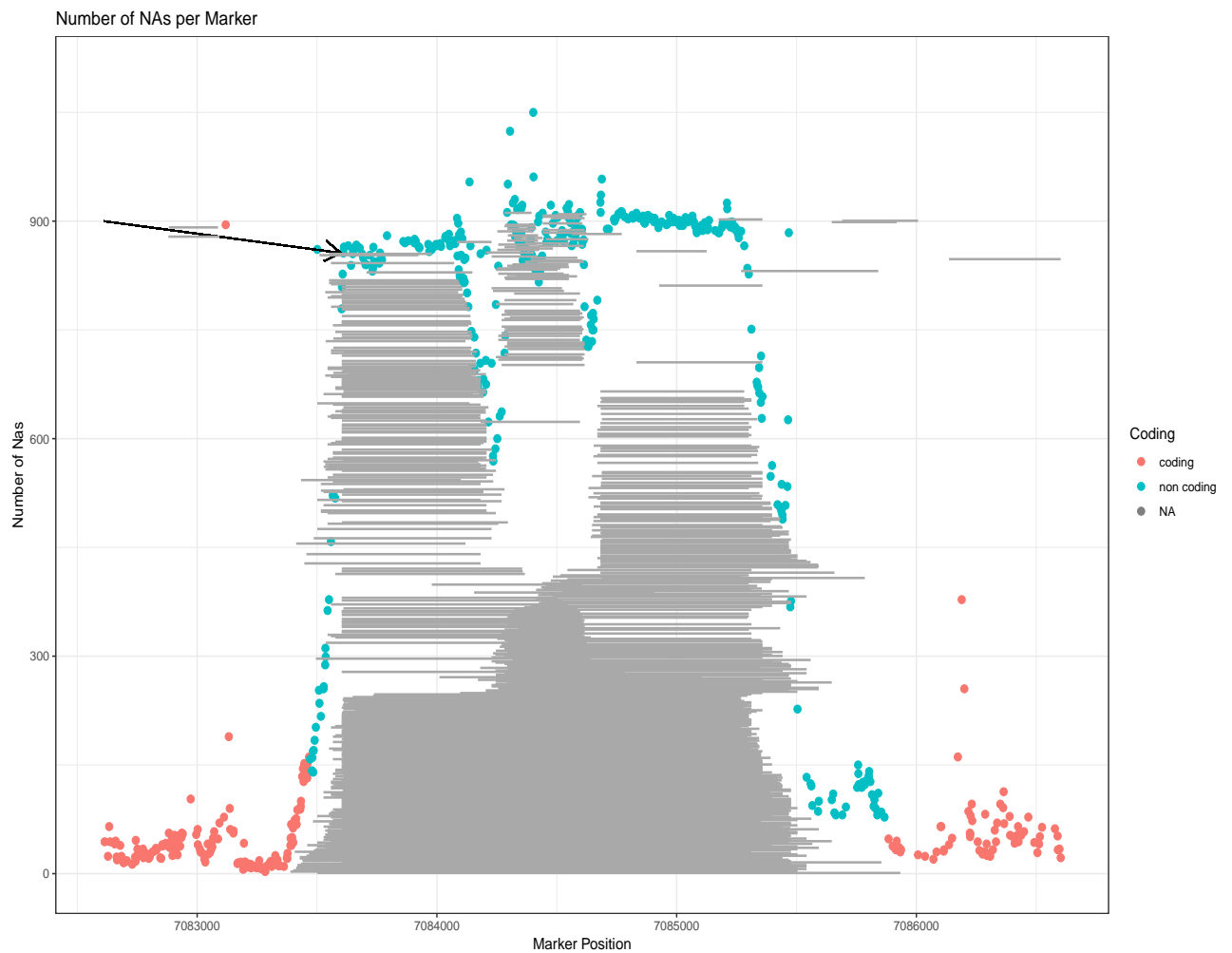


FIGURE 2.6: Number of segregating haplotypes with a polymorphism in at least one position over a stretch of 1 kBP.

3 GWAS-Flow a gpu-accelerated software for large-scale genome-wide association studies

The following chapter has been published in a similar version on the bioRxiv preprint server *Freudenthal et al., 2019a* and has been submitted for publication to Oxford Bioinformatics. The experiments and the software have been designed and conducted author. The manuscript has been prepared by the author, with minor corrections from Prof. Arthur Korte & Dominik Grimm. All authors approved of the final manuscript.

3.1 Introduction

Genome-wide association studies, pioneered in human genetics *Hirschhorn and Daly, 2005* in the last decade, have become the predominant method to detect associations between phenotypes and the genetic variations present in a population. Understanding the genetic architecture of traits and mapping the underlying genomic polymorphisms is of paramount importance for successful breeding both in plants and animals, as well as for studying the genetic risk factors of diseases. Over the last decades, the cost for genotyping have been reduced dramatically. Early GWAS consisted of a few hundred individuals which have been phenotyped and genotyped on a couple of hundreds to thousands of genomic markers. Nowadays, marker density

for many species easily exceed millions of genomic polymorphisms. Albeit commonly SNPs are used for association studies, standard GWAS models are flexible to handle different genomic features as input. The *Arabidopsis* 1001 genomes project features for example 1135 sequenced *Arabidopsis thaliana* accessions with over 10 million genomic markers that segregate in the population *Alonso-Blanco et al., 2016*. Other genome projects also yielded large amounts of genomic data for a substantial amount of individuals, as exemplified in the 1000 genomes project for humans *Siva, 2008*, the 2000 yeast genomes project or the 3000 rice genomes project *Li, Wang, and Zeigler, 2014*. Thus, there is an increasing demand for GWAS models that can analyze these data in a reasonable time frame. One critical step of GWAS is to determine the threshold at which an association is termed significant. Classically the conservative Bonferroni threshold is used, which accounts for the number of statistical tests that are performed, while many recent studies try to significance thresholds that are based on the false-discovery rate (FDR) *Storey and Tibshirani, 2003*. An alternative approach are permutation-based thresholds *Che et al., 2014*. Permutation-based thresholds estimate the significance by shuffling phenotypes and genotypes before each GWAS run, thus any signal left in the data should not have a genetic cause, but might represent model mis-specifications or uneven phenotypic distributions. Typically this process is repeated hundreds to thousands of times and will lead to a distinct threshold for each phenotype analyzed *Togninalli et al., 2017*. The computational demand of permutation-based thresholds is immense, as per analysis not one, but at least hundreds of GWAS need to be performed. Here the main limitation is the pure computational demand. Thus, faster GWAS models could easily make the estimation of permutation-based thresholds the default choice.

3.2 Methods

GWAS Model

The GWAS model used for GWAS-Flow is based on a fast approximation of the linear-mixed-model described in Kang et al., 2010; Zhang et al., 2010, which estimates the variance components σ_g and σ_e only once in a null model that includes the genetic relationship matrix, but no distinct genetic markers. These components are thereafter used for the tests of each specific marker. Here, the underlying assumption is, that the ratio of these components stays constant, even if distinct genetic markers are included into the GWAS model. This holds true for nearly all markers and only markers which possess a big effect will alter this ratio slightly, where now σ_g would become smaller compared to the null model. Thus, the p-values calculated by the approximation might be a little higher (less significant) for strongly associated markers.

The GWAS-Flow Software

The GWAS-Flow software was designed to provide a fast and robust GWAS implementation that can easily handle large data and allows to perform permutations in a reasonable time frame. Traditional GWAS implementations that are implemented using Python Van Rossum and Drake Jr, 1995 or R R Core Team, 2019 cannot always meet these demands. We tried to overcome those limitations by using TensorFlow Abadi et al., 2015, a multi-language machine learning framework published and developed by Google. GWAS calculations are composed of a series of matrix computations that can be highly parallelized, and easily integrated into the architecture provided by TensorFlow. Our implementation allows both, the classical parallelization of code on multiple processors (CPUs) and the use of graphical processing units (GPUs). GWAS-Flow is written using the Python TensorFlow API. Data import is done with pandas McKinney, 2010 and/or HDF5 for Python Collette, 2013. Preprocessing of the data (e.g filtering by minor Allele count (MAC)) is performed with numpy

Oliphant, 2006. Variance components for residual and genomic effects are estimated with a slightly altered function based on the Python package *limix* Lippert et al., 2014. The GWAS model is based on the following linear mixed model that takes into account the effect of every marker with respect to the kinship:

$$Y = \beta_0 + X_i\beta_i + u + \epsilon, u \sim N(0, \sigma_g K), \epsilon \sim N(0, \sigma_e I) \quad (3.1)$$

From this LMM the residual sum of squares for marker i are calculated as described in 3.2

$$RSS_i = \sum Y - (X_i\beta_0 + I_i\beta_1) \quad (3.2)$$

The residuals are used to calculate a p-value for each marker according to an overall F-test that compares the model including a distinct genetic effect to a model without this genetic effect:

$$F = \frac{RSS_{env} - R1_{full}}{\frac{R1_{full}}{n-3}} \quad (3.3)$$

Apart from the p-values that derive from the F-distribution, GWAS-Flow also report summary statistics, such as the estimated effect size (β_i) and its standard error for each marker.

Calculation of permutation-based thresholds for GWAS

To calculate a permutation-based threshold, we essentially perform n repetitions ($n > 100$) of the GWAS on the same data with the sole difference that before each GWAS we randomize the phenotypic values. Thus any correlation between the phenotype and the genotype will be broken and indeed for over 90% of these analyses the estimated pseudo-heritability is close to zero. On the other hand, the phenotypic distribution will stay unaltered by this randomization. Hence, any remaining signal in the GWAS has to be of a non-genetic origin and could be caused by e.g. model mis-specifications. Now we take the lowest p-value (after filtering for the

desired minor allele count) for each permutation and take the 5% lowest value as the permutation-based threshold for the GWAS.

Benchmarking

For benchmarking of GWAS-Flow we used data from the *Arabidopsis* 1001 Genomes Project *Alonso-Blanco et al., 2016*. The genomic data we used were subsets between 10,000 and 100,000 markers. We chose not to include subsets that exceed 100,000 markers, because there is a linear relationship between the number of markers and the computational time demanded, as all markers are tested independently. We used phenotypic data for flowering time at ten degrees (FT10) for *A. thaliana*, published and downloaded from the AraPheno database *Seren et al., 2016*. We down- and up-sampled sets to generate phenotypes for sets between 100 and 5000 accessions. For each set of phenotypes and markers we ran 10 permutations to assess the computational time needed. All analyses have been performed with a custom R script that has been used previously *Togninalli et al., 2017*, GWAS-Flow using either a CPU or a GPU architecture and GEMMA *Zhou and Stephens, 2012*. GEMMA is a fast and efficient implementation of the mixed model that is broadly used to perform GWAS. All calculations were run on the same machine using 16 i9 virtual CPUs. The GPU version ran on an NVIDIA Tesla P100 graphic card. Additionally to the analyses of the simulated data, we compared the times required by GEMMA and both GWAS-Flow implementations for > 200 different real datasets from *A. thaliana* that have been downloaded from the AraPheno *Seren et al., 2016* database and have been analyzed with the available fully imputed genomic dataset of ca. 10 million markers, filtered for a minor allele count greater five.

3.3 Results

The two main factors influencing the computational time for GWAS are the number of markers incorporated in such an analysis and the number of different accessions, while the latter has an approximate quadratic effect in classical GWAS implementations *Zhou and Stephens, 2012*. Figure 1A shows the time demand as a function of the number of accessions used in the analysis with 10,000 markers. The quadratic increase in time demand is clearly visible for the custom R implementation, as well as for the CPU-based GWAS-Flow implementation and *GEMMA*. The GWAS-Flow implementation and *GEMMA* clearly outperforms the R implementation in general, while for a small number of accessions GWAS-Flow is slightly faster than *GEMMA*. For the GPU-based implementation the increase in run-time with larger sample sizes is much less pronounced. While for small ($< 1,000$ individuals) data, there is no benefit compared to running GWAS-Flow on CPUs or running *GEMMA*, the GPU-version clearly outperforms the other implementations if the number of accessions increases. Figure 1B shows the computational time in relation to the number of markers and a fixed amount of 2000 accessions for the two different GWAS-Flow implementations. Here, a linear relationship is visible in both cases. To show the performance of GWAS-Flow not only for simulated data, we also run both implementations on more than 200 different real datasets downloaded from the AraPheno database. Figure 1C shows the computational time demands for all analyses comparing both GWAS-Flow implementation to *GEMMA*. Here, the CPU-based GWAS-Flow performs comparable to *GEMMA*, while the GPU-based implementation outperforms both, if the number of accessions is above 500. Importantly all obtained GWAS results (p-values, beta estimates and standard errors of the beta estimates) are nearly (apart from some mathematical inaccuracies) identical between the three different implementations.

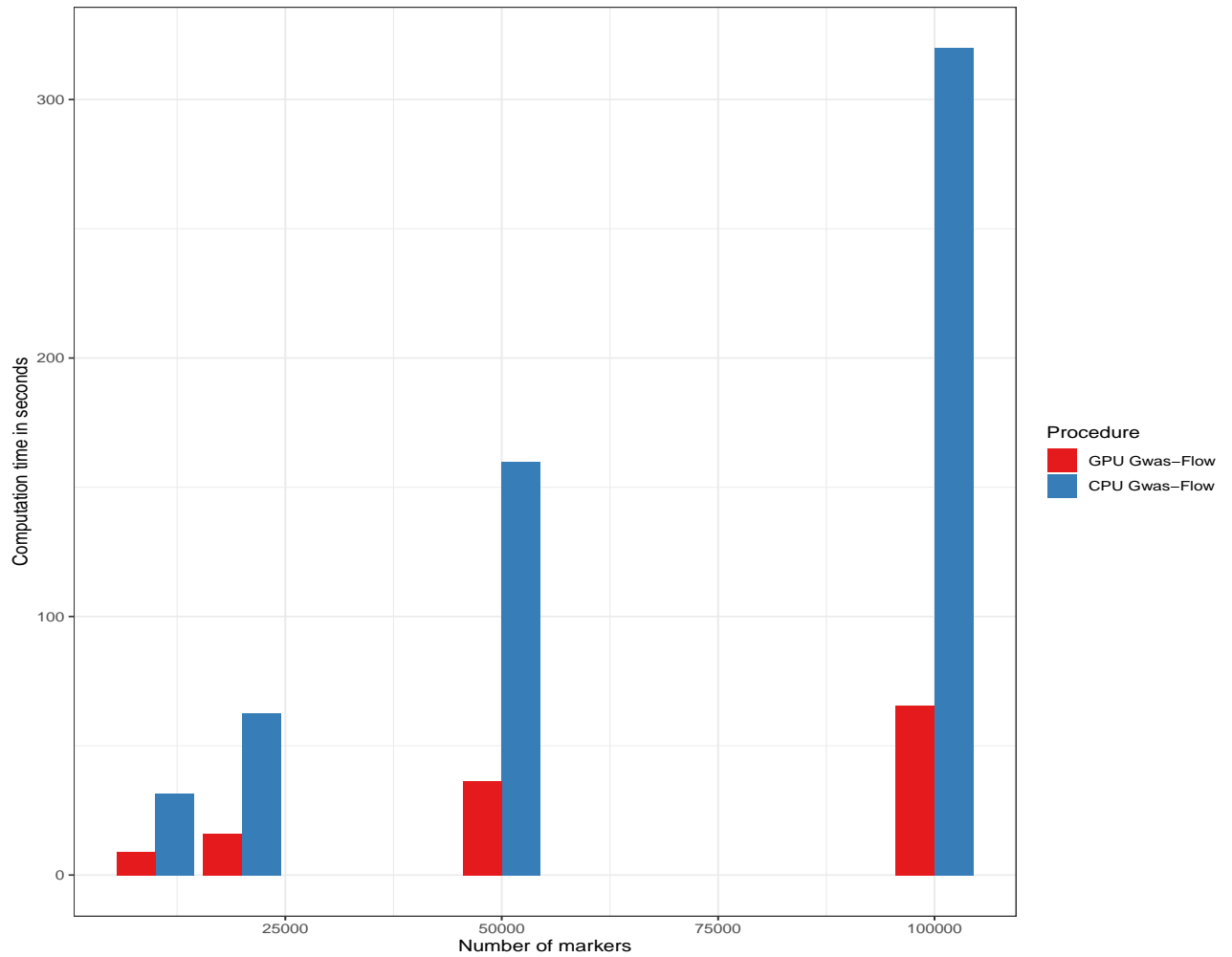


FIGURE 3.1: Computational time as a function of the number of genetic markers with constantly 2000 accessions for both GWAS-Flow versions

3.4 Disucssion

We made use of recent developments of computational architecture and software to cope with the increasing computational demand in analyzing large GWAS datasets. With GWAS-Flow we implemented both, a CPU- and a GPU-based version of the classical linear mixed model commonly used for GWAS. Both implementations outperform custom R scripts on simulated and real data. While the CPU-based version performs nearly identical compared to *GEMMA*, a commonly used GWAS implementation, the GPU-based implementation outperforms both, if the number of individuals, which have been phenotyped, increases. For analyzing big data, here the

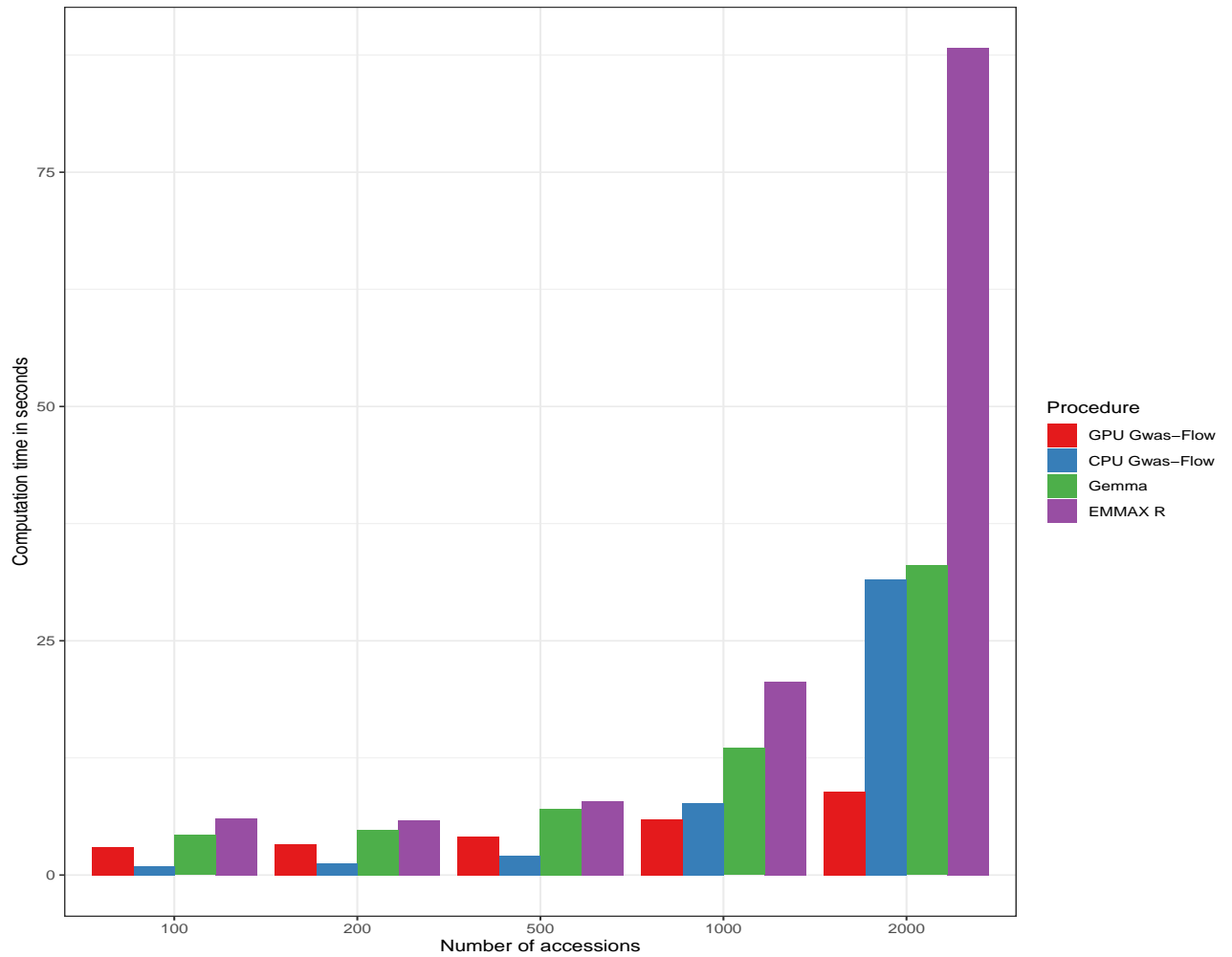


FIGURE 3.2: Computational time as a function of the number of accessions with 10000 markers each.

main limitation would be the RAM of the GPU, but as the individual test for each marker are independent, this can be easily overcome programmatically. The presented GWAS-Flow implementations are markedly faster compared to custom GWAS scripts and even outperform efficient fast implementations like *GEMMA* in terms of speed. This readily enables the use of permutation-based thresholds, as with GWAS-Flow hundred permutations can be performed in a reasonable time even for big data. Thus, it is possible for each analyzed phenotype to create a specific, permutation-based threshold that might present a more realistic scenario. Importantly the permutation-based threshold can be easily adjusted to different minor allele counts, generating different significance thresholds depending on the allele

count. This could help to distinguish false and true associations even for rare alleles. GWAS-Flow is a versatile and fast software package. Currently GWAS-Flow is and will remain under active development to make the software more versatile. This will e.g. include the compatibility with TensorFlow v2.0.0 and enable data input formats, such as PLINK *Purcell et al., 2007*. The whole framework is flexible, so it is easy to include predefined co-factors e.g to enable multi-locus models *Segura et al., 2012* or account for multi-variate models like the multi-trait mixed model *Korte et al., 2012*. Standard GWAS are good in detecting additive effects with comparably large effect sizes, but lack the ability to detect epistatic interactions and their influence on complex traits *Mckinney and Pajewski, 2012; Korte and Farlow, 2013*. To catch the effects of these gene-by-gene or SNP-by-SNP interactions, a variety of genome-wide association interaction studies (GWAIS) have been developed, thoroughly reviewed in *Ritchie and Van Steen, 2018*. Here, GWAS-Flow might provide a tool that enables to test the full pairwise interaction matrix of all SNPs. Although this might be a statistic nightmare, it now would be computationally feasible.

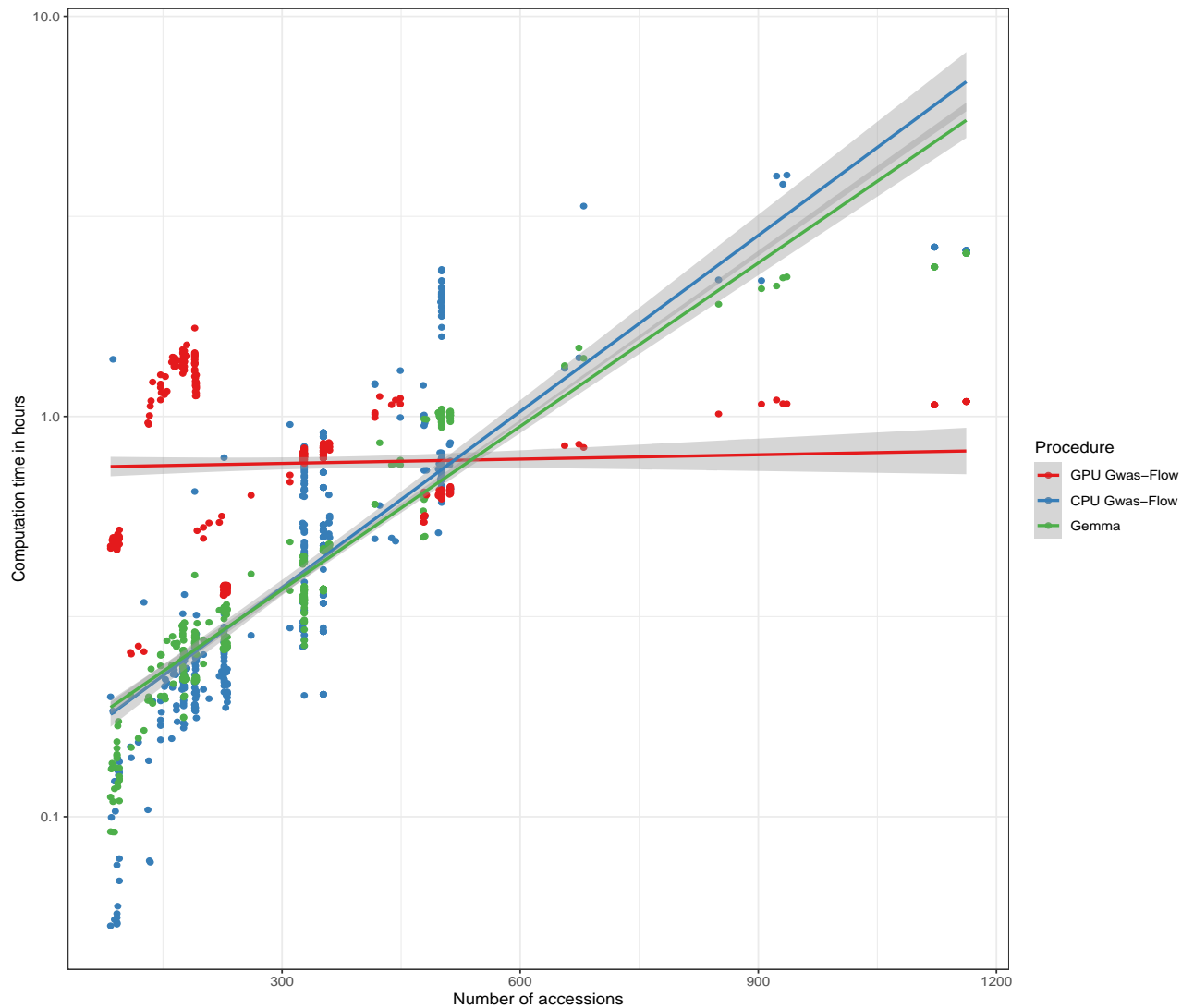


FIGURE 3.3: Comparison of the computational time for the analyses of > 200 phenotypes from *Arabidopsis thaliana* as a function of the number of accessions for GEMMA and the CPU- and GPU-based version of GWAS-Flow. GWAS was performed with a fully imputed genotype matrix containing 10.7 M markers and a minor allele filter of $MAC > 5$

4 Genomic prediction of phenotypic values of quantitative traits using artificial neural networks

4.1 Introduction

4.1.1 A brief history of machine learning

Basic perceptron model

While machine learning, neural networks, deep learning became essential tools for many applications in more recent years, their mathematical principals date back to the early 1950s and 1960s. Figure 4.1 schematically show the basic perceptron model as proposed by Rosenblatt, which was designed to mimic the information flow in biological nervous systems *Rosenblatt, 1961*

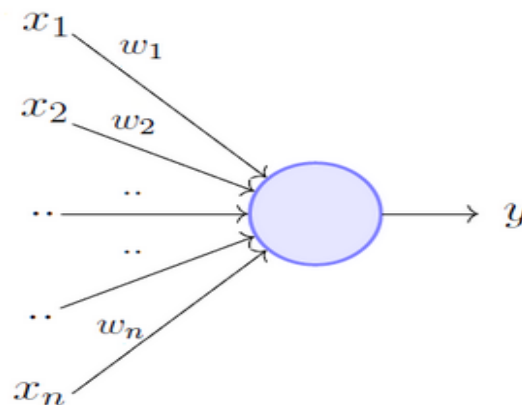


FIGURE 4.1: Basic perceptron model as proposed by Rosenblatt

This basic perceptron, which contrary to perceptrons used nowadays does not have an activation function, takes n binary inputs x_1, x_2, \dots, x_n and produces a single, likewise binary, output y after being processed by the perceptron or neuron. To achieve this Rosenblatt introduced the concept of weights which indicated a certain relative importance to the outcome of the output. w_1, w_2, \dots, w_n . The output y is determined by the weighted sum of the weights and biases $\sum_i w_i x_i$. If a certain threshold value is met the neuron is either activated and outputs 1 or not and outputs 0. This is algebraically represented in 4.1

$$0 = \text{if } \sum_i^n w_i x_i - \theta \leq 0 \quad (4.1a)$$

$$1 = \text{if } \sum_i^n w_i x_i - \theta > 0 \quad (4.1b)$$

Next to the weights w_n and the inputs x_n a third term θ is introduced in equation 4.1 which represents the activation threshold in per definition is negative. A single perceptron is a linear classifier and can only be trained on linearly separable functions and can be used as shown by Rosenblatt, 1961 to solve simple logical operations as AND, OR and not. The simple perceptron fails, due to non-linearity, to perform XOR operations as shown by Marvin and Seymour, 1969. This discovery led to a near still stance in the research of artificial neural networks in the 1970s. This time period is now often referred to as the first AI-winter. Another reason that massively hindered the applications and research of machine learning during that time, was the compared to modern times incredibly small amount of computational power available Nguyen and Widrow, 1990.

More complex decision making, like solving XOR problems, requires more complex structures than a single perceptron. Continuing the trend of mimicking human neural networks, multiple artificial neurons are stacked into layers and these layers, are connected to each other allowing communication between the many perceptrons

in a such generated network. Figure 4.2 shows schematically the basic structure of such a network, now container three types of layers. (i) the input layer, (ii) one or more hidden layers and (iii) one output layer, which in this case only consists of one neuron.

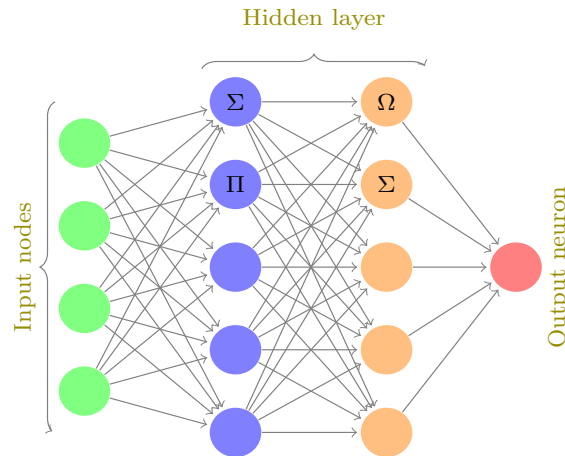


FIGURE 4.2: Schematic layout of a simple multi-layer perceptron

In the sample layout of figure 4.2 the neurons in the first column weigh the inputs and pass those the the neurons on the second layer. In this case all neurons on the first layer or connected to all neurons on the second layer, such layers are referred to fully-connected layers (FLC) , and their resulting networks are often called multi-layer perceptrons (MLP). This architecture enables the network to perform more complex calculations and result in more abstract decisions than single neurons or single layer architectures.

Activation functions

The neurons discussed so far are only capable of outputting binary results. Either 0 or 1, depending on the threshold values being met or not. For more complex estimations it is desirable that small changes in the input also result in small changes of the output. This requirement can not be met with binary outputs. Activation functions for a given node provides rules for the output in accordance to the inputs Žilinskas, 2006.

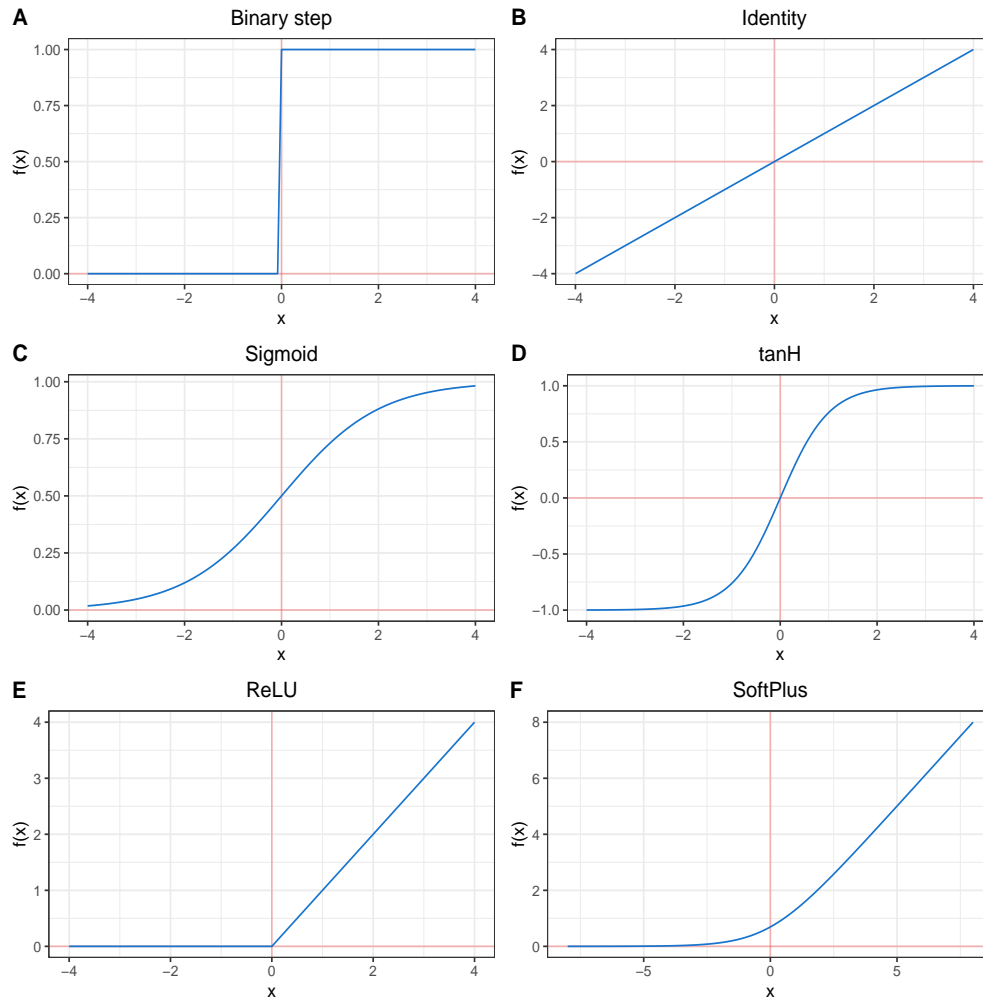


FIGURE 4.3: Popular activation functions used in neural networks. **A** Binary step activation function. **B** Identity activation function. **C** Sigmoid or logistic activation function. **D** tangens hyperbolicus activation function. **E** rectified linear units activation function . **F** SoftPlus activation function.

Figure 4.3 A shows six of the most commonly used activation functions Warner and Misra, 1996. The simplest one was introduced, is the binary step activation function equation 4.2, which properties have been discussed along the perceptron model. All other activation produce continuous outputs from any given input. Basically any mathematical function can serve as an activation function in neural nets, starting with a simple identity function 4.3 , 4.3 B. Sigmoid figure 4.3 C, equation 4.4 and tanh figure 4.3 D, equation 4.5, when $x \rightarrow \infty$ or $x \rightarrow -\infty$ they have similar properties to the binary function, but produce continuous output around 0.

$$f(x) = \sigma(x) = \begin{cases} 0 & \text{for } x < 0 \\ 1 & \text{for } x \geq 0 \end{cases} \quad (4.2)$$

$$f(x) = \sigma(x) = x \quad (4.3)$$

$$f(x) = \sigma(x) = \frac{1}{1 + e^{-x}} \quad (4.4)$$

$$f(x) = \sigma(x) = \frac{e^x - e^{-x}}{e^x + e^{-x}} \quad (4.5)$$

$$f(x) = \sigma(x) = \begin{cases} 0 & \text{for } x < 0 \\ x & \text{for } x \geq 0 \end{cases} \quad (4.6)$$

$$f(x) = \ln(1 + e^x) \quad (4.7)$$

ReLU (equation 4.6) and the softplus (equation 4.7) share similar properties as well, the latter one being a smoothed version of ReLU. Rectifiers as activation functions have been introduced in 2000s *Hahnloser et al., 2000* and have since then overtaken all others as the most popular activations functions in neural networks and deep learning today *LeCun, Bengio, and Hinton, 2015* and they have proven to be superior in deep-learning algorithms that sigmoid or logistic functions. One of the advantages leading to the superiority of ReLUs is that with randomly initialized weights only half of the ReLU neurons are activated, compared to tanh and sigmoid activation *Glorot, Bordes, and Bengio, 2011*. All activation functions shown in figure 4.3, but the binary step function, share one common property: a small change of the input weight will result in small changes in the output, while a small change of the input for the binary step function leads to either no or a complete change of the output. This property is, as described below, is an important prerequisite for networks being able to learn.

Gradient descent algorithm

Let the network shown in 4.2 be for the classification of a arbitrary phenotype like blue petals with $x_1...x_4$ on the input layers being genetic markers as features. And the output layer displaying a value from 0 to 1, meaning yes: blue petals from 0 - 0.5 and no blue petals from 0.5 to 1. To quantify how well the network performs on achieving that goal a loss function is applied *Schmidhuber, 2015*. There is a large variety of different loss functions available for neural networks like mean squared error (MSE), root mean squared error (RMSE), cross-entropy and many others. In general MSE, MSE are commonly used for regression problems, with the latter being less popular and cross-entropy also called log loss is used for binary or multi-class classification problems *Janocha and Czarnecki, 2017*. Since all problems presented in due course or regression problems, that use MSE as their loss function, this will be the only one emphasized.

$$MSE = \frac{1}{n} \sum_{i=1}^n (y_i - \tilde{y})^2 \quad (4.8)$$

Equation 4.8 shows the MSE function which is the sum of the squares of the differences of all the predicted and the real values. The same function can be rewritten with the previously used terminology of weights and biases in equation 4.8.

$$L(w, b) = \frac{1}{2n} \sum_x \|y(x) - \tilde{y}\|^2. \quad (4.9)$$

With w and b as the collection of all the weights and the biases in the network used to optimize the function $y(x)$. Giving the quadratic nature of the function the $L(w, b)$ will always be positive. And if $L(w, b) \rightarrow 0$ the loss is minimal, meaning that the real and predicted values are close together and the network found weights and biases that explain the output well.

A widely used function to find the optimum for such a loss function is gradient descent. Its objective is to find the minimum for the loss function *Bottou, 1991*. The behind gradient descent or other optimizing algorithms is start with randomly initialized weights and biases and repeatedly move them in direction Δw and Δb . This results in a change of the loss function as shown in equation 4.10, making use of partial derivatives.

$$\Delta L = \frac{\partial L}{\partial w} \Delta w + \frac{\partial L}{\partial b} \Delta b \quad (4.10)$$

Ideally ΔL is negative and the optimization algorithm found Δw and Δb that lead to a reduction of the loss. To simplify this problem let Δd be the vector of changes: $\Delta d = (\Delta w, \Delta b)^T$ and ∇L the vector of the partial derivatives: equation 4.11

$$\nabla L = \left(\frac{\partial L}{\partial w}, \frac{\partial L}{\partial b} \right)^T \quad (4.11)$$

Having defined ∇L and Δd the term 4.10 can be simplified as equation 4.12

$$\Delta C = \nabla L * \Delta d \quad (4.12)$$

Now the task of gradient descent or any other optimizer is to find Δd that results in ΔC being negative as shown in equation 4.13

$$\Delta d = -\eta \nabla L \quad (4.13)$$

In this case η is a small positive decimal number, commonly referred to as the learning rate, which usually, but not exclusively ranges from 0.1 to 0.001. However it can be larger or much smaller in some cases. Having found a way to ensure that ΔL always decreases according to equation 4.13 it is utilized to repeatedly update the gradient ∇L . To make the gradient descent algorithm efficient the learning rate η must be chosen correctly. If η is too large, the gradient ΔL might end up being larger than zero, leading to an increase of the loss, and if the step size is too small

convergence will either take too long or not take place at all *Bergstra et al., 2011*. In practical machine learning approaches different learning rates are tested. There are also algorithmic approaches. While equation 4.10 only accounts for two inputs features, it can be generalized to compute n inputs shown in equation 4.14.

$$\nabla L = \left(\frac{\partial L}{\partial w_1}, \dots, \frac{\partial L}{\partial w_n} \right)^T \quad (4.14)$$

Equation 4.15 shows the gradient descent how it is used to repetitively update the weights and biases to optimize the loss function $L(c, w)$ with w and b as the weight and bias matrices and the learning rate η . In machine learning each iterative update of the network is often called epoch or training epoch.

$$w = w_i - \eta \frac{\partial}{\partial w} L(w) \quad (4.15a)$$

$$b = b_i - \eta \frac{\partial}{\partial b} L(b) \quad (4.15b)$$

$$(4.15c)$$

Substituting the partial differentials with ∇L equation 4.15 a simplifies to:

$$w = w_i - \eta \nabla L \quad (4.16)$$

Optimizers

The previous section introduced the concept of gradient descent, an algorithm to minimize the loss function of the weights and biases of a neural network. All other optimizers introduced here, are either variations or extensions of the basic gradient descent algorithm (GD) shown in 4.15. One disadvantage of gradient descent is that

if the data sets grow larger, the demand in memory for computation increases exponentially. Taking into consideration machine learning is a popular method in big data applications this is a serious drawback. Methods to overcome that are stochastic gradient descent and mini-batch gradient descent. The idea behind the latter is to randomly divide the entity of the training data in sub-samples called mini-batches *Bottou and Bousquet, 2008*. The network is then trained iteratively over the mini batches. The batch size influences the accuracy and the training speed and is another hyperparameter which has to be tuned. If the batch size is 1 mini batch GD is also referred to as stochastic gradient descent (SGD). During the optimization process optimizers can find local minima in the cost function without being able to overcome them to find the desired global minimum. An algorithm extending GD to accelerate the search of the global minimum is momentum. Which allows the GD to speed up when the loss is decreasing and to slow down when going in the wrong direction - increasing the loss function $L(w, b)$. This is achieved by accounting for the gradient of the previous step in the calculation of the current step. This concept was introduced by *Polyak, 1964* and re-popularized alongside backpropagation learning by *Rumelhart, Hinton, and Williams, 1988*.

$$w = w_i - \eta \nabla L + \alpha \Delta w \quad (4.17)$$

Equation 4.17 shows how the momentum is mathematically represented in GD to update the weights w or likewise the biases the delta of the weights multiplied by the coefficient α - the momentum, which usually ranges from 0.1 to 0.9 and is another parameter to tuned for successful training. If the momentum is too small the GD will not be able to overcome local minima and if α is too large the loss functions tends to oscillate without finding an optimum *LeCun, Bengio, and Hinton, 2015*. For both of the momentum and the learning rate it is impractical to remain on the same level during all training epochs. Because after each epoch the loss function is either closer or further away from its global minima and depending on the distance to that

minimum it is desirable to have larger or smaller learning rates and momenta. This can be achieved with naive approaches for example using a step function to gradually decrease those values after each iteration, or to utilize algorithmic approaches *Michie, Spiegelhalter, and Taylor, 1994*. There is a large variety of optimizers trying to find optimal values for α and η and till today this field is under active research *Goodfellow, Bengio, and Courville, 2016*. Popular among those are: RMSprop *Hinton, Srivastava, and Swersky, 2012*; Nesterov momentum *Dozat, 2016*; Adadelta *Zeiler, 2012*; Adagrad *Ruder, 2016* and Adam *Kingma and Ba, 2014*. With Adam being the most widely used optimizer today. Nesterov momentum is slight change to the normal momentum capable of having huge impacts in practical applications, because it helps avoiding oscillations around the minimum by using intermediate information to adapt the momentum.

RMSProp - root mean square propagation - is a method aiming to adapt the learning rate algorithmically, by choosing η for each parameter. And lastly the wide-spread Adam optimizer combines both of the features of momentum and RMSProp and adapts the learning rate as well as the momentum iteratively *Kingma and Ba, 2014*.

Backpropagation

maybe i will leave out backpropagation ☺

Backpropagation *Rumelhart, Hinton, and Williams, 1988*

Regularization parameters

When applying the combined aforementioned algorithms and optimizers to find global minima of a loss function of a neural network a problem arises, because optimizers like Adam work “too” well. This issues is due to the fact that neural networks have 100s of thousand of free parameters to be trained, deep neural networks have billions and trillions of parameters. If training of the neural net continues for enough epochs eventually. The loss function will approach a minimum and as $L(w, b) \rightarrow 0$ the initial conclusion could be that the training was quite successful,

but when trying to apply the network trained on the training data set (TRN) to a testing data set (TST). The loss and accuracy of the prediction of TST and TST are very large or accordingly small. This phenomenon is know as overfitting and a lot of fine tuning of hyperparameters is devoted to minimizing this effect Tetko, Livingstone, and Luik, 1995. Figure 4.4 visualizes the effects of overfitting during training Goodfellow, Bengio, and Courville, 2016.

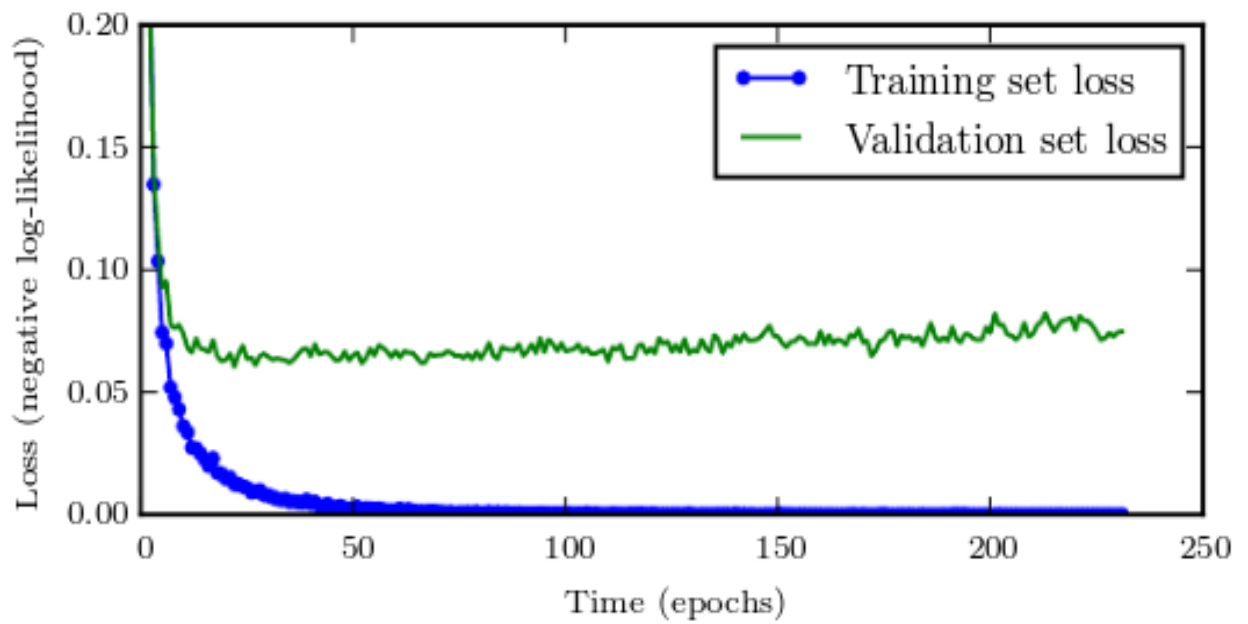


FIGURE 4.4: Learning curves showing how a loss function changes during training in the loss and validation data set. While the training loss approaches 0 the validation loss starts increasing after hitting a minimum. This effect is due to overfitting on the training data set. Figure from Goodfellow, Bengio, and Courville, 2016.

Cross-validation

A method that is used in basically every training of neural network is splitting up the data sets in multiple sub-sets. More specifically a training set (TRN) and a testing set (TST). The training set is used to minimize the loss functions and its success is evaluated on the TRN set, by comparing the predicted values \hat{y} with the

real values in TST y . For all neural nets in this study person's correlation coefficient was chosen as performance metric, as in equation 4.18 *Soper et al., 1917*.

$$\rho(y, \hat{y}) = \frac{cov(y, \hat{y})}{\sigma_y \sigma_{\hat{y}}} \quad (4.18)$$

There are other popular performance metrics, especially for classification problems, like AUC (area under the curve) and ROC (receiver operating characteristics), which basically evaluate by weighing sensitivity and specificity. In cross-validation compared to single validation the initial data set is split into TRN and TST multiple times e.g. if the ratio is 80:20 5 times, and each TRN-TST pair is evaluated individually. Sometimes it becomes necessary to use a third subset - the validation data. Because hyperparameter tuning is performed with the TRN and TST sets, a third portion of the data needs to be assessed to check whether the neural network is able to generalize on global data.

L1 and L2 loss

L1 and L2

Dropout

4.1.2 On the nature of quantitative traits

According to the omnigenic model which is an extension of the polygenic model proposed by *Boyle, Li, and Pritchard, 2017* and thoroughly reviewed in *Timpson et al., 2018* all traits or phenotypic values are influenced by a great number or all genes in the genome. Therefore resulting in traits following certain gradual statistical distributions instead of being binned in classes or even binary. Intuitively this might be contradicting with the foundation of modern Genetics - Mendel's three laws. That where derived from observations with where mainly influenced by one locus. But staying with one of Mendel's examples the round or wrinkled surfaces of peas

Pisum sativum, an assessment of a couple of thousands peas, would most likely inevitably lead to the conclusion that from the “roundest” to the “wrinkliest” pea any gradual step between those is possible and observable. Mendel’s third law of independent segregation also only holds true under certain assumptions. The most simplest one being that the traits under investigation have to be located on different linkage groups. Otherwise for the 7 traits used in Mendel’s initial studies would not have segregated independently. The odds of 7 randomly selected traits being on 7 different linkage groups are rather small, especially taking into account, that the genome of the *P. sativum* consists of only 7 chromosomes itself Kalo et al., 2004. Mendel probably new about traits not following its own laws, as well as being aware of the quantitative nature of traits such as the constitution of surfaces of peas or the color of petals. But being the pioneer of a then rather unexplored field of science, some of which big questions we fail to satisfactory answer today, he did not have the resources or the knowledge to explain behavior’s not “mendeling”, that were only able to be deciphered in later decades and centuries based on his ground-breaking work.

Initially thought to be contradicting to Mendel’s ideas Darwin proposed the concept’s of evolution due to natural selection which also introduce the idea of traits following a gradual distribution Darwin, 1859. This contrast led to a long lasting debate in the scientific community in the early 1900s, between the Mendelians and the biometricians who believed in the quantitative nature of continuous traits. This conflict has eventually been solved by Fisher’s fundamental work published in 1918 Fisher, 1919. His theories combined the then in all fields of science popular research of distributions with genomics. He he mathematically proved that traits influenced by many genes, with randomly-sampled alleles follow a continuous normal distribution in a population. While this combined the ideas of Mendel and the biometricians it opened an other long debated question of effect size and the overall architecture of complex traits. While in the theory of monogenic traits the effect size of the single gene on the trait is 1 or 100 % with an increasing number of genes

influencing a complex traits the *per se* contribution of single gene has to decrease with an increasing number of loci determining the value a given trait. In the 1990s it has been thought, that complex traits are predominantly controlled from few genes with a large to medium effect size, while others had a minimal influence *Zhang et al., 2018*.

With the upcoming popularity of GWAS as the favored method to decipher genetic architectures of traits, or having pioneered in human genetics it became clear that the majority of the effect sizes are tiny $< 1\%$ while there are very few loci which have a moderate effect on the phenotypic variance of a population with around 10% or less *Korte and Farlow, 2013, Stringer et al., 2011*. This nature of quantitative traits present great challenges to animal *Goddard and Hayes, 2009* and plant breeding *Würschum, 2012*, in further improving crop or livestock performances, as well complicating the decomposition of genomic causes for diseases like schizophrenia or autism in human medicine *De Rubeis et al., 2014, Purcell et al., 2014*.

While the complex nature of the architecture of quantitative traits provide enough challenges as is, all traits will also be influenced by the environment from which an individual originates. Therefore the distribution of trait values in a given population can be expressed as the addition of the variances of its genetic and the environmental effects **4.19**.

$$\sigma_P = \sigma_G + \sigma_E \quad (4.19)$$

The genomic and the environmental effects not only influence the phenotypic variance directly, but the environment also has an influence on gene expression methylation of DNA bases etc. and therefore the equation **4.19** needs to be extend by the variance of the gene-environment interactions $\sigma_{G \times E}$ **4.20**, *Lynch and Walsh, 1998, Walsh and Lynch, 2018*.

$$\sigma_P = \sigma_G + \sigma_E + \sigma_{G \times E} \quad (4.20)$$

Equation 4.20 shows the decomposition of the phenotypic variance, to thoroughly understand complex genetic architectures of traits the genetic variance needs to be decomposed further in its additive, dominance and epistatic components 4.21

$$\sigma_G = \sigma_A + \sigma_D + \sigma_I \quad (4.21)$$

The additive effects are caused by single, for this model mostly homozygous, loci while the variance caused by dominance effects, is caused by heterozygous loci and their resulting interactions being full-, over-, co- or underdominant. And lastly the interaction effects that are a result of two or more genes only having an impact if the involved genes co-occur in a certain state. The resulting variance is commonly known as gene-gene interactions and/or epistasis *Falconer and Mackay, 1996*. Since possible interactions in a genome can happen between additive or dominant or a combination of those loci. The variance due to interaction effects σ_I can be further dissembled in the variance resulting from additive-additive σ_{AA} dominant-dominant σ_{DD} and additive-dominant σ_{AD} terms as represented in equation 4.22.

$$\sigma_I = \sigma_{AxA} + \sigma_{DxD} + \sigma_{AxD} \quad (4.22)$$

Knowledge of the variance components involved in the expression of a trait in population, lead up to the estimation of the total influence of all genetic variances and the environmental variance on the phenotypic distribution. This concept is called heritability. The heritability of a trait H^2 accounts for the proportion of the phenotypic variance controlled by the total genetic variance as shown in equation 4.23. This is also referred to as broad sense heritability, because all genetic effects including additive, dominance and epistatic effects are included *Brooker, 1999*.

$$H^2 = \frac{\sigma_A + \sigma_D + \sigma_I}{\sigma_P} \quad (4.23)$$

The concept of narrow-sense heritability 4.24 is similar to the broad-sense heritability, but only the additive genetic effects are included in the genetic part of the equation. This differentiation is important for natural and artificial selection and thus is commonly used in evolutionary genomics and breeding. Because in diploid species each parent only passes down on a single allele of a given locus. Dominance effects or interaction effects are not commonly inherited from one parent. Therefore it is mainly the additive genetic effects of a parent that influences its offspring. While the dominance and epistatic variances are controlled by the combination of the parents Falconer and Mackay, 1996, Walsh and Lynch, 2018.

$$h^2 = \frac{\sigma_A}{\sigma_P} \quad (4.24)$$

4.1.3 Artificial selection in plant and animal breeding in the genomics era

Introduction to genomic selection

Genomic prediction has been applied to almost all relevant crop and model species. Including: *A.thaliana* Hu et al., 2015; Shen et al., 2013. Alfalfa (*Medicago sativa*) Li and Brummer, 2012; Annicchiarico et al., 2015; Li et al., 2015; Biazzi et al., 2017; Hawkins and Yu, 2018. Barley Neyhart, Lorenz, and Smith, 2019; Oakey et al., 2016; Zhong et al., 2009. Cassava (*Manihot esculenta*) Elias et al., 2018a; Elias et al., 2018b. Cauliflower (*Brassica olearacea* spp) Thorwarth, Yousef, and Schmid, 2018. Cotton (*Gossypium* spp. Gapare et al., 2018. Maze (*Zea mays*) Moeinizada et al., 2019; Allier et al., 2019; Brauner et al., 2018; Schrag et al., 2018; Schopp et al., 2017b; Sousa et al., 2017; Schopp et al., 2017a; Kadam et al., 2016; Bustos-Korts et al., 2016a; Montesinos-López et al., 2015; Owens et al., 2014; Lehermeier et al., 2014; Technow et al., 2014; Peiffer et al., 2014; Riedelsheimer et al., 2013; Guo et al., 2013; Technow, Bürger, and Melchinger, 2013; Windhausen et al., 2012; Rincant et al., 2012. Potato (*Solanum tuberosum*); Enciso-Rodriguez et al., 2018; Endelman et al., 2018. Rape seed (*Brassica naps*) Würschum, Abel, and Zhao, 2014; Jan

et al., 2016; Luo et al., 2017; Werner et al., 2018; Snowdon and Iniguez Luy, 2012; Qian, Qian, and Snowdon, 2014. Rice (*Oryza sativa*) Momen et al., 2019; Hassen et al., 2018; Xu, 2013; Grenier et al., 2015. Rye (*Secale cereale*) Auinger et al., 2016; Bernal-Vasquez et al., 2014; Wang et al., 2014; Bernal-Vasquez et al., 2017; Marulanda et al., 2016. Soybean (*Glycine max*) Stewart-Brown et al., 2019; Jarquin, Specht, and Lorenz, 2016; Xavier, Muir, and Rainey, 2016. Switchgrass (*Panicum virgatum*) Poudel et al., 2019; Ramstein and Casler, 2019; Ramstein et al., 2016. Wheat (*Triticum aestivum*) Cuevas et al., 2019a; Howard et al., 2019; Krause et al., 2019; Rincient et al., 2018; Norman et al., 2018; Belamkar et al., 2018; Ovenden et al., 2018; Sukumaran et al., 2016; Bustos-Korts et al., 2016b; Gianola et al., 2016; Crossa et al., 2016; Thavamanikumar, Dolferus, and Thumma, 2015; Lopez-Cruz et al., 2015. As well as various tree species Almeida Filho et al., 2019; Rincient et al., 2018; Kainer et al., 2018; Ratcliffe et al., 2017; El-Dien et al., 2016; Kumar et al., 2015; Jaramillo-Correa et al., 2014; Zapata-Valenzuela et al., 2013; Holliday, Wang, and Aitken, 2012; Resende et al., 2012.

Even though GS finds broad application in plant breeding it has been originally developed for the use in animal breeding Hayes and Goddard, 2010; Goddard, Hayes, and Meuwissen, 2011. The gold standard is a method known as genomic BLUP VanRaden, 2008 which utilizes a relationship matrix based on the co-occurrence of genetic markers. This method is derived from the pre-genomic era in animal breeding where the relationship matrix was constructed after pedigrees according to the best linear unbiased predictors based linear mixed models developed by Henderson, 1975. GBLUP accounts only for additive-genetic effects VanRaden, 2008. There are other methods that are able to account for more complex genomic effects that are non-additive. Popular among those are reproducing Kernel Hilbert Spaces (RKHS) Gianola and Kaam, 2008. Alternatively to linear mixed models a variety of different Bayesian methods became popular, basically differing in the degree of shrinkage of the assumed marker distribution Hayes and Goddard, 2001; Gianola et al., 2009; Habier et al., 2011; Gianola, 2013; Crossa et al., 2017a; Azodi et al., 2019.

Genomic BLUP and Bayesian methods

All methods share a common statistical obstacle which is commonly referred to as the $n \gg p$ problematic, which arises because the number n marker is usually significantly larger than the number of observations p . In practical applications it is not uncommon to have more than 100 000 markers while the number of phenotypes is no larger than 100. This does not allow to obtain genomic estimated breeding values (GEBV) by single marker regression as done by GWAS, which have highly inflated over all SNP-effects Korte and Farlow, 2013. One possible is to include effect sizes as random effects and make prior assumptions about their distribution. The difference in prior distribution is the main distinction between the methods of the Bayesian alphabet Gianola, 2013. Methods as Bayes A, Bayes B and Bayes C allow

4.1.4 Genomic selection using artificial neural networks

Genomic selection (GS) has been successfully applied in animal Gianola and Rosa, 2015, Hayes and Goddard, 2010 and plant breeding Crossa et al., 2010, Desta and Ortiz, 2014, Heffner et al., 2010, Crossa et al., 2017b as well as in medical applications, since it was first reported Hayes and Goddard, 2001. Since then the repertoire of methods for predicting phenotypic values has increased rapidly e.g. De Los Campos et al., 2009, Habier et al., 2011, Gianola, 2013, Crossa et al., 2017a. The most commonly applied methods include GULP and a set of related algorithms known as the bayesian alphabet Gianola et al., 2009. Genomic prediction in general has repeatedly been shown to outperform pedigree-based methods Crossa et al., 2010, Albrecht et al., 2011 and is nowadays used in many plant and animal breeding schemes. It has also been shown that using whole-genome information is superior to using only feature-selected markers with known QTLs for a given trait Bernardo and Yu, 2007, Heffner, Jannink, and Sorrells, 2011 in some cases. A more recent study Azodi et al., 2019 compared 11 different genomic prediction algorithms with a variety of data sets and found contradicting results, indicating that feature selection can be useful in some

cases the when the whole genome regression is performed by neural nets 1 While every new method is a valuable addition to the tool-kits for genomic selection, some fundamental problems remain unsolved, of which the $n \gg p$ problematic stands out. Usually in genomic selection settings the size of the training population (TRN) with n phenotypes is substantially smaller than the number of markers (p) *Fan, Han, and Liu, 2014*. Making the number of features immensely large, even when SNP-SNP interactions are not considered. Furthermore each marker is treated as an independent observation neglecting collinearity and linkage disequilibrium (LD). Further difficulties arise through non-additive, epistatic and dominance marker effects. The main problem with epistasis issue quantitative genetics is the almost infinite amount of different marker combinations, that cannot be represented within the size of TRN in the thousands, the same problems arises for example in GWA studies *Korte and Farlow, 2013*. With already large p the number of possible additive SNP-SNP interactions potentiates to $p^{(p-1)}$. Methods that attempt to overcome those issues are EGBLUP, using an enhanced epistatic kinship matrix and reproducing kernel Hilbert space regression (RKHS) *Jiang and Reif, 2015, Martini et al., 2017*.

In the past 10 years, due to increasing availability of high performance computational hardware with decreasing costs and parallel development of free easy-to-use software, most prominent being googles library TensorFlow *Abadi et al., 2016* and Keras *Chollet, 2015*, machine learning (ML) has experienced a renaissance. ML is a set of methods and algorithms used widely for regression and classification problems. popular among those are e.g. support vector machines, multi-layer perceptrons (MLP) and convolutional neural networks. The machine learning mimics the architecture of neural networks and are therefore commonly referred to as artificial neural networks (ANN). Those algorithms have widely been applied in many biological fields *Min, Lee, and Yoon, 2017, Lan et al., 2018, Mamoshina et al., 2016, Angermueller et al., 2016, Webb, 2018, Rampasek and Goldenberg, 2016*.

A variety of studies assessed the usability of ML in genomic prediction *González-Camacho et al., 2018, González-Camacho et al., 2016, Ogutu, Piepho, and Schulz-Streeck,*

2011, Montesinos-López et al., 2019a, Grinberg, Orhobor, and King, 2018, Cuevas et al., 2019b, Montesinos-López et al., 2019b, Ma et al., 2017, Qiu et al., 2016, González-Camacho et al., 2012 Li et al., 2018. Through all those studies the common denominator is that there is no such thing as a gold standard for genomic prediction. No single algorithm was able to outperform all the others tested in a single of those studies, let alone in all. While the generally aptitude of ML for genomic selection has been repeatedly shown, how no evidence exists that neural networks can outperform or in many cases perform on that same level as mixed-model approaches as GBLUP Hayes and Goddard, 2001. While in other fields like image classification neural networks have up to 100s of hidden layers He et al., 2016 the commonly used fully-connected networks in genomic prediction of 1 - 3 hidden layers. With 1 layer networks often being the most successful among those. Contradicting to the idea behind machine learning in genomic selection 1 hidden layer networks will be inapt to capture interactions between loci and thus only account for additive effects. As shown in Azodi et al., 2019 convolutional networks perform worse than fully-connected networks in genomic selection, which again is contradicting to other fields where convolutional layers are applied successfully, e.g natural language processing Dos Santos and Gatti, 2014 or medical image analysis Litjens et al., 2017. Instead of using convolutional layers and fully-connected layers only, as show in Pook et al 2019, we also propose to use locally-connected layer in combination with fully-connected layers. While CL and LCL are closely related they have a significant difference. While in CL weights are shared between neurons in LCLs each neuron as its own weight. This leads to a reduced number of parameters to be trained in the following FCLs, and should therefore theoretically lead to a decrease in overfitting a common problem in machine learning. To evaluate the results of Pook et al. 2019 accomplished with simulated data we used the data sets generated in the scope of the 1001 genome project of *Arabidopsis thaliana* Alonso-Blanco et al., 2016

4.2 Proof of concept for ANN-based genomic selection

Having established the quantitative architecture of traits in section 4.1.2 and the basics of machine learning and neural nets in section 4.1.1, that knowledge can be used to provide a proof of concept that neural networks are a candidate for GP. Table 4.1 provides also the possible genotypes that can be derived by two bi-allelic markers $G_1 \dots G_4$ on a fictional haploid organism. In this simulation the effect sizes for each marker β_1 and β_2 are constant with a value of 1.

TABLE 4.1: Simple simulated phenotypes and genotypes for genomic prediction with genotypes $G_1 \dots G_4$, M_1 and M_2 and phenotypes based on additive effects or *and*, *or*, *xor* logic gates.

	M_1	M_2	Y_{ADD}	Y_{AND}	Y_{OR}	Y_{XOR}
G_1	0	0	0	0	0	0
G_2	0	1	1	0	1	1
G_3	1	0	1	0	1	1
G_4	1	1	2	1	1	0

The four phenotypes Y_{ADD} , Y_{AND} , Y_{OR} and Y_{XOR} , which were derived from their respective marker effects. Y_{ADD} is a phenotype with purely additive effects. So in the nomenclature introduced in chapter 4.1.2 $\sigma_A = \sigma_G$ and $\sigma_I = 0$. Since the hypothetical organism is haploid there are dominance effects to be accounted for $\sigma_D = 0$. Since all the genetic effects are caused by additive effects and there are now environmental effects σ_E , the narrow sense heritability h^2 - equation 4.24 - and the broad sense heritability H^2 - equation 4.23 - are equally 1. The other three phenotypes are based on epistatic effects σ_I generated by passing the markers M_1 and M_2 through their respective logic gates. This theoretically results in $h^2 = 0$ and $H^2 = 1$, because there are no additive effects. For y_{AND} however $h \approx 0.5$, because there is a correlation between Y_{ADD} and Y_{AND} . In practical applications this allows

methods like GBLUP, designed to account for additive genetic effects to capture some of the epistatic effects of σ_I Vieira et al., 2017.

According to chapter 4.1.1 a single perceptron would fail to solve *xor* gates. While a network with multiple nodes and layers should be able to overcome that deficit. A relatively simple neural network with two fully-connected hidden layers with 10 and 5 nodes, was trained for the prediction of each phenotypes. To keep the simulation as possible, no regularization parameters, dropout etc. was included. The activation function was ReLU (4.6) with an Adam optimizer. The results of the prediction are shown in table 4.2.

TABLE 4.2: Results of genomic prediction from phenotypes and genotypes in table 4.1

	M_1	M_2	\hat{Y}_{ADD}	\hat{Y}_{AND}	\hat{Y}_{OR}	\hat{Y}_{XOR}
G_1	0	0	0.01	0.00	0.00	0.01
G_2	0	1	0.99	0.01	0.99	0.98
G_3	1	0	0.99	0.00	0.99	1.01
G_4	1	1	1.99	0.98	1.01	0.02

Not surprisingly, the simple network is able to solve all four phenotypes and predicting the phenotypes accurately. The task was rather easy because the training data set and the testing data set were the same, but it served the purpose of showing that neural networks are generally apt to solve different marker interactions. *In natura* those interactions and the overall genetic architecture is much more complex. Effect sizes are not constant and epistasis may be caused by interactions by more than just two markers, and with an increasing number of markers n the number of possible two-way interactions increases even more so to 2^{n-1} . Smaller interaction effects could be obscured under larger additive effects, gene-environment might have a significant influence leading to a model that does not converge.

4.3 Material

4.3.1 DH populations derived from MAZE landraces

4.3.2 A. thaliana

4.4 Methods

4.4.1 ANN

4.4.2 GBLUP

4.5 Results

4.6 Discussion

5 GWAS

5.1 Reevalulation of 463 phenotypes from the AraPheno database

5.1.1 Introduction

5.1.2 Material and Methods

5.1.3 Results

5.1.4 Results

5.1.5 Disucssion

5.2 GWAS in DH landrace populatios of maze across and within environments

5.2.1 Introduction

5.2.2 Material and Methods

5.2.3 Results

5.2.4 Results

5.2.5 Disucssion

A Source code GWAS-Flow

A.1 gwas.py

```
1 import os
2 import sys
3 import time
4 import numpy as np
5 import pandas as pd
6 import main
7 import h5py
8
9 # set defaults
10 mac_min = 1
11 batch_size = 500000
12 out_file = "results.csv"
13 m = 'phenotype_value'
14 perm = 1
15 mac_min= 6
16
17 X_file = 'gwas_sample_data/AT_geno.hdf5'
18 Y_file = 'gwas_sample_data/phenotype.csv'
19 K_file = 'gwas_sample_data/kinship_ibs_binary_mac5.h5py'
20
21
22
23 for i in range (1,len(sys.argv),2):
24     if sys.argv[i] == "-x" or sys.argv[i] == "--genotype":
25         X_file = sys.argv[i+1]
26     elif sys.argv[i] == "-y" or sys.argv[i] == "--phenotype":
27         Y_file = sys.argv[i+1]
28     elif sys.argv[i] == "-k" or sys.argv[i] == "--kinship":
```

```

29     K_file = sys.argv[i+1]
30     elif sys.argv[i] == "-m":
31         m = sys.argv[i+1]
32     elif sys.argv[i] == "-a" or sys.argv[i] == "--mac_min":
33         mac_min = int(sys.argv[i+1])
34     elif sys.argv[i] == "-bs" or sys.argv[i] == "--batch-size":
35         batch_size = int(sys.argv[i+1])
36     elif sys.argv[i] == "-p" or sys.argv[i] == "--perm":
37         perm = int(sys.argv[i+1])
38     elif sys.argv[i] == "-o" or sys.argv[i] == "--out":
39         out_file = sys.argv[i+1]
40     elif sys.argv[i] == "-h" or sys.argv[i] == "--help":
41         print("-x , --genotype :file containing marker information in
42 csv or hdf5 format of size")
43         print("-y , --phenotype: file container phenotype information
44 in csv format" )
45         print("-k , --kinship : file containing kinship matrix of size
46 k X k in csv or hdf5 format")
47         print("-m : name of columnn containing the phenotype : default
48 m = phenotype_value")
49         print("-a , --mac_min : integer specifying the minimum minor
50 allele count necessary for a marker to be included. Default a = 1"
51 )
52         print("-bs, --batch-size : integer specifying the number of
53 markers processed at once. Default -bs 500000" )
54         print("-p , --perm : single integer specifying the number of
55 permutations. Default 1 == no perm ")
56         print("-o , --out : name of output file. Default -o results.
57 csv ")
58         print("-h , --help : prints help and command line options")
59         quit()
60     else:
61         print('unknown option ' + str(sys.argv[i]))
62         quit()
63
64 print("parsed commandline args")

```

```

58
59 start = time.time()
60
61 X,K,Y_,markers = main.load_and_prepare_data(X_file,Y_file,K_file,m)
62
63
64 ## MAF filterin
65 markers_used , X , macs = main.mac_filter(mac_min,X,markers)
66
67 ## prepare
68 print("Begin performing GWAS on ", Y_file)
69
70 if perm == 1:
71     output = main.gwas(X,K,Y_,batch_size)
72     if( X_file.split(".")[ -1] == 'csv'):
73         chr_pos = np.array(list(map(lambda x : x.split("- "),
74 markers_used)))
75     else:
76         chr_reg = h5py.File(X_file,'r')['positions'].attrs['
chr_regions']
77         mk_index= np.array(range(len(markers)),dtype=int)[macs >=
mac_min]
78         chr_pos = np.array([list(map(lambda x: sum(x > chr_reg[:,1]) +
1, mk_index)), markers_used]).T
79         my_time = np.repeat((time.time()-start),len(chr_pos))
80     pd.DataFrame({
81         'chr' : chr_pos[:,0] ,
82         'pos' : chr_pos[:,1] ,
83         'pval': output[:,0] ,
84         'mac' : np.array(macs[macs >= mac_min],dtype=np.int) ,
85         'eff_size': output[:,1] ,
86         'SE' : output[:,2]}) .to_csv(out_file,index=False)
87 elif perm > 1:
88     min_pval = []
89     perm_seeds = []
90     my_time = []
91     for i in range(perm):
92         start_perm = time.time()

```

```

92     print("Running permutation ", i+1, " of ",perm)
93     my_seed = np.asscalar(np.random.randint(9999,size=1))
94     perm_seeds.append(my_seed)
95     np.random.seed(my_seed)
96     Y_perm = np.random.permutation(Y_)
97     output = main.gwas(X,K,Y_perm,batch_size)
98     min_pval.append(np.min(output[:,0]))
99     print("Elapsed time for permuatation",i+1 ," with p_min",
min_pval[i]," is",": ", round(time.time() - start_perm,2))
100     my_time.append(time.time()-start_perm)
101     pd.DataFrame({
102         'time': my_time ,
103         'seed': perm_seeds ,
104         'min_p': min_pval }).to_csv(out_file,index=False)
105
106 print("done")
107
108 end = time.time()
109 eltime = np.round(end -start,2)
110
111 if eltime <= 59:
112     print("Total time elapsed", eltime, "seconds")
113 elif eltime > 59 and eltime <= 3600:
114     print("Total time elapsed", np.round(eltime / 60,2) , "minutes")
115 elif eltime > 3600 :
116     print("Total time elapsed", np.round(eltime / 60 / 60,2), "hours"
117     )
118

```

A.2 main.py

```

1     import pandas as pd
2     import numpy as np
3     from scipy.stats import f
4     import tensorflow as tf
5     import limix
6     import herit

```

```

7   import h5py
8   import limix
9   import multiprocessing as mlt
10
11  def load_and_prepare_data(X_file,Y_file,K_file,m):
12      type_K = K_file.split(".")[1]
13      type_X = X_file.split(".")[1]
14
15      ## load and preprocess genotype matrix
16      Y = pd.read_csv(Y_file,engine='python').sort_values(['accession_id',
17      '']).groupby('accession_id').mean()
18      Y = pd.DataFrame({'accession_id' : Y.index, 'phenotype_value' : Y
19      [m]})
20
21      if type_X == 'hdf5' or type_X == 'h5py' :
22          SNP = h5py.File(X_file,'r')
23          markers= np.asarray(SNP['positions'])
24          acc_X = np.asarray(SNP['accessions'][:],dtype=np.int)
25      elif type_X == 'csv' :
26          X = pd.read_csv(X_file,index_col=0)
27          markers = X.columns.values
28          acc_X = X.index
29          X = np.asarray(X,dtype=np.float32)/2
30      else :
31          sys.exit("Only hdf5, h5py and csv files are supported")
32
33      if type_K == 'hdf5' or type_K == 'h5py':
34          k = h5py.File(K_file,'r')
35          acc_K = np.asarray(k['accessions'][:],dtype=np.int)
36      elif type_K == 'csv':
37          k = pd.read_csv(K_file,index_col=0)
38          acc_K = k.index
39          k = np.array(k, dtype=np.float32)
40
41      acc_Y = np.asarray(Y[['accession_id']]).flatten()
42      acc_isec = [isec for isec in acc_X if isec in acc_Y]
43
44      idx_acc = list(map(lambda x: x in acc_isec, acc_X))
45      idy_acc = list(map(lambda x: x in acc_isec, acc_Y))

```

```

43     idk_acc = list(map(lambda x: x in acc_isec, acc_K))
44
45     Y_ = np.asarray(Y.drop('accession_id',1),dtype=np.float32)[idy_acc
46     ,:]
47
48     if type_X == 'hdf5' or type_X == 'h5py' :
49         X = np.asarray(SNP['snps'][0:(len(SNP['snps'])+1)],dtype=np.
50         float32)[: ,idx_acc].T
51         X = X[np.argsort(acc_X[idx_acc]),:]
52         k1 = np.asarray(k['kinship'][:])[idk_acc,:]
53         K = k1[:,idk_acc]
54         K = K[np.argsort(acc_X[idx_acc]),:]
55         K = K[:,np.argsort(acc_X[idx_acc])]
56     else:
57         X = X[idx_acc,:]
58         k1 = k[idk_acc,:]
59         K = k1[:,idk_acc]
60
61     print("data has been imported")
62     return X,K,Y_,markers
63
64 def mac_filter(mac_min, X, markers):
65     ac1 = np.sum(X,axis=0)
66     ac0 = X.shape[0] - ac1
67     macs = np.minimum(ac1,ac0)
68     markers_used = markers[macs >= mac_min]
69     X = X[:,macs >= mac_min]
70     return markers_used, X, macs
71
72 def gwas(X,K,Y,batch_size):
73     n_marker = X.shape[1]
74     n = len(Y)
75     ## REML
76     K_stand = (n-1)/np.sum((np.identity(n) - np.ones((n,n))/n) * K) *
77     K

```

```

77     vg, delta, ve = herit.estimate(Y,"normal",K_stand,verbose = False
    )
78     print(" Pseudo-heritability is " , vg / (ve + vg + delta))
79     print(" Performing GWAS on ", n , " phenotypes and ", n_marker , "
    markers")
80     ## Transform kinship-matrix, phenotypes and estimate intercpt
81     Xo = np.ones(K.shape[0]).flatten()
82     M = np.transpose(np.linalg.inv(np.linalg.cholesky(vg * K_stand +
    ve * np.identity(n))))).astype(np.float32)
83     Y_t = np.sum(np.multiply(np.transpose(M),Y),axis=1).astype(np.
    float32)
84     int_t = np.sum(np.multiply(np.transpose(M),np.ones(n)),axis=1).
    astype(np.float32)
85     ## EMMAX Scan
86     RSS_env = (np.linalg.lstsq(np.reshape(int_t,(n,-1)) , np.reshape(
    Y_t,(n,-1))))[1]).astype(np.float32)
87     ## calculate betas and se of betas
88     def stderr(a,M,Y_t2d,int_t):
89         x = tf.stack((int_t,tf.squeeze(tf.matmul(M.T,tf.reshape(a,(n
    ,-1))))),axis=1)
90         coeff = tf.matmul(tf.matmul(tf.linalg.inv(tf.matmul(tf.
    transpose(x),x)),tf.transpose(x)),Y_t2d)
91         SSE = tf.reduce_sum(tf.math.square(tf.math.subtract(Y_t,tf.
    math.add(tf.math.multiply(x[:,1],coeff[0,0]),tf.math.multiply(x
   [:,1],coeff[1,0])))))
92         SE = tf.math.sqrt(SSE/(471-(1+2)))
93         StdERR = tf.sqrt(tf.linalg.diag_part(tf.math.multiply(SE , tf
    .linalg.inv(tf.matmul(tf.transpose(x),x))))) [1]
94         return tf.stack((coeff[1,0],StdERR))
95     ## calculate residual sum squares
96     def rss(a,M,y,int_t):
97         x_t = tf.reduce_sum(tf.math.multiply(M.T,a),axis=1)
98         lm_res = tf.linalg.lstsq(tf.transpose(tf.stack((int_t,x_t),
    axis=0)),Y_t2d)
99         lm_x = tf.concat((tf.squeeze(lm_res),x_t),axis=0)
100        return tf.reduce_sum(tf.math.square(tf.math.subtract(tf.
    squeeze(Y_t2d),tf.math.add(tf.math.multiply(lm_x[1],lm_x[2:]), tf.
    multiply(lm_x[0],int_t)))))

```

```

101     ## loop over the batches
102     for i in range(int(np.ceil(n_marker/batch_size))):
103         tf.reset_default_graph()
104         if n_marker < batch_size:
105             X_sub = X
106         else:
107             lower_limit = batch_size * i
108             upper_limit = batch_size * i + batch_size
109             if upper_limit <= n_marker :
110                 X_sub = X[:,lower_limit:upper_limit]
111                 print("Working on markers ", lower_limit , " to ",
upper_limit, " of ", n_marker )
112             else:
113                 X_sub = X[:,lower_limit:]
114                 print("Working on markers ", lower_limit , " to ",
n_marker, " of ", n_marker )
115             config = tf.ConfigProto()
116             n_cores = mlt.cpu_count()
117             config.intra_op_parallelism_threads = n_cores
118             config.inter_op_parallelism_threads = n_cores
119             sess = tf.Session(config=config)
120             Y_t2d = tf.cast(tf.reshape(Y_t,(n,-1)),dtype=tf.float32)
121             y_tensor = tf.convert_to_tensor(Y_t,dtype = tf.float32)
122             StdERR = tf.map_fn(lambda a : stderr(a,M,Y_t2d,int_t), X_sub.T
)
123             R1_full = tf.map_fn(lambda a: rss(a,M,Y_t2d,int_t), X_sub.T)
124             F_1 = tf.divide(tf.subtract(RSS_env, R1_full),tf.divide(
R1_full,(n-3)))
125             if i == 0 :
126                 output = sess.run(tf.concat([tf.reshape(F_1,(X_sub.shape
[1],-1)),StdERR],axis=1))
127             else :
128                 tmp = sess.run(tf.concat([tf.reshape(F_1,(X_sub.shape
[1],-1)),StdERR],axis=1))
129                 output = np.append(output,tmp,axis=0)
130             sess.close()
131             F_dist = output[:,0]
132             pval = 1 - f.cdf(F_dist,1,n-3)

```



```

133     output[:,0] = pval
134     return output
135
136
137

```

A.3 herit.py

```

1
2 def estimate(y, lik, K, M=None, verbose=True):
3     from numpy_sugar.linalg import economic_qs
4     from numpy import pi, var, diag
5     from glimix_core.glmm import GLMMExpFam
6     from glimix_core.lmm import LMM
7     from limix._data._assert import assert_likelihoood
8     from limix._data import normalize_likelihoood, conform_dataset
9     from limix.qtl._assert import assert_finite
10    from limix._display import session_block, session_line
11    lik = normalize_likelihoood(lik)
12    lik_name = lik[0]
13    with session_block("Heritability analysis", disable=not verbose):
14        with session_line("Normalising input...", disable=not verbose):
15            :
16                data = conform_dataset(y, M=M, K=K)
17                y = data["y"]
18                M = data["M"]
19                K = data["K"]
20                assert_finite(y, M, K)
21                if K is not None:
22                    # K = K / diag(K).mean()
23                    QS = economic_qs(K)
24                else:
25                    QS = None
26                if lik_name == "normal":
27                    method = LMM(y.values, M.values, QS, restricted=True)
28                    method.fit(verbose=verbose)
29                else:
30                    method = GLMMExpFam(y, lik, M.values, QS, n_int=500)

```

```
30         method.fit(verbose=verbose, factr=1e6, pgtol=1e-3)
31     g = method.scale * (1 - method.delta)
32     e = method.scale * method.delta
33     if lik_name == "bernoulli":
34         e += pi * pi / 3
35     v = var(method.mean())
36     return g , v , e
```

Bibliography

- Abadi, Martín et al. (2015). *TensorFlow: Large-Scale Machine Learning on Heterogeneous Systems*. Software available from tensorflow.org. URL: <https://www.tensorflow.org/>.
- Abadi, Martín et al. (2016). “TensorFlow: A System for Large-scale Machine Learning”. In: *Proceedings of the 12th USENIX Conference on Operating Systems Design and Implementation*. OSDI’16. Savannah, GA, USA: USENIX Association, pp. 265–283. ISBN: 978-1-931971-33-1. URL: <http://dl.acm.org/citation.cfm?id=3026877.3026899>.
- Albrecht, Theresa et al. (2011). “Genome-based prediction of testcross values in maize”. In: *Theoretical and Applied Genetics* 123.2, p. 339.
- Allier, Antoine et al. (2019). “Usefulness Criterion and post-selection Parental Contributions in Multi-parental Crosses: Application to Polygenic Trait Introgression”. In: *G3: Genes, Genomes, Genetics* 9.5, pp. 1469–1479.
- Almeida Filho, Janeo Eustáquio de et al. (2019). “Genomic Prediction of Additive and Non-additive Effects Using Genetic Markers and Pedigrees”. In: *G3: Genes, Genomes, Genetics* 9.8, pp. 2739–2748. DOI: [10.1534/g3.119.201004](https://doi.org/10.1534/g3.119.201004). URL: <https://doi.org/10.1534/g3.119.201004>.
- Alonso-Blanco, Carlos et al. (2016). “1,135 genomes reveal the global pattern of polymorphism in *Arabidopsis thaliana*”. In: *Cell* 166.2, pp. 481–491.
- Angermueller, Christof et al. (2016). “Deep learning for computational biology”. In: *Molecular systems biology* 12.7, p. 878.
- Ankenbrand, Markus et al. (Jan. 2018). “chloroExtractor: extraction and assembly of the chloroplast genome from whole genome shotgun data”. In: *The Journal of Open Source Software* 3.21, p. 464. ISSN: 2475-9066. DOI: [10.21105/joss.00464](https://doi.org/10.21105/joss.00464). URL: <http://joss.theoj.org/papers/10.21105/joss.00464>.

- Ankenbrand, Markus J. and Frank Förster (Apr. 2019). *Simulated Arabidopsis thaliana sequencing datasets for chloroplast assembler benchmarking*. DOI: [10.5281/zenodo.2622875](https://doi.org/10.5281/zenodo.2622875). URL: <https://doi.org/10.5281/zenodo.2622875>.
- Ankenbrand, Markus J. et al. (June 2017). "AliTV—interactive visualization of whole genome comparisons". In: *PeerJ Computer Science* 3, e116. ISSN: 2376-5992. DOI: [10.7717/peerj-cs.116](https://doi.org/10.7717/peerj-cs.116). URL: <https://doi.org/10.7717/peerj-cs.116>.
- Annicchiarico, Paolo et al. (2015). "Accuracy of genomic selection for alfalfa biomass yield in different reference populations". In: *BMC genomics* 16.1, p. 1020.
- Archibald, John M (2015). "Endosymbiosis and eukaryotic cell evolution". In: *Current Biology* 25.19, R911–R921.
- Auinger, Hans-Jürgen et al. (2016). "Model training across multiple breeding cycles significantly improves genomic prediction accuracy in rye (*Secale cereale* L.)" In: *Theoretical and Applied Genetics* 129.11, pp. 2043–2053.
- Azodi, Christina B et al. (2019). "Benchmarking algorithms for genomic prediction of complex traits". In: *bioRxiv*, p. 614479.
- Bakker, Freek T. et al. (Jan. 2016). "Herbarium genomics: plastome sequence assembly from a range of herbarium specimens using an Iterative Organelle Genome Assembly pipeline". en. In: *Biological Journal of the Linnean Society* 117.1, pp. 33–43. ISSN: 00244066. DOI: [10.1111/bij.12642](https://doi.org/10.1111/bij.12642). URL: <https://academic.oup.com/biolinnean/article-lookup/doi/10.1111/bij.12642>.
- Belamkar, Vikas et al. (2018). "Genomic Selection in Preliminary Yield Trials in a Winter Wheat Breeding Program". In: *G3: Genes, Genomes, Genetics* 8.8, pp. 2735–2747. DOI: [10.1534/g3.118.200415](https://doi.org/10.1534/g3.118.200415). URL: <https://doi.org/10.1534>.
- Bendich, Arnold J. (1987). "Why do chloroplasts and mitochondria contain so many copies of their genome?" In: *BioEssays* 6.6, pp. 279–282. DOI: [10.1002/bies.950060608](https://doi.org/10.1002/bies.950060608). eprint: <https://onlinelibrary.wiley.com/doi/pdf/10.1002/bies.950060608>. URL: <https://onlinelibrary.wiley.com/doi/abs/10.1002/bies.950060608>.
- Berardini, Tanya Z. et al. (2015). "The *Arabidopsis* information resource: Making and mining the "gold standard" annotated reference plant genome". In: *genesis* 53.8, pp. 474–485. DOI: [10.1002/dvg.22877](https://doi.org/10.1002/dvg.22877). eprint: <https://onlinelibrary.wiley.com/doi/abs/10.1002/dvg.22877>.

- [com/doi/pdf/10.1002/dvg.22877](https://doi.org/10.1002/dvg.22877). URL: <https://onlinelibrary.wiley.com/doi/abs/10.1002/dvg.22877>.
- Bergstra, James S et al. (2011). "Algorithms for hyper-parameter optimization". In: *Advances in neural information processing systems*, pp. 2546–2554.
- Bernal-Vasquez, Angela-Maria et al. (2014). "The importance of phenotypic data analysis for genomic prediction-a case study comparing different spatial models in rye". In: *BMC genomics* 15.1, p. 646.
- Bernal-Vasquez, Angela-Maria et al. (2017). "Genomic prediction in early selection stages using multi-year data in a hybrid rye breeding program". In: *BMC genetics* 18.1, p. 51.
- Bernardo, Rex and Jianming Yu (2007). "Prospects for genomewide selection for quantitative traits in maize". In: *Crop Science* 47.3, pp. 1082–1090.
- Biazzi, Elisa et al. (2017). "Genome-wide association mapping and genomic selection for alfalfa (*Medicago sativa*) forage quality traits". In: *PLoS One* 12.1, e0169234.
- Bock, Ralph (2017). "Witnessing genome evolution: experimental reconstruction of endosymbiotic and horizontal gene transfer". In: *Annual review of genetics* 51, pp. 1–22.
- Bottou, Léon (1991). "Stochastic gradient learning in neural networks". In: *Proceedings of Neuro-Nimes* 91.8, p. 12.
- Bottou, Léon and Olivier Bousquet (2008). "The Tradeoffs of Large Scale Learning". In: *Advances in Neural Information Processing Systems 20 (NIPS 2007)*. Ed. by J.C. Platt et al. NIPS Foundation (<http://books.nips.cc>), pp. 161–168. URL: <http://leon.bottou.org/papers/bottou-bousquet-2008>.
- Boyle, Evan A, Yang I Li, and Jonathan K Pritchard (2017). "An expanded view of complex traits: from polygenic to omnigenic". In: *Cell* 169.7, pp. 1177–1186.
- Brauner, Pedro C et al. (2018). "Genomic prediction within and among doubled-haploid libraries from maize landraces". In: *Genetics* 210.4, pp. 1185–1196.
- Brooker, Robert J (1999). *Genetics: analysis & principles*. Addison-Wesley Reading, MA.
- Bustos-Korts, Daniela et al. (2016a). "Improvement of predictive ability by uniform coverage of the target genetic space". In: *G3: Genes, Genomes, Genetics* 6.11, pp. 3733–3747.

- Bustos-Korts, Daniela et al. (2016b). "Improvement of Predictive Ability by Uniform Coverage of the Target Genetic Space". In: *G3: Genes, Genomes, Genetics* 6.11, pp. 3733–3747. DOI: [10.1534/g3.116.035410](https://doi.org/10.1534/g3.116.035410). URL: <https://doi.org/10.1534>.
- Chan, Cheong Xin and Mark A. Ragan (2013). "Next-generation phylogenomics". In: *Biology direct* 8, pp. 3–3. ISSN: 1745-6150. DOI: [10.1186/1745-6150-8-3](https://doi.org/10.1186/1745-6150-8-3). URL: <https://www.ncbi.nlm.nih.gov/pubmed/23339707>.
- Chat, J. et al. (July 2002). "A Case of Chloroplast Heteroplasmy in Kiwifruit (*Actinidia deliciosa*) That Is Not Transmitted During Sexual Reproduction". In: *Journal of Heredity* 93.4, pp. 293–300. ISSN: 0022-1503. DOI: [10.1093/jhered/93.4.293](https://doi.org/10.1093/jhered/93.4.293). eprint: <http://oup.prod.sis.lan/jhered/article-pdf/93/4/293/6454216/293.pdf>. URL: <https://doi.org/10.1093/jhered/93.4.293>.
- Che, Ronglin et al. (2014). "An adaptive permutation approach for genome-wide association study: evaluation and recommendations for use". In: *BioData mining* 7.1, p. 9.
- Chollet, François et al. (2015). *Keras*. <https://keras.io>.
- Coissac, Eric et al. (2016). "From barcodes to genomes: extending the concept of DNA barcoding". In: *Molecular Ecology* 25.7, pp. 1423–1428. ISSN: 1365-294X. DOI: [10.1111/mec.13549](https://doi.org/10.1111/mec.13549). URL: <https://onlinelibrary.wiley.com/doi/abs/10.1111/mec.13549> (visited on 05/16/2019).
- Collette, Andrew (2013). *Python and HDF5*. O'Reilly.
- Corriveau, Joseph L. and Annette W. Coleman (1988). "Rapid Screening Method to Detect Potential Biparental Inheritance of Plastid DNA and Results for Over 200 Angiosperm Species". In: *American Journal of Botany* 75.10, pp. 1443–1458. ISSN: 00029122, 15372197. URL: <http://www.jstor.org/stable/2444695>.
- Crossa, José et al. (2010). "Prediction of genetic values of quantitative traits in plant breeding using pedigree and molecular markers". In: *Genetics*.
- Crossa, José et al. (2016). "Genomic Prediction of Gene Bank Wheat Landraces". In: *G3: Genes, Genomes, Genetics* 6.7, pp. 1819–1834. DOI: [10.1534/g3.116.029637](https://doi.org/10.1534/g3.116.029637). URL: <https://doi.org/10.1534>.
- Crossa, José et al. (2017a). "Genomic selection in plant breeding: Methods, models, and perspectives". In: *Trends in plant science*.

- Crossa, José et al. (2017b). "Genomic selection in plant breeding: methods, models, and perspectives". In: *Trends in plant science* 22.11, pp. 961–975.
- Cuevas, Jaime et al. (2019a). "Deep Kernel for Genomic and Near Infrared Predictions in Multi-environment Breeding Trials". In: *G3: Genes, Genomes, Genetics* 9.9, pp. 2913–2924. DOI: [10.1534/g3.119.400493](https://doi.org/10.1534/g3.119.400493). URL: <https://doi.org/10.1534>.
- Cuevas, Jaime et al. (2019b). "Deep Kernel for Genomic and Near Infrared Predictions in Multi-environment Breeding Trials". In: *G3: Genes, Genomes, Genetics* 9.9, pp. 2913–2924.
- Daniell, Henry et al. (June 23, 2016). "Chloroplast genomes: diversity, evolution, and applications in genetic engineering". In: *Genome Biology* 17. ISSN: 1474-7596. DOI: [10.1186/s13059-016-1004-2](https://www.ncbi.nlm.nih.gov/pmc/articles/PMC4918201/). URL: <https://www.ncbi.nlm.nih.gov/pmc/articles/PMC4918201/> (visited on 05/20/2019).
- Darwin, Charles (1859). *On the Origin of Species by Means of Natural Selection. or the Preservation of Favored Races in the Struggle for Life*. London: Murray.
- De Los Campos, Gustavo et al. (2009). "Predicting quantitative traits with regression models for dense molecular markers and pedigree". In: *Genetics* 182.1, pp. 375–385.
- De Rubeis, Silvia et al. (2014). "Synaptic, transcriptional and chromatin genes disrupted in autism". In: *Nature* 515.7526, p. 209.
- Deiner, Kristy et al. (2017). "Environmental DNA metabarcoding: Transforming how we survey animal and plant communities". In: *Molecular Ecology* 26.21, pp. 5872–5895. ISSN: 1365-294X. DOI: [10.1111/mec.14350](https://onlinelibrary.wiley.com/doi/abs/10.1111/mec.14350). URL: <https://onlinelibrary.wiley.com/doi/abs/10.1111/mec.14350> (visited on 05/21/2019).
- Desta, Zeratsion Abera and Rodomiro Ortiz (2014). "Genomic selection: genome-wide prediction in plant improvement". In: *Trends in plant science* 19.9, pp. 592–601.
- Dierckxsens, Nicolas, Patrick Mardulyn, and Guillaume Smits (Feb. 28, 2017). "NOVO-Plasty: de novo assembly of organelle genomes from whole genome data". In: *Nucleic Acids Research* 45.4, e18–e18. ISSN: 0305-1048. DOI: [10.1093/nar/gkw955](https://academic.oup.com/nar/article/45/4/e18/2290925). URL: <https://academic.oup.com/nar/article/45/4/e18/2290925> (visited on 01/26/2018).

- Docker Hub Group for Benchmark Project. URL: <https://cloud.docker.com/u/chloroextractorteam/>.
- Dos Santos, Cicero and Maira Gatti (2014). "Deep convolutional neural networks for sentiment analysis of short texts". In: *Proceedings of COLING 2014, the 25th International Conference on Computational Linguistics: Technical Papers*, pp. 69–78.
- Dozat, Timothy (2016). "Incorporating nesterov momentum into adam". In: *El-Dien, Omnia Gamal et al. (2016). "Implementation of the Realized Genomic Relationship Matrix to Open-Pollinated White Spruce Family Testing for Disentangling Additive from Nonadditive Genetic Effects". In: G3: Genes, Genomes, Genetics 6.3, pp. 743–753. DOI: 10.1534/g3.115.025957. URL: https://doi.org/10.1534.*
- Elias, Ani A et al. (2018a). "Improving genomic prediction in cassava field experiments by accounting for interplot competition". In: *G3: Genes, Genomes, Genetics 8.3, pp. 933–944.*
- (2018b). "Improving genomic prediction in cassava field experiments using spatial analysis". In: *G3: Genes, Genomes, Genetics 8.1, pp. 53–62.*
- Enciso-Rodriguez, Felix et al. (2018). "Genomic selection for late blight and common scab resistance in tetraploid potato (*Solanum tuberosum*)". In: *G3: Genes, Genomes, Genetics 8.7, pp. 2471–2481.*
- Endelman, Jeffrey B. et al. (Mar. 2018). "Genetic Variance Partitioning and Genome-Wide Prediction with Allele Dosage Information in Autotetraploid Potato". In: *Genetics 209.1, pp. 77–87. DOI: 10.1534/genetics.118.300685. URL: https://doi.org/10.1534/genetics.118.300685.*
- Falconer, DS and TFC Mackay (1996). "Introduction to quantitative genetics. 1996". In: *Harlow, Essex, UK: Longmans Green 3.*
- Fan, Jianqing, Fang Han, and Han Liu (2014). "Challenges of big data analysis". In: *National science review 1.2, pp. 293–314.*
- Fisher, Ronald A (1919). "XV.—The correlation between relatives on the supposition of Mendelian inheritance." In: *Earth and Environmental Science Transactions of the Royal Society of Edinburgh 52.2, pp. 399–433.*

- Förster, Frank and Markus J. Ankenbrand (May 2019). *chloroExtractorTeam/benchmark: Benchmark container setup v2.0.1*. DOI: [10.5281/zenodo.2628061](https://doi.org/10.5281/zenodo.2628061). URL: <https://doi.org/10.5281/zenodo.2628061>.
- Freudenthal, Jan A. et al. (2019a). “GWAS-Flow: A GPU accelerated framework for efficient permutation based genome-wide association studies”. In: DOI: [10.1101/783100](https://doi.org/10.1101/783100). URL: <https://doi.org/10.1101/783100>.
- Freudenthal, Jan A et al. (2019b). “The landscape of chloroplast genome assembly tools”. In: *bioRxiv*, p. 665869.
- Fuentes, Ignacia et al. (2014). “Horizontal genome transfer as an asexual path to the formation of new species”. In: *Nature* 511.7508, p. 232.
- Gapare, Washington et al. (2018). “Historical Datasets Support Genomic Selection Models for the Prediction of Cotton Fiber Quality Phenotypes Across Multiple Environments”. In: *G3: Genes, Genomes, Genetics* 8.5, pp. 1721–1732.
- Gianola, Daniel (2013). “Priors in whole-genome regression: the Bayesian alphabet returns”. In: *Genetics* 194.3, pp. 573–596.
- Gianola, Daniel and Johannes BCHM van Kaam (2008). “Reproducing kernel Hilbert spaces regression methods for genomic assisted prediction of quantitative traits”. In: *Genetics* 178.4, pp. 2289–2303.
- Gianola, Daniel and Guilherme JM Rosa (2015). “One hundred years of statistical developments in animal breeding”. In: *Annu. Rev. Anim. Biosci.* 3.1, pp. 19–56.
- Gianola, Daniel et al. (2009). “Additive genetic variability and the Bayesian alphabet”. In: *Genetics* 183.1, pp. 347–363.
- Gianola, Daniel et al. (2016). “Genome-Wide Association Studies with a Genomic Relationship Matrix: A Case Study with Wheat and Arabidopsis”. In: *G3: Genes, Genomes, Genetics* 6.10, pp. 3241–3256. DOI: [10.1534/g3.116.034256](https://doi.org/10.1534/g3.116.034256). URL: <https://doi.org/10.1534/g3.116.034256>.
- GitHub Repository for Benchmark Project. URL: <https://github.com/chloroExtractorTeam/benchmark>.
- Glorot, Xavier, Antoine Bordes, and Yoshua Bengio (2011). “Deep sparse rectifier neural networks”. In: *Proceedings of the fourteenth international conference on artificial intelligence and statistics*, pp. 315–323.

- Goddard, Michael E and Ben J Hayes (2009). "Mapping genes for complex traits in domestic animals and their use in breeding programmes". In: *Nature Reviews Genetics* 10.6, p. 381.
- Goddard, Michael E, Ben J Hayes, and Theo HE Meuwissen (2011). "Using the genomic relationship matrix to predict the accuracy of genomic selection". In: *Journal of animal breeding and genetics* 128.6, pp. 409–421.
- González-Camacho, JM et al. (2012). "Genome-enabled prediction of genetic values using radial basis function neural networks". In: *Theoretical and Applied Genetics* 125.4, pp. 759–771.
- González-Camacho, Juan Manuel et al. (2016). "Genome-enabled prediction using probabilistic neural network classifiers". In: *BMC genomics* 17.1, p. 208.
- González-Camacho, Juan Manuel et al. (2018). "Applications of machine learning methods to genomic selection in breeding wheat for rust resistance". In: *The plant genome* 11.2.
- Goodfellow, Ian, Yoshua Bengio, and Aaron Courville (2016). *Deep learning*. MIT press.
- Green, Beverley R. (2011). "Chloroplast genomes of photosynthetic eukaryotes". In: *The Plant Journal* 66.1, pp. 34–44. ISSN: 1365-313X. DOI: [10.1111/j.1365-313X.2011.04541.x](https://doi.org/10.1111/j.1365-313X.2011.04541.x). URL: <https://onlinelibrary.wiley.com/doi/abs/10.1111/j.1365-313X.2011.04541.x> (visited on 05/16/2019).
- Grenier, Cécile et al. (2015). "Accuracy of genomic selection in a rice synthetic population developed for recurrent selection breeding". In: *PloS one* 10.8, e0136594.
- Grinberg, Nastasiya F, Oghenejokpeme I Orhobor, and Ross D King (2018). "An Evaluation of Machine-learning for Predicting Phenotype: Studies in Yeast, Rice and Wheat". In: *BioRxiv*, p. 105528.
- Guo, Zhigang et al. (2013). "Accuracy of across-environment genome-wide prediction in maize nested association mapping populations". In: *G3: Genes, Genomes, Genetics* 3.2, pp. 263–272.
- Habier, David et al. (2011). "Extension of the Bayesian alphabet for genomic selection". In: *BMC bioinformatics* 12.1, p. 186.
- Hahnloser, Richard HR et al. (2000). "Digital selection and analogue amplification coexist in a cortex-inspired silicon circuit". In: *Nature* 405.6789, p. 947.

- Hassen, Manel Ben et al. (May 2018). "Genomic Prediction Accounting for Genotype by Environment Interaction Offers an Effective Framework for Breeding Simultaneously for Adaptation to an Abiotic Stress and Performance Under Normal Cropping Conditions in Rice". In: *G3: Genes, Genomes, Genetics* 8.7, pp. 2319–2332. DOI: [10.1534/g3.118.200098](https://doi.org/10.1534/g3.118.200098). URL: <https://doi.org/10.1534/g3.118.200098>.
- Hawkins, Charles and Long-Xi Yu (2018). "Recent progress in alfalfa (*Medicago sativa* L.) genomics and genomic selection". In: *The Crop Journal* 6.6, pp. 565–575.
- Hayes, Ben and Mike Goddard (2010). "Genome-wide association and genomic selection in animal breeding". In: *Genome* 53.11, pp. 876–883.
- Hayes, BJ, ME Goddard, et al. (2001). "Prediction of total genetic value using genome-wide dense marker maps". In: *Genetics* 157.4, pp. 1819–1829.
- He, Kaiming et al. (2016). "Deep residual learning for image recognition". In: *Proceedings of the IEEE conference on computer vision and pattern recognition*, pp. 770–778.
- Heffner, Elliot L, Jean-Luc Jannink, and Mark E Sorrells (2011). "Genomic selection accuracy using multifamily prediction models in a wheat breeding program". In: *The Plant Genome* 4.1, pp. 65–75.
- Heffner, Elliot L et al. (2010). "Plant breeding with genomic selection: gain per unit time and cost". In: *Crop science* 50.5, pp. 1681–1690.
- Henderson, Charles R (1975). "Best linear unbiased estimation and prediction under a selection model". In: *Biometrics*, pp. 423–447.
- Hinton, Geoffrey, Nitish Srivastava, and Kevin Swersky (2012). "Neural networks for machine learning lecture 6a overview of mini-batch gradient descent". In: *Cited on 14*, p. 8.
- Hirschhorn, Joel N. and Mark J. Daly (2005). "Genome-wide association studies for common diseases and complex traits". In: *Nature Reviews Genetics* 6.2, pp. 95–108. ISSN: 1471-0064. DOI: [10.1038/nrg1521](https://doi.org/10.1038/nrg1521). URL: <https://doi.org/10.1038/nrg1521>.
- Holliday, Jason A., Tongli Wang, and Sally Aitken (2012). "Predicting Adaptive Phenotypes From Multilocus Genotypes in Sitka Spruce (*Picea sitchensis*) Using Random Forest". In: *G3: Genes, Genomes, Genetics* 2.9, pp. 1085–1093. DOI: [10.1534/g3.112.002733](https://doi.org/10.1534/g3.112.002733). URL: <https://doi.org/10.1534/g3.112.002733>.

- Howard, Réka et al. (2019). "Joint Use of Genome, Pedigree, and Their Interaction with Environment for Predicting the Performance of Wheat Lines in New Environments". In: *G3: Genes, Genomes, Genetics* 9.9, pp. 2925–2934. DOI: [10.1534/g3.119.400508](https://doi.org/10.1534/g3.119.400508). URL: <https://doi.org/10.1534>.
- Hu, Yaodong et al. (2015). "Prediction of plant height in *Arabidopsis thaliana* using DNA methylation data". In: *Genetics* 201.2, pp. 779–793.
- Jan, Habib U et al. (2016). "Genomic prediction of testcross performance in canola (*Brassica napus*)". In: *PLoS One* 11.1, e0147769.
- Janocha, Katarzyna and Wojciech Marian Czarnecki (2017). "On loss functions for deep neural networks in classification". In: *arXiv preprint arXiv:1702.05659*.
- Jaramillo-Correa, Juan-Pablo et al. (2014). "Molecular Proxies for Climate Maladaptation in a Long-Lived Tree (*Pinus pinaster* Aiton, Pinaceae)". In: *Genetics* 199.3, pp. 793–807. DOI: [10.1534/genetics.114.173252](https://doi.org/10.1534/genetics.114.173252). URL: <https://doi.org/10.1534>.
- Jarquín, Diego, James Specht, and Aaron Lorenz (2016). "Prospects of Genomic Prediction in the USDA Soybean Germplasm Collection: Historical Data Creates Robust Models for Enhancing Selection of Accessions". In: *G3: Genes, Genomes, Genetics* 6.8, pp. 2329–2341. DOI: [10.1534/g3.116.031443](https://doi.org/10.1534/g3.116.031443). URL: <https://doi.org/10.1534>.
- Jette, Morris A., Andy B. Yoo, and Mark Grondona (2002). "SLURM: Simple Linux Utility for Resource Management". In: *In Lecture Notes in Computer Science: Proceedings of Job Scheduling Strategies for Parallel Processing (JSSPP) 2003*. Springer-Verlag, pp. 44–60.
- Jiang, Yong and Jochen C Reif (2015). "Modeling epistasis in genomic selection". In: *Genetics* 201.2, pp. 759–768.
- Jin, Jian-Jun et al. (Mar. 2018). "GetOrganelle: a simple and fast pipeline for de novo assembly of a complete circular chloroplast genome using genome skimming data". In: *bioRxiv*. DOI: [10.1101/256479](https://doi.org/10.1101/256479). URL: <http://biorxiv.org/lookup/doi/10.1101/256479>.
- Kadam, Dnyaneshwar C et al. (2016). "Genomic prediction of single crosses in the early stages of a maize hybrid breeding pipeline". In: *G3: Genes, Genomes, Genetics* 6.11, pp. 3443–3453.

- Kainer, David et al. (2018). "Accuracy of Genomic Prediction for Foliar Terpene Traits in *Eucalyptus polybractea*". In: *G3: Genes, Genomes, Genetics* 8.8, pp. 2573–2583. DOI: [10.1534/g3.118.200443](https://doi.org/10.1534/g3.118.200443). URL: <https://doi.org/10.1534>.
- Kalo, P et al. (2004). "Comparative mapping between *Medicago sativa* and *Pisum sativum*". In: *Molecular Genetics and Genomics* 272.3, pp. 235–246.
- Kang, Hyun Min et al. (2010). "Variance component model to account for sample structure in genome-wide association studies". In: *Nature genetics* 42.4, p. 348.
- Kim, Sung et al. (2007). "Recombination and linkage disequilibrium in *Arabidopsis thaliana*". In: *Nature genetics* 39.9, p. 1151.
- Kingma, Diederik P and Jimmy Ba (2014). "Adam: A method for stochastic optimization". In: *arXiv preprint arXiv:1412.6980*.
- Koch, Marcus A and Michaela Matschinger (2007). "Evolution and genetic differentiation among relatives of *Arabidopsis thaliana*". In: *Proceedings of the National Academy of Sciences* 104.15, pp. 6272–6277.
- Korte, Arthur and Ashley Farlow (2013). "The advantages and limitations of trait analysis with GWAS: a review". In: *Plant methods* 9.1, p. 29.
- Korte, Arthur et al. (2012). "A mixed-model approach for genome-wide association studies of correlated traits in structured populations". In: *Nature genetics* 44.9, p. 1066.
- Krause, Margaret R. et al. (2019). "Hyperspectral Reflectance-Derived Relationship Matrices for Genomic Prediction of Grain Yield in Wheat". In: *G3: Genes, Genomes, Genetics*, g3.200856.2018. DOI: [10.1534/g3.118.200856](https://doi.org/10.1534/g3.118.200856). URL: <https://doi.org/10.1534>.
- Kumar, Rachana A., Delene J. Oldenburg, and Arnold J. Bendich (Sept. 2014). "Changes in DNA damage, molecular integrity, and copy number for plastid DNA and mitochondrial DNA during maize development". In: *Journal of Experimental Botany* 65.22, pp. 6425–6439. ISSN: 0022-0957. DOI: [10.1093/jxb/eru359](https://doi.org/10.1093/jxb/eru359). eprint: <http://oup.prod.sis.lan/jxb/article-pdf/65/22/6425/16935653/eru359.pdf>. URL: <https://doi.org/10.1093/jxb/eru359>.

- Kumar, Satish et al. (2015). "Genome-Enabled Estimates of Additive and Nonadditive Genetic Variances and Prediction of Apple Phenotypes Across Environments". In: *G3: Genes, Genomes, Genetics* 5.12, pp. 2711–2718. DOI: [10.1534/g3.115.021105](https://doi.org/10.1534/g3.115.021105). URL: <https://doi.org/10.1534>.
- Kurtzer, Gregory M, Vanessa Sochat, and Michael W Bauer (2017). "Singularity: Scientific containers for mobility of compute". In: *PloS one* 12.5, e0177459.
- Kutschera, Ulrich and Karl J Niklas (2005). "Endosymbiosis, cell evolution, and speciation". In: *Theory in Biosciences* 124.1, pp. 1–24.
- Lan, Kun et al. (2018). "A survey of data mining and deep learning in bioinformatics". In: *Journal of medical systems* 42.8, p. 139.
- LeCun, Yann, Yoshua Bengio, and Geoffrey Hinton (2015). "Deep learning". In: *nature* 521.7553, p. 436.
- Lehermeier, Christina et al. (2014). "Usefulness of multiparental populations of maize (*Zea mays* L.) for genome-based prediction". In: *Genetics* 198.1, pp. 3–16.
- Leinonen, Rasko et al. (Nov. 2010). "The Sequence Read Archive". In: *Nucleic Acids Research* 39.suppl_1, pp. D19–D21. ISSN: 0305-1048. DOI: [10.1093/nar/gkq1019](https://doi.org/10.1093/nar/gkq1019). eprint: http://oup.prod.sis.lan/nar/article-pdf/39/suppl_1/D19/7624335/gkq1019.pdf. URL: <https://doi.org/10.1093/nar/gkq1019>.
- Li, Bo et al. (2018). "Genomic prediction of breeding values using a subset of SNPs identified by three machine learning methods". In: *Frontiers in genetics* 9, p. 237.
- Li, Heng (2018). "Minimap2: pairwise alignment for nucleotide sequences". In: *Bioinformatics* 34.18, pp. 3094–3100.
- Li, Jia-Yang, Jun Wang, and Robert S Zeigler (2014). "The 3,000 rice genomes project: new opportunities and challenges for future rice research". In: *GigaScience* 3.1, p. 8.
- Li, Peijin et al. (2014). "Multiple FLC haplotypes defined by independent cis-regulatory variation underpin life history diversity in *Arabidopsis thaliana*". In: *Genes & Development* 28.15, pp. 1635–1640.
- Li, Xuehui and E Charles Brummer (2012). "Applied genetics and genomics in alfalfa breeding". In: *Agronomy* 2.1, pp. 40–61.
- Li, Xuehui et al. (2015). "Genomic prediction of biomass yield in two selection cycles of a tetraploid alfalfa breeding population". In: *The Plant Genome* 8.2.

- Lippert, Christoph et al. (2014). "LIMIX: genetic analysis of multiple traits". In: *bioRxiv*. DOI: 10.1101/003905. eprint: <https://www.biorxiv.org/content/early/2014/05/22/003905.full.pdf>. URL: <https://www.biorxiv.org/content/early/2014/05/22/003905>.
- Litjens, Geert et al. (2017). "A survey on deep learning in medical image analysis". In: *Medical image analysis* 42, pp. 60–88.
- Lopez-Cruz, Marco et al. (2015). "Increased Prediction Accuracy in Wheat Breeding Trials Using a Marker x Environment Interaction Genomic Selection Model". In: *G3: Genes, Genomes, Genetics* 5.4, pp. 569–582. DOI: 10.1534/g3.114.016097. URL: <https://doi.org/10.1534>.
- Luo, Xiang et al. (2017). "Genomic prediction of genotypic effects with epistasis and environment interactions for yield-related traits of rapeseed (*Brassica napus* L.)". In: *Frontiers in genetics* 8, p. 15.
- Lynch, Michael, Bruce Walsh, et al. (1998). *Genetics and analysis of quantitative traits*. Vol. 1. Sinauer Sunderland, MA.
- Ma, Wenlong et al. (2017). "DeepGS: Predicting phenotypes from genotypes using Deep Learning". In: *bioRxiv*, p. 241414.
- Mamoshina, Polina et al. (2016). "Applications of deep learning in biomedicine". In: *Molecular pharmaceutics* 13.5, pp. 1445–1454.
- Martin, William et al. (Sept. 17, 2002). "Evolutionary analysis of Arabidopsis, cyanobacterial, and chloroplast genomes reveals plastid phylogeny and thousands of cyanobacterial genes in the nucleus". In: *Proceedings of the National Academy of Sciences of the United States of America* 99.19, pp. 12246–12251. ISSN: 0027-8424. DOI: 10.1073/pnas.182432999. URL: <https://www.ncbi.nlm.nih.gov/pmc/articles/PMC129430/> (visited on 05/20/2019).
- Martini, Johannes WR et al. (2017). "Genomic prediction with epistasis models: on the marker-coding-dependent performance of the extended GBLUP and properties of the categorical epistasis model (CE)". In: *BMC bioinformatics* 18.1, p. 3.
- Marulanda, Jose J et al. (2016). "Optimum breeding strategies using genomic selection for hybrid breeding in wheat, maize, rye, barley, rice and triticale". In: *Theoretical and applied genetics* 129.10, pp. 1901–1913.
- Marvin, Minsky and Papert Seymour (1969). *Perceptrons*.

- McKain, Michael and Afinit (Sept. 2017). *Mrmckain/Fast-Plast: Fast-Plast V.1.2.6*. DOI: [10.5281/zenodo.973887](https://doi.org/10.5281/zenodo.973887). URL: <https://zenodo.org/record/973887>.
- Mckinney, Brett and Nicholas Pajewski (2012). "Six degrees of epistasis: statistical network models for GWAS". In: *Frontiers in genetics* 2, p. 109.
- McKinney, Wes (2010). "Data Structures for Statistical Computing in Python". In: *Proceedings of the 9th Python in Science Conference*. Ed. by Stéfan van der Walt and Jarrod Millman, pp. 51–56.
- Mereschkowsky, Constantin (1905). "Über natur und ursprung der chromatophoren im pflanzenreiche". In: *Biologisches Centralblatt* 25, pp. 293–604.
- Merkel, Dirk (2014). "Docker: lightweight linux containers for consistent development and deployment". In: *Linux Journal* 2014.239, p. 2.
- Michie, Donald, David J Spiegelhalter, CC Taylor, et al. (1994). "Machine learning". In: *Neural and Statistical Classification* 13.
- Min, Seonwoo, Byunghan Lee, and Sungroh Yoon (2017). "Deep learning in bioinformatics". In: *Briefings in bioinformatics* 18.5, pp. 851–869.
- Moeinizade, Saba et al. (2019). "Optimizing Selection and Mating in Genomic Selection with a Look-Ahead Approach: An Operations Research Framework". In: *G3: Genes, Genomes, Genetics*, g3–200842.
- Momen, Mehdi et al. (Aug. 2019). "Predicting Longitudinal Traits Derived from High-Throughput Phenomics in Contrasting Environments Using Genomic Legendre Polynomials and B-Splines". In: *G3: Genes, Genomes, Genetics* 9.10, pp. 3369–3380. DOI: [10.1534/g3.119.400346](https://doi.org/10.1534/g3.119.400346). URL: <https://doi.org/10.1534/g3.119.400346>.
- Montesinos-López, Osva A et al. (2015). "Threshold models for genome-enabled prediction of ordinal categorical traits in plant breeding". In: *G3: Genes, Genomes, Genetics* 5.2, pp. 291–300.
- Montesinos-López, Osva A et al. (2019a). "A benchmarking between deep learning, support vector machine and Bayesian threshold best linear unbiased prediction for predicting ordinal traits in plant breeding". In: *G3: Genes, Genomes, Genetics* 9.2, pp. 601–618.
- (2019b). "New deep learning genomic-based prediction model for multiple traits with binary, ordinal, and continuous phenotypes". In: *G3: Genes, Genomes, Genetics* 9.5, pp. 1545–1556.

- National Center for Biotechnology Information. NCBI Taxonomy. Accessed: 2019-10-01.
URL: <https://www.ncbi.nlm.nih.gov/Taxonomy/taxonomyhome.html/>.
- Neyhart, Jeffrey, Aaron J Lorenz, and Kevin P Smith (2019). "Multi-Trait Improvement by Predicting Genetic Correlations in Breeding Crosses". In: *bioRxiv*, p. 593210.
- Nguyen, Derrick and Bernard Widrow (1990). "The truck backer-upper: An example of self-learning in neural networks". In: *Advanced neural computers*. Elsevier, pp. 11–19.
- Nordborg, Magnus et al. (2002). "The extent of linkage disequilibrium in *Arabidopsis thaliana*". In: *Nature genetics* 30.2, p. 190.
- Norman, Adam et al. (2018). "Optimising Genomic Selection in Wheat: Effect of Marker Density, Population Size and Population Structure on Prediction Accuracy". In: *G3: Genes, Genomes, Genetics* 8.9, pp. 2889–2899. DOI: [10.1534/g3.118.200311](https://doi.org/10.1534/g3.118.200311). URL: <https://doi.org/10.1534>.
- Oakey, Helena et al. (2016). "Genomic selection in multi-environment crop trials". In: *G3: Genes, Genomes, Genetics* 6.5, pp. 1313–1326.
- Ogutu, Joseph O, Hans-Peter Piepho, and Torben Schulz-Streeck (2011). "A comparison of random forests, boosting and support vector machines for genomic selection". In: *BMC proceedings*. Vol. 5. 3. BioMed Central, S11.
- Ohyama, Kanji et al. (Aug. 1986). "Chloroplast gene organization deduced from complete sequence of liverwort *Marchantia polymorpha* chloroplast DNA". In: *Nature* 322.6079, p. 572. ISSN: 1476-4687. DOI: [10.1038/322572a0](https://doi.org/10.1038/322572a0). URL: <https://www.nature.com/articles/322572a0> (visited on 05/20/2019).
- Olejniczak, Szymon Adam et al. (2016). "Chloroplasts: state of research and practical applications of plastome sequencing". In: *Planta* 244.3, pp. 517–527.
- Oliphant, Travis E (2006). *A guide to NumPy*. Vol. 1. Trelgol Publishing USA.
- Ovenden, Ben et al. (2018). "Accounting for Genotype-by-Environment Interactions and Residual Genetic Variation in Genomic Selection for Water-Soluble Carbohydrate Concentration in Wheat". In: *G3: Genes, Genomes, Genetics* 8.6, pp. 1909–1919. DOI: [10.1534/g3.118.200038](https://doi.org/10.1534/g3.118.200038). URL: <https://doi.org/10.1534>.
- Owens, Brenda F et al. (2014). "A foundation for provitamin A biofortification of maize: genome-wide association and genomic prediction models of carotenoid levels". In: *Genetics* 198.4, pp. 1699–1716.

- Palmer, Jeffrey D. (1985). "COMPARATIVE ORGANIZATION OF CHLOROPLAST GENOMES". In: *Annual Review of Genetics* 19.1. PMID: 3936406, pp. 325–354. DOI: [10.1146/annurev.ge.19.120185.001545](https://doi.org/10.1146/annurev.ge.19.120185.001545). eprint: <https://doi.org/10.1146/annurev.ge.19.120185.001545>. URL: <https://doi.org/10.1146/annurev.ge.19.120185.001545>.
- Peiffer, Jason A et al. (2014). "The genetic architecture of maize height". In: *Genetics* 196.4, pp. 1337–1356.
- Polyak, Boris T (1964). "Some methods of speeding up the convergence of iteration methods". In: *USSR Computational Mathematics and Mathematical Physics* 4.5, pp. 1–17.
- Poudel, Hari P. et al. (2019). "Genomic Prediction for Winter Survival of Lowland Switchgrass in the Northern USA". In: *G3: Genes, Genomes, Genetics*, g3.400094.2019. DOI: [10.1534/g3.119.400094](https://doi.org/10.1534/g3.119.400094). URL: <https://doi.org/10.1534>.
- Purcell, Shaun et al. (2007). "PLINK: a tool set for whole-genome association and population-based linkage analyses". In: *The American journal of human genetics* 81.3, pp. 559–575.
- Purcell, Shaun M et al. (2014). "A polygenic burden of rare disruptive mutations in schizophrenia". In: *Nature* 506.7487, p. 185.
- Qian, Lunwen, Wei Qian, and Rod J Snowdon (2014). "Sub-genomic selection patterns as a signature of breeding in the allopolyploid *Brassica napus* genome". In: *BMC genomics* 15.1, p. 1170.
- Qiu, Zhixu et al. (2016). "Application of machine learning-based classification to genomic selection and performance improvement". In: *International Conference on Intelligent Computing*. Springer, pp. 412–421.
- R Core Team (2019). *R: A Language and Environment for Statistical Computing*. R Foundation for Statistical Computing. Vienna, Austria. URL: <https://www.R-project.org/>.
- Rampasek, Ladislav and Anna Goldenberg (2016). "Tensorflow: Biology's gateway to deep learning?" In: *Cell systems* 2.1, pp. 12–14.
- Ramstein, Guillaume P. and Michael D. Casler (2019). "Extensions of BLUP Models for Genomic Prediction in Heterogeneous Populations: Application in a Diverse

- Switchgrass Sample". In: *G3: Genes, Genomes, Genetics*, g3.200969.2018. DOI: 10.1534/g3.118.200969. URL: <https://doi.org/10.1534>.
- Ramstein, Guillaume P. et al. (2016). "Accuracy of Genomic Prediction in Switchgrass (*Panicum virgatum*L.) Improved by Accounting for Linkage Disequilibrium". In: *G3: Genes, Genomes, Genetics* 6.4, pp. 1049–1062. DOI: 10.1534/g3.115.024950. URL: <https://doi.org/10.1534>.
- Ratcliffe, Blaise et al. (2017). "Single-Step BLUP with Varying Genotyping Effort in Open-Pollinated *Picea glauca*". In: *G3: Genes, Genomes, Genetics* 7.3, pp. 935–942. DOI: 10.1534/g3.116.037895. URL: <https://doi.org/10.1534>.
- Resende, M. F. R. et al. (2012). "Accuracy of Genomic Selection Methods in a Standard Data Set of Loblolly Pine (*Pinus taeda* L.)" In: *Genetics* 190.4, pp. 1503–1510. DOI: 10.1534/genetics.111.137026. URL: <https://doi.org/10.1534>.
- Riedelsheimer, Christian et al. (2013). "Genomic predictability of interconnected biparental maize populations". In: *Genetics* 194.2, pp. 493–503.
- Rincent, Renaud et al. (2012). "Maximizing the reliability of genomic selection by optimizing the calibration set of reference individuals: comparison of methods in two diverse groups of maize inbreds (*Zea mays* L.)" In: *Genetics* 192.2, pp. 715–728.
- Rincent, Renaud et al. (2018). "Phenomic Selection Is a Low-Cost and High-Throughput Method Based on Indirect Predictions: Proof of Concept on Wheat and Poplar". In: *G3: Genes, Genomes, Genetics*, g3.200760.2018. DOI: 10.1534/g3.118.200760. URL: <https://doi.org/10.1534>.
- Ritchie, Marylyn D and Kristel Van Steen (2018). "The search for gene-gene interactions in genome-wide association studies: challenges in abundance of methods, practical considerations, and biological interpretation". In: *Annals of translational medicine* 6.8.
- Rocaps Lab. CpBase. Accessed: 2019-04-01, Version: 8/20/2017. URL: http://rocaplab.ocean.washington.edu/old_website/tools/cpbase.
- Rosenblatt, Frank (1961). *Principles of neurodynamics. perceptrons and the theory of brain mechanisms*. Tech. rep. Cornell Aeronautical Lab Inc Buffalo NY.
- Ruder, Sebastian (2016). "An overview of gradient descent optimization algorithms". In: *arXiv preprint arXiv:1609.04747*.

- Rumelhart, David E, Geoffrey E Hinton, Ronald J Williams, et al. (1988). "Learning representations by back-propagating errors". In: *Cognitive modeling* 5.3, p. 1.
- Sancho, Rubén et al. (June 2018). "Comparative plastome genomics and phylogenomics of *Brachypodium* : flowering time signatures, introgression and recombination in recently diverged ecotypes". en. In: *New Phytologist* 218.4, pp. 1631–1644. ISSN: 0028646X. DOI: [10.1111/nph.14926](https://doi.org/10.1111/nph.14926). URL: <http://doi.wiley.com/10.1111/nph.14926>.
- Scarcelli, N. et al. (2016). "Intra-individual polymorphism in chloroplasts from NGS data: where does it come from and how to handle it?" In: *Molecular Ecology Resources* 16.2, pp. 434–445. DOI: [10.1111/1755-0998.12462](https://doi.org/10.1111/1755-0998.12462). eprint: <https://onlinelibrary.wiley.com/doi/pdf/10.1111/1755-0998.12462>. URL: <https://onlinelibrary.wiley.com/doi/abs/10.1111/1755-0998.12462>.
- Schmidhuber, Jürgen (2015). "Deep learning in neural networks: An overview". In: *Neural networks* 61, pp. 85–117.
- Schopp, Pascal et al. (2017a). "Accuracy of genomic prediction in synthetic populations depending on the number of parents, relatedness, and ancestral linkage disequilibrium". In: *Genetics* 205.1, pp. 441–454.
- Schopp, Pascal et al. (2017b). "Genomic prediction within and across biparental families: means and variances of prediction accuracy and usefulness of deterministic equations". In: *G3: Genes, Genomes, Genetics* 7.11, pp. 3571–3586.
- Schrag, Tobias A et al. (2018). "Beyond genomic prediction: combining different types of omics data can improve prediction of hybrid performance in maize". In: *Genetics* 208.4, pp. 1373–1385.
- Segura, Vincent et al. (2012). "An efficient multi-locus mixed-model approach for genome-wide association studies in structured populations". In: *Nature genetics* 44.7, p. 825.
- Seren, Ümit et al. (2016). "AraPheno: a public database for *Arabidopsis thaliana* phenotypes". In: *Nucleic acids research*, gkw986.
- Shen, Wei et al. (Oct. 2016). "SeqKit: A Cross-Platform and Ultrafast Toolkit for FASTA/Q File Manipulation". In: *PLOS ONE* 11.10, pp. 1–10. DOI: [10.1371/journal.pone.0163962](https://doi.org/10.1371/journal.pone.0163962). URL: <https://doi.org/10.1371/journal.pone.0163962>.

- Shen, Xia et al. (2013). "A novel generalized ridge regression method for quantitative genetics". In: *Genetics* 193.4, pp. 1255–1268.
- Shinozaki, K. et al. (1986). "The complete nucleotide sequence of the tobacco chloroplast genome: its gene organization and expression". In: *The EMBO Journal* 5.9, pp. 2043–2049. ISSN: 1460-2075. DOI: [10.1002/j.1460-2075.1986.tb04464.x](https://doi.org/10.1002/j.1460-2075.1986.tb04464.x). URL: <https://onlinelibrary.wiley.com/doi/abs/10.1002/j.1460-2075.1986.tb04464.x> (visited on 05/20/2019).
- Siva, Nayanah (2008). *1000 Genomes project*.
- Snowdon, Rod J and Federico L Iniguez Luy (2012). "Potential to improve oilseed rape and canola breeding in the genomics era". In: *Plant breeding* 131.3, pp. 351–360.
- Soper, HE et al. (1917). "On the distribution of the correlation coefficient in small samples. Appendix II to the papers of" Student" and RA Fisher". In: *Biometrika* 11.4, pp. 328–413.
- Sousa, Massaine Bandeira e et al. (2017). "Genomic-enabled prediction in maize using kernel models with genotype \times environment interaction". In: *G3: Genes, Genomes, Genetics* 7.6, pp. 1995–2014.
- Stegemann, Sandra and Ralph Bock (2009). "Exchange of genetic material between cells in plant tissue grafts". In: *science* 324.5927, pp. 649–651.
- Stewart-Brown, Benjamin B. et al. (2019). "Genomic Selection for Yield and Seed Composition Traits Within an Applied Soybean Breeding Program". In: *G3: Genes, Genomes, Genetics* 9.7, pp. 2253–2265. DOI: [10.1534/g3.118.200917](https://doi.org/10.1534/g3.118.200917). URL: <https://doi.org/10.1534/g3.118.200917>.
- Storey, John D. and Robert Tibshirani (2003). "Statistical significance for genomewide studies". In: *Proceedings of the National Academy of Sciences* 100.16, pp. 9440–9445. ISSN: 0027-8424. DOI: [10.1073/pnas.1530509100](https://doi.org/10.1073/pnas.1530509100). eprint: <https://www.pnas.org/content/100/16/9440.full.pdf>. URL: <https://www.pnas.org/content/100/16/9440>.
- Stringer, Sven et al. (2011). "Underestimated effect sizes in GWAS: fundamental limitations of single SNP analysis for dichotomous phenotypes". In: *PloS one* 6.11, e27964.
- Sukumaran, Sivakumar et al. (2016). "Genomic Prediction with Pedigree and Genotype Environment Interaction in Spring Wheat Grown in South and West Asia,

- North Africa, and Mexico". In: *G3: Genes, Genomes, Genetics* 7.2, pp. 481–495. DOI: [10.1534/g3.116.036251](https://doi.org/10.1534/g3.116.036251). URL: <https://doi.org/10.1534>.
- Tang, Chunlao et al. (2007). "The evolution of selfing in *Arabidopsis thaliana*". In: *Science* 317.5841, pp. 1070–1072.
- Technow, Frank, Anna Bürger, and Albrecht E Melchinger (2013). "Genomic prediction of northern corn leaf blight resistance in maize with combined or separated training sets for heterotic groups". In: *G3: Genes, Genomes, Genetics* 3.2, pp. 197–203.
- Technow, Frank et al. (2014). "Genome properties and prospects of genomic prediction of hybrid performance in a breeding program of maize". In: *Genetics* 197.4, pp. 1343–1355.
- Tetko, Igor V, David J Livingstone, and Alexander I Luik (1995). "Neural network studies. 1. Comparison of overfitting and overtraining". In: *Journal of chemical information and computer sciences* 35.5, pp. 826–833.
- Thavamanikumar, Saravanan, Rudy Dolferus, and Bala R. Thumma (2015). "Comparison of Genomic Selection Models to Predict Flowering Time and Spike Grain Number in Two Hexaploid Wheat Doubled Haploid Populations". In: *G3: Genes, Genomes, Genetics* 5.10, pp. 1991–1998. DOI: [10.1534/g3.115.019745](https://doi.org/10.1534/g3.115.019745). URL: <https://doi.org/10.1534>.
- Thorwarth, Patrick, Eltohamy AA Yousef, and Karl J Schmid (2018). "Genomic Prediction and Association Mapping of Curd-Related Traits in Gene Bank Accessions of Cauliflower". In: *G3: Genes, Genomes, Genetics* 8.2, pp. 707–718.
- Timpson, Nicholas J et al. (2018). "Genetic architecture: the shape of the genetic contribution to human traits and disease". In: *Nature Reviews Genetics* 19.2, p. 110.
- Togninalli, Matteo et al. (2017). "The AraGWAS Catalog: a curated and standardized *Arabidopsis thaliana* GWAS catalog". In: *Nucleic acids research* 46.D1, pp. D1150–D1156.
- Twyford, Alex D. and Rob W. Ness (Sept. 1, 2017). "Strategies for complete plastid genome sequencing". In: *Molecular Ecology Resources* 17.5, pp. 858–868. ISSN: 1755-0998. DOI: [10.1111/1755-0998.12626](https://doi.org/10.1111/1755-0998.12626). URL: <http://onlinelibrary.wiley.com/doi/10.1111/1755-0998.12626/abstract> (visited on 01/26/2018).

- Van Rossum, Guido and Fred L Drake Jr (1995). *Python tutorial*. Centrum voor Wiskunde en Informatica Amsterdam, The Netherlands.
- VanRaden, Paul M (2008). "Efficient methods to compute genomic predictions". In: *Journal of dairy science* 91.11, pp. 4414–4423.
- Vieira, IC et al. (2017). "Assessing non-additive effects in GBLUP model". In: *Genetics and molecular research: GMR* 16.2.
- Vinga, Susana et al. (2012). "Pattern matching through Chaos Game Representation: bridging numerical and discrete data structures for biological sequence analysis". In: *Algorithms for molecular biology : AMB* 7.1. 22551152[pmid], pp. 10–10. ISSN: 1748-7188. DOI: [10.1186/1748-7188-7-10](https://doi.org/10.1186/1748-7188-7-10). URL: <https://www.ncbi.nlm.nih.gov/pubmed/22551152>.
- Walsh, Bruce and Michael Lynch (2018). *Evolution and selection of quantitative traits*. Oxford University Press.
- Wang, Weiwen et al. (2018). "Assembly of chloroplast genomes with long- and short-read data: a comparison of approaches using *Eucalyptus pauciflora* as a test case". In: *BMC genomics* 19.1. 30594129[pmid], pp. 977–977. ISSN: 1471-2164. DOI: [10.1186/s12864-018-5348-8](https://doi.org/10.1186/s12864-018-5348-8). URL: <https://www.ncbi.nlm.nih.gov/pubmed/30594129>.
- Wang, Yu et al. (2014). "The accuracy of prediction of genomic selection in elite hybrid rye populations surpasses the accuracy of marker-assisted selection and is equally augmented by multiple field evaluation locations and test years". In: *BMC genomics* 15.1, p. 556.
- Warner, Brad and Manavendra Misra (1996). "Understanding neural networks as statistical tools". In: *The american statistician* 50.4, pp. 284–293.
- Webb, Sarah (2018). "Deep learning for biology". In: *Nature* 554.7693.
- Werner, Christian R et al. (2018). "Effective genomic selection in a narrow-genepool crop with low-density markers: Asian rapeseed as an example". In: *The plant genome* 11.2.
- Wicke, Susann et al. (July 1, 2011). "The evolution of the plastid chromosome in land plants: gene content, gene order, gene function". In: *Plant Molecular Biology* 76.3, pp. 273–297. ISSN: 1573-5028. DOI: [10.1007/s11103-011-9762-4](https://doi.org/10.1007/s11103-011-9762-4). URL: <https://doi.org/10.1007/s11103-011-9762-4> (visited on 05/16/2019).

- Windhausen, Vanessa S et al. (2012). "Effectiveness of genomic prediction of maize hybrid performance in different breeding populations and environments". In: *G3: Genes, Genomes, Genetics* 2.11, pp. 1427–1436.
- Würschum, Tobias (2012). "Mapping QTL for agronomic traits in breeding populations". In: *Theoretical and Applied Genetics* 125.2, pp. 201–210.
- Würschum, Tobias, Stefan Abel, and Yusheng Zhao (2014). "Potential of genomic selection in rapeseed (*Brassica napus* L.) breeding". In: *Plant Breeding* 133.1, pp. 45–51.
- Xavier, Alencar, William M. Muir, and Katy Martin Rainey (2016). "Assessing Predictive Properties of Genome-Wide Selection in Soybeans". In: *G3* 6.8, pp. 2611–2616. DOI: [10.1534/g3.116.032268](https://doi.org/10.1534/g3.116.032268). URL: <https://doi.org/10.1534>.
- Xiao-Ming, Zheng et al. (May 8, 2017). "Inferring the evolutionary mechanism of the chloroplast genome size by comparing whole-chloroplast genome sequences in seed plants". In: *Scientific Reports* 7.1, p. 1555. ISSN: 2045-2322. DOI: [10.1038/s41598-017-01518-5](https://doi.org/10.1038/s41598-017-01518-5). URL: <https://www.nature.com/articles/s41598-017-01518-5> (visited on 05/16/2019).
- Xu, Shizhong (Aug. 2013). "Genetic Mapping and Genomic Selection Using Recombination Breakpoint Data". In: *Genetics* 195.3, pp. 1103–1115. DOI: [10.1534/genetics.113.155309](https://doi.org/10.1534/genetics.113.155309). URL: <https://doi.org/10.1534/genetics.113.155309>.
- Zapata-Valenzuela, Jaime et al. (2013). "Genomic Estimated Breeding Values Using Genomic Relationship Matrices in a Cloned Population of Loblolly Pine". In: *G3: Genes, Genomes, Genetics* 3.5, pp. 909–916. DOI: [10.1534/g3.113.005975](https://doi.org/10.1534/g3.113.005975). URL: <https://doi.org/10.1534>.
- Zeiler, Matthew D (2012). "ADADELTA: an adaptive learning rate method". In: *arXiv preprint arXiv:1212.5701*.
- Zhang, Yan et al. (2018). "Estimation of complex effect-size distributions using summary-level statistics from genome-wide association studies across 32 complex traits". In: *Nature genetics* 50.9, p. 1318.
- Zhang, Zhiwu et al. (Mar. 2010). "Mixed linear model approach adapted for genome-wide association studies". In: *Nature Genetics* 42.4, pp. 355–360. DOI: [10.1038/ng.546](https://doi.org/10.1038/ng.546). URL: <https://doi.org/10.1038/ng.546>.

- Zhong, Shengqiang et al. (2009). "Factors affecting accuracy from genomic selection in populations derived from multiple inbred lines: a barley case study". In: *Genetics* 182.1, pp. 355–364.
- Zhou, Xiang and Matthew Stephens (June 2012). "Genome-wide efficient mixed-model analysis for association studies". In: *Nature Genetics* 44.7, pp. 821–824. DOI: [10 . 1038/ng.2310](https://doi.org/10.1038/ng.2310). URL: <https://doi.org/10.1038/ng.2310>.
- Žilinskas, A (2006). *Practical mathematical optimization: An introduction to basic optimization theory and classical and new gradient-based algorithms*.